



# **AMERICAN COLLEGE OF VETERINARY RADIOLOGY**

**2011 Annual Scientific Meeting**

**October 11-14, 2011**

**HYATT REGENCY ALBUQUERQUE**

**ALBUQUERQUE, NEW MEXICO**

## **PROGRAM COMMITTEE**

**Jay Stefanacci, Program Chair**

**Sloan Dupree, Program Co-Chair (Forum Focus)**

**Sheri Siegel, Program Co-Chair (Radiation Oncology)**

**Nathan Nelson, Program Co-Chair (Image Interpretation Session)**

**Anthony Pease, President Ultrasound Society**

**Federica Morandi, President Society of Veterinary Nuclear Medicine**

**John Hathcock, President CT/MRI Society**

**Jessica Winger, ACVR Meeting Manager**

**Susie Wilson, ACVR Administrator**

## **ACVR ADMINISTRATION**

**Val Samii, President**

**Kari Anderson, President - Elect**

**Rob McLear, Treasurer**

**Tom Nyland, Webmaster/Secretary**

**Mary K. Klein, President, Radiation Oncology**

**Robert D. Pechman, Executive Director**

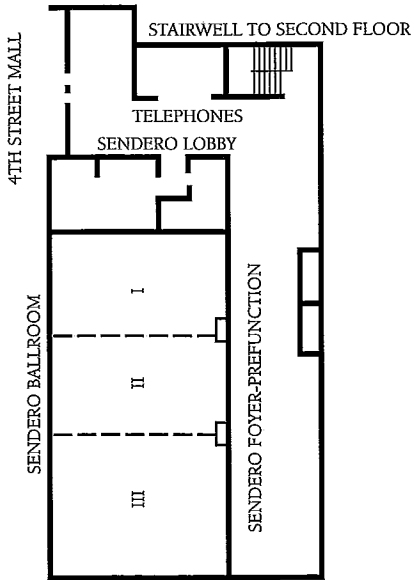
**Darryl N. Biery, Assistant Executive Director**

## TABLE OF CONTENTS

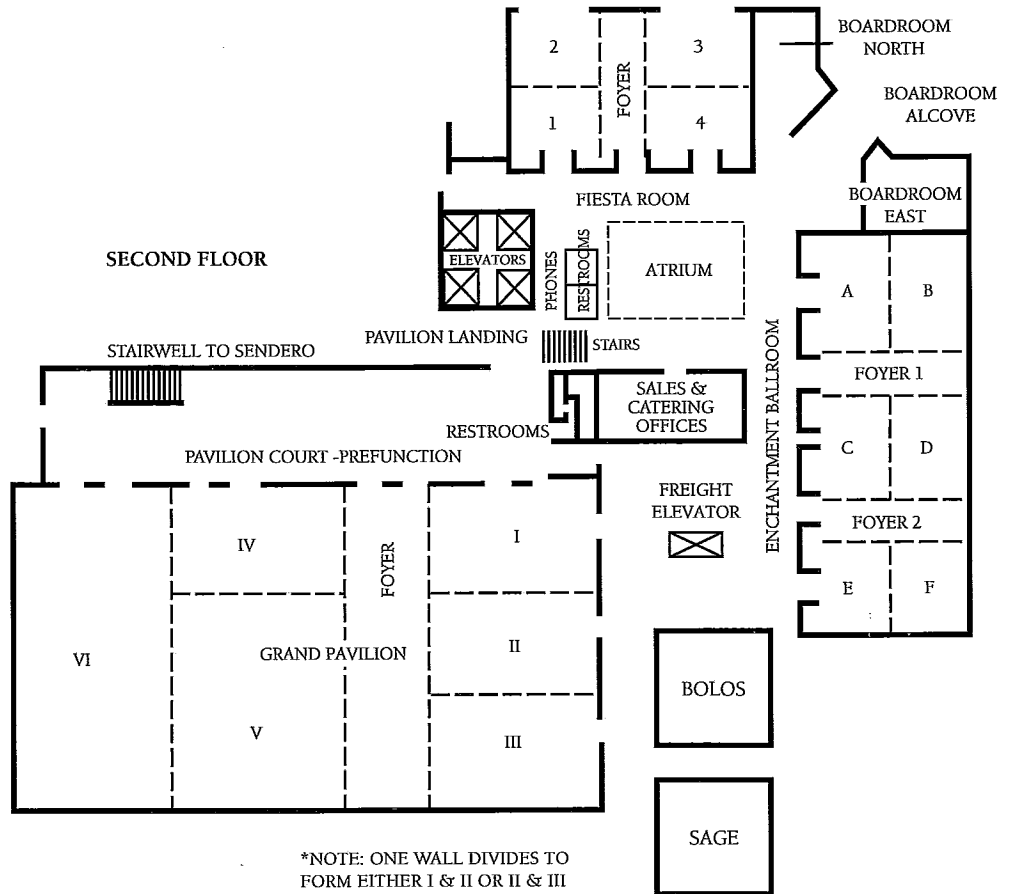
I.	2011 Conference General Information.....	4
	Hotel floor plan	
	Registration will be located at Pavilion Landing	
II.	Corporate Partners.....	5
III.	Program Overview.....	14
IV.	Monday, October 10, 2011.....	18
	Interventional Radiology Laboratory: Tracheal and Urethral Stenting	
	Sponsored by Infiniti Medical, Off-Site Location	
IV.	Tuesday, October 11, 2011.....	18
	Special Guest Speaker, Dr. Jeffrey Solomon	
	ACVR Forum	
V.	Wednesday, October 12, 2011.....	19
	Conference Welcome, Dr. Jay Stefanacci, 2011 Program Chair	
	ACVR Presidential Address, Dr. Val Samii	
	Resident Authored Paper Award	
	ACVR Keynote Address, Dr. Donald Thrall	
	Radiology Scientific Session	
	Ultrasound Keynote Address, Dr. Natasha Werpy	
	Ultrasound Scientific Session	
	Opportunity to Meet with the Residency Directors	
	Welcome Reception, Sponsored by Universal Medical Systems, Inc.	
VI.	Thursday, October 13, 2011, ACVR.....	39
	Society of Veterinary Nuclear Medicine Meeting	
	Nuclear Medicine Roundtable Discussion	
	Nuclear Medicine Scientific Session	
	Meet the New Diplomates	
	Image Interpretation Session	
	ACVR Business Meeting	
	LADIS Meeting	

VII.	Thursday, October 13, 2011, RO.....	46
	VRTOG/RO Scientific Session	
	Image Interpretation Session	
	ACVR Business Meeting	
	LADIS Meeting	
VIII.	Friday, October 14, 2011, ACVR.....	58
	CT/MRI Society Meeting	
	CT/MRI Society Keynote Address, Dr. Charles Ho	
	CT/MRI Scientific Session	
	Poster Session with Authors	
	LADIS Scientific Session	
IX.	Friday, October 14, 2011, RO.....	99
	Radiation Oncology Keynote Address, Dr. Phillip Devlin	
	VRTOG Society Meeting	
	Welcome New Diplomates/RO Business Meeting	
	RO Scientific Session	
X.	Special Activities .....	100
XI.	Conference Registrants.....	101
	Identification of Registrants	
	Registrant list	

FIRST FLOOR



SECOND FLOOR





**THE AMERICAN COLLEGE OF VETERINARY RADIOLOGY  
GRATEFULLY ACKNOWLEDGES THE SUPPORT OF THE  
FOLLOWING COMPANIES AND WISHES TO THANK THEM  
FOR THEIR CONTRIBUTIONS**

**ANIMAGE LLC**

Dr. Horst Bruning, President  
3825 Hopyard Road, Suite 220  
Pleasanton CA 94588  
Phone: 925-416-1900 ext.111  
Email: [hbruning@exxim-cc.com](mailto:hbruning@exxim-cc.com)  
Website: [www.animagellc.com](http://www.animagellc.com)

Animage LLC presents Fidex, a veterinary diagnostic imaging system with CT, DR, and fluoroscopy in one machine. Fidex can be CT-only, CT+DR, CT+fluoroscopy, or a three-modality system. Fidex plugs into 110 V or 220 V outlets; has dramatically lower costs of installation, operation, & maintenance; and has better spatial resolution than refurbished human CT scanners. Fidex requires no more shielding than a standard X-ray machine and no special cooling.

## **ANTECH IMAGING SERVICES**

17672-B Cowan Avenue

Irvine, CA 92614

Phone: 877-727-6800

Website: [www.antechimagingervices.com](http://www.antechimagingervices.com)

For more than 10 years, AIS has been providing telemedicine and cloud storage to more veterinarians and clinics than any other service in the world. AIS has over 20 full time staff radiologists, and sponsors radiology residents at 6 Universities. We are proud to play a leading role in the advancement of telemedicine and the radiology profession.

## **ASTERIS, INC.**

Box 285

Stephentown, NY 12168

Phone: 877-7ASTERIS

877-727-8374

Email: [info@asteris.biz](mailto:info@asteris.biz)

Website: [www.asteris.biz](http://www.asteris.biz)

ASTERIS is an innovative, progressive corporation focusing on technology solutions for the veterinary industry. Founded in 2004, ASTERIS delivers inimitable PACS (Picture Archiving and Communication Systems) solutions and a groundbreaking veterinary information communication platform. A revolutionary concept, ASTERIS Veterinary Communication Network (VCN) enables veterinary practices, universities, and clients to access and share the full breadth of patient medical data at any time, from anywhere in the world.

## **ATLANTIS WORLDWIDE LLC**

761 Nepperhan Avenue

Yonkers, NY 10703

Phone: 1-800-533-3356

Email: [info@atlantisworldwide.com](mailto:info@atlantisworldwide.com)

Website: [www.atlantisworldwide.com](http://www.atlantisworldwide.com)

Used & Refurbished Diagnostic Imaging Equipment for Vets. As one of the oldest and largest providers of used & refurbished diagnostic imaging equipment, Atlantis can provide your facility with high quality imaging systems. With a solid reputation of delivering reliable refurbished medical equipment our strategy has always been to partner with our clients to find the appropriate technology at the appropriate price. All modalities, all manufacturers! We sell C-Arms, CT, MRI, X-Ray and Ultrasound. Installation & Training -Financing- Customized Turnkey Solutions

**CANON (VIRTUAL IMAGING, INC.)**

720 S Powerline Road, Suite E  
Deerfield Beach, FL 33442  
Phone: 954-428-6191  
Fax: 954-428-6195  
Email: [info@virtualimaging-fl.com](mailto:info@virtualimaging-fl.com)  
Website: [www.virtualimaging-fl.com](http://www.virtualimaging-fl.com)

Virtual Imaging, Inc. is a wholly owned subsidiary of Canon U.S.A., Inc. Combining unmatched experience, extensive resources and broad business functions, Virtual Imaging collaborates with large complex hospital and government organizations as well as imaging centers and private physician offices to support them in becoming efficient, high-performance healthcare providers and professionals. Recently, Virtual Imaging has broadened its capabilities and solutions to channel the same business acumen to veterinary practices and organizational groups for the better treatment and care of animals. We assist in the advancement of our clients forward thinking goals, from strategic planning to day-to-day operations, with our commitment to provide products and services for diagnostic equipment, imaging solutions, and digital flat panel technology. With over 130 employees, 50+ Service Engineers, 55+ dealers nationwide and a proven track record; Virtual Imaging is able to combine the necessary expertise, skills and technologies that facilitate healthcare and veterinary providers to better diagnose diseases and treat conditions.

**COACTIV PACS 4VETS**

900 Ethan Allen Highway  
Ridgefield, CT 06877  
Phone: 877-COACTIV  
877-262-2848  
Fax: 203-438-5004  
Email: [molly.mcdougall@coactiv.com](mailto:molly.mcdougall@coactiv.com)  
Website: [www.pacs4vets.com](http://www.pacs4vets.com)

CoActive Medical develops and markets a complete line of PACS and Medical Imaging products and services for the management of digital radiography images. CoActiv has designed PACS4VETS®, a state-of-the-art PACS, based on EXAM-PACS®, CoActiv's human PACS, which enables veterinarians to view, manage, distribute and archive exams produced by imaging modalities. CoActiv is dedicated to delivering affordable and easy-to-use digital imaging management tools to the veterinary profession, resulting in improved diagnostic capabilities that also have FDA and HIPAA certification.

**CUATTRO**

1618 Valle Vista Boulevard  
Pekin, IL 61554

Website: [www.cuattro.com](http://www.cuattro.com)

Cuattro's flat panel digital radiography systems improve efficiency and workflow, for increased productivity and lower costs. Cuattro digital flat panel same-day retrofits, complete rooms and mobile digital x-ray systems, and cloud-based archiving and PACS, deliver better performance, perfect images, in half the time of CR or film.

**FUJIFILM MEDICAL SYSTEMS U.S.A., INC.**

419 West Avenue  
Stamford, CT 06902

Website: [www.fujiprivatepractice.com](http://www.fujiprivatepractice.com)

FUJIFILM Medical Systems, the inventor and world leader in digital x-ray, will showcase the FDR D-EVO, a new digital flat panel detector enabling veterinary practices to transition to DR with no modification to an existing radiographic room. The digital flat panel detector was designed to deliver Fujifilm's renowned image quality and intuitive functionality designed to address the needs of your practice. Systems for viewing, archiving and storing digital x-rays are also available. For more information: [www.fujiprivatepractice.com](http://www.fujiprivatepractice.com).

**HITACHI ALOKA MEDICAL**

10 Fairfield Boulevard  
Wallingford, CT 06942  
Phone: 203-269-5088  
Toll Free: 1-800-872-5652  
Fax: 203-269-6075

Email: [inquiry@hitachi-aloka.com](mailto:inquiry@hitachi-aloka.com)

Website: [www.hitachi-aloka.com](http://www.hitachi-aloka.com)

Hitachi Aloka Medical offers small, portable, easy to use systems for every veterinary application. Known for our unparalleled image quality, superior system reliability, and incredible penetration, our systems employ innovative technologies for easier diagnosis and faster exam times.

## **IDEXX TELEMEDICINE CONSULTANTS**

16900 SE 82nd Drive  
Clackamas, OR 97015  
Phone: 1-800-726-1212  
Website: [www.idexx.com](http://www.idexx.com)

Radiology, cardiology, specialty services and more- everything we do is focused on helping you take swift, precise action to improve patient outcomes. All while making the entire experience easy and professionally rewarding. Our consultants work with you to provide not just a quality report, but a critical understanding of the specialized medicine behind each expert evaluation. And it's how we ensure our work together will inform confident medical decisions for all your complex and routine patient cases.

## **ORTHOPEDIC FOUNDATION FOR ANIMALS**

2300 East Nifong Boulevard  
Columbia, MO 65201-3806  
Phone: 573-442-0418  
Fax: 573-875-5073  
Email: [ofa@offa.org](mailto:ofa@offa.org)  
Website: [www.offa.org](http://www.offa.org)

Established as a 501c(3) not-for-profit organization in 1966, the OFA has funded over two million dollars towards animal wellness. The OFA has evolved from solely a hip registry into genetic counseling for hip and elbow dysplasia, congenital cardiac disease, autoimmune thyroiditis, patella luxation, and other inherited canine diseases.

## **PARAMED MEDICAL SYSTEMS, INC.**

39 High Street  
North Andover, MA 01845

Paramed Medical Systems is a young, dynamic, innovative and forward thinking company dedicated to developing and marketing revolutionary advances in truly open and stand up MRI systems including the MrV designed specifically for veterinary medicine. Its open structure and specific table design make positioning the animal extremely simple. The MrV provides the best cost/quality ratio available and can be easily installed in areas where space is limited.

## **SCIL ANIMAL CARE COMPANY**

151 N Greenleaf Street  
Gurnee, IL 60031  
Phone: 847-223-6323  
Fax: 847-223-3374  
Website: [www.scilvet.com](http://www.scilvet.com)

Scil animal care company is an international organization with 22 company locations throughout Europe, Asia, the U.S. and Canada, and is dedicated to delivering animal health professionals the highest quality veterinary products. We understand that high quality products are not enough in today's modern veterinary laboratory. Post-acquisition in-hospital training, support and service make the critical difference to the ongoing performance of the instrument, as well as its financial contribution to the veterinary practice. Scil animal care company is here to support you! Scil offers chemistry analyzers, hematology analyzers, vital signs monitors, surgical power tools by Aesculap, equipment accessories, and more! Scil is also proud to service the industry with impeccable customer service, 24/7 telephone technical support, on-site equipment installations, equipment training, and continuing education.

## **SOUND-EKLIN**

5817 Dryden Place, Suite 100  
Carlsbad, CA 92008  
Website: [www.soundeklin.com](http://www.soundeklin.com)

Sound-Eklin is the industry's uncontested leader in veterinary imaging including digital radiography, ultrasound, imaging data management, viewing and advanced imaging tools. Sound-Eklin is driving the industry forward with a commitment to open standards supported by strength, synergy and freedom of choice.

## **ULTRASONIX MEDICAL CORPORATION**

130-4311 Viking Way  
Richmond, BC V6V2K9  
Website: [www.ultrasonix.com](http://www.ultrasonix.com)

Ultrasonix develops and manufactures diagnostic ultrasound imaging systems with customizable touch screens to simplify workflows. The company's systems are built on an open software platform that enables remote service and easy updates to keep current with advancements in imaging technology. Founded in 2000, Ultrasonix is a privately-held company headquartered in Richmond, British Columbia, Canada.

## **UNIVERSAL IMAGING**

299 Adams Street

Bedford Hills, NY 10507

Phone: 1-800-842-0607

Fax: 914-666-2454

Email: [pbrunelli@UniversalUltrasound.com](mailto:pbrunelli@UniversalUltrasound.com)

Website: <http://www.universalultrasound.com>

Universal Ultrasound has been the leading supplier of veterinary ultrasound for over 36 years. We have partnered with over 16,000 veterinarians to bring affordable imaging diagnostics into their practices. Universal Ultrasound offers the largest variety of ultrasound and digital radiography packages for both beginning and advanced users, featuring all digital technology, portability, veterinary specific applications, complete connectivity, PACS and comprehensive training. Our technology partners include Toshiba, Sedecal, Fuji, Canon, Sonocape and more. See the difference veterinary imaging can make in your practice today.

Universal Ultrasound has partnered with over 16,000 veterinarians to bring affordable imaging diagnostics into their practices. Universal offers a variety of packages for both beginning and advanced users, featuring all digital technology, portability, veterinary specific applications, complete connectivity, PACS and comprehensive training.

## **UNIVERSAL MEDICAL SYSTEMS, INC.**

D.R. Zavagno

29500 Aurora Road, Unit 16

Solon, OH 44139

Phone: 440-349-3210

Fax: 440-498-2188

Website: [www.veterinary-imaging.com](http://www.veterinary-imaging.com)

Universal Medical Systems, Inc. (Ohio) is the only LICENSED AUTHORIZED DISTRIBUTOR serving the veterinary market selling CT and MRI scanners exclusively from Toshiba, Esaote, Neurologica and Philips designed specifically to meet your needs. New or certified systems are available with a variety of financing and service options. Visit us today.

## **VETEL DIAGNOSTICS**

4850 Davenport Creek Road

San Luis Obispo, CA 93401

Phone: 1-800-458-8890

Fax: 805-549-9237

Email: [info@veteldiagnostics.com](mailto:info@veteldiagnostics.com)

Website: [www.veteldiagnostics.com](http://www.veteldiagnostics.com)

Vetel Diagnostics is a diagnostic imaging company devoted exclusively to the veterinarian. With imaging tools including Flat Panel and Computed Radiography, Ultrasound, Dental Digital Radiography, CT /MRI, and Thermography, Vetel offers specific solutions for every veterinarian. Imaging software, PACS, data archival and after sale support complete your diagnostic imaging needs. Vetel Diagnostics, for a Better Look Inside.

## **VET RAY TECHNOLOGY BY SEDECAL**

230 Lexington Drive

Buffalo Grove, IL 60089

Phone: 847-394-6960

Fax: 847-394-6966

Website: [www.vetray.com](http://www.vetray.com)

Vet Ray Technology by Sedecal, is the world's largest manufacturer of Veterinary specific x-ray equipment. Vet Ray Technology has the top selling small animal table for both digital and film applications and supplies a wide variety of large animal products ranging from Over Head Tube Cranes to portable digital equipment.

## **VIN**

Phone: 1-800-700-4636

Email: [VINGRAM@vin.com](mailto:VINGRAM@vin.com).

Website: [www.VIN.com](http://www.VIN.com)

The Veterinary Information Network (VIN) is the premier online community, continuing education, and information resource for veterinarians. Founded in 1991, VIN reaches over 45,000 veterinarians, veterinary students, and industry partners worldwide. VIN is the leader in unlimited access to medical, product and practice management information. For a FREE one month trial membership, join us at [www.VIN.com](http://www.VIN.com), phone 800-700-4636, or email [VINGRAM@vin.com](mailto:VINGRAM@vin.com). Let us show you why VIN is the BEST online resource for veterinarians. VIN will provide a free cyber café at the ACVR Annual Conference, so please stop by to check your Email, surf the web, and try VIN!

# American College of Veterinary Radiology

## Special Thanks to the following Corporate Partners:

2011 Conference Bag Sponsor  
CoActiv PACS 4 Vets

Badge Neck Lanyard Sponsor  
Universal Imaging

Cyber Café  
Veterinary Information Network (VIN)

ACVR Reception Sponsors  
Universal Medical Systems, Inc.

Lunch Sponsor  
Orthopedic Foundation for Animals

***Program Overview***  
**2011 ACVR Scientific Meeting**  
**October 11-14, 2011**  
**Hyatt Regency**  
**Albuquerque, NM**

**Monday, October 10, 2011**

8:30 am – 5:00 pm **Interventional Radiology Laboratory: Tracheal and Urethral Stenting**  
Sponsored by Infiniti Medical  
**Off-Site Location**

**Tuesday, October 11, 2011**

7:00 am	<i>Registration opens</i>	Pavilion Landing
8:00 am	<u>Special Guest Speaker</u> <b>Innovation and Veterinary Medicine: Interventional Radiology as a Template for Change and What This Means to You</b> Dr. Jeffrey Solomon	Pavilion IV - VI
9:00 am	<u>ACVR Forum</u> <b>Current Trends in and Uses of CT in Veterinary Medicine</b> A Roundtable Discussion	
9:00 am	<b>Lumbosacral Disease</b> Dr. Jeryl Jones	
10:00 am	<i>Break</i>	
10:15 am	<b>Abdominal Disease</b> Dr. Gabrielle Seiler	
11:15 am	<b>Respiratory Tract Imaging</b> Dr. Robert O'Brien	
12:15 pm	<i>Lunch</i>	Back of Pavilion IV - VI
1:15 pm	<b>Dynamic Vascular Imaging</b> Dr. Allison Zwingenberger	
2:15 pm	<b>Detector Design</b> Dr. Tobias Schwartz	
3:15 pm	<i>Break</i>	
3:30 pm	<b>Large Animal Imaging</b> Dr. Peter Scrivani	
4:30 pm	<b>Question and Answer Panel</b>	
5:00 pm	<i>Adjourn for the Day</i>	

**Wednesday, October 12, 2011**

7:00 am	<i>Registration opens</i>	Pavilion Landing
7:00 am	Veterinary Ultrasound Society Meeting	Pavilion IV - VI
8:00 am	<b>2011 ACVR Meeting Opening Welcome</b> Dr. Jay Stefanacci, Program Chair	
8:15 am	<b>ACVR President's Address</b> Dr. Val Samii	
8:45 am	Resident Authored Paper Award	
9:00 am	<u>ACVR Keynote Address</u> <b>ACVR 2011: Time to Kick the Tires</b> Dr. Donald Thrall	
10:00 am	<i>Break with Exhibitors</i>	Pavilion I - III
10:30 am	Radiology Scientific Session	
12:00 pm	<i>Lunch</i>	Sendero Ballroom
1:00 pm	<u>Ultrasound Keynote Address</u> <b>Advanced and Interventional Equine Sonography</b> Dr. Natasha Werpy	
2:00 pm	Ultrasound Scientific Session 1	
2:30 pm	<i>Break with Exhibitors</i>	Pavilion I - III
3:00 pm	Ultrasound Scientific Session 2	
5:00 pm	<i>Adjourn for the Day</i>	
5:30 pm	Meet with the Residency Directors	Pavilion IV - VI
6:30 pm	<i>ACVR Welcome Reception</i>	Sendero Ballroom

**Thursday, October 13, 2011 (ACVR and RO simultaneous sessions)**

**ACVR**

7:00 am	<i>Registration opens</i>	Pavilion Landing
7:00 am	Society of Veterinary Nuclear Medicine Meeting	Pavilion IV - VI
8:00 am	<u>Nuclear Medicine Roundtable Discussion:</u> <b>Feline Hyperthyroidism—Diagnosis and Treatment...Where Are We?</b> Panelists: Dr. Greg Daniel Dr. Peter Scrivani Dr. Seth Wallack Dr. David Herring	
9:30 am	Nuclear Medicine Scientific Session	
10:30 am	<i>Break with Exhibitors</i>	Pavilion I - III
11:00 am	Meet the New Diplomates	
12:00 pm	<i>Lunch</i>	Sendero Ballroom
1:00 pm	Image Interpretation Session	Pavilion IV - VI
2:30 pm	<i>Break with Exhibitors</i>	Pavilion I - III
3:00 pm	ACVR Business Meeting	Pavilion IV - VI
5:00 pm	<i>Adjourn for the Day</i>	
5:00 pm	LADIS Meeting	Pavilion IV - VI

**RO**

8:00 am	VRTOG/RO Scientific Session 1	Enchantment A - D
10:30 am	<i>Break with Exhibitors</i>	Pavilion I - III
11:00 am	VRTOG/RO Scientific Session 2	
12:00 pm	<i>Lunch</i>	Sendero Ballroom
1:00 pm	Image Interpretation Session	Pavilion IV - VI
2:30 pm	<i>Break with Exhibitors</i>	Pavilion I - III
3:00 pm	ACVR Business Meeting	Pavilion IV - VI
5:00 pm	<i>Adjourn for the Day</i>	
5:00 pm	LADIS Meeting	Pavilion IV - VI

**Friday October 14, 2011 (ACVR and RO simultaneous sessions)**

**ACVR**

7:00 am	CT/MRI Society Meeting	Pavilion IV - VI
7:30 am	<i>Registration opens</i>	Pavilion Landing
8:00 am	<u>CT/MRI Society Keynote Address</u> <b>Applications of MRI in Human Orthopedic Sports Medicine</b> Charles P. Ho, PhD, MD, Director of Imaging Research, Steadman Philippon Research Institute, Vail, CO	
9:00 am	CT/MRI Scientific Session 1	
10:30 am	<i>Break with Exhibitors</i>	Pavilion I - III
11:00 am	CT/MRI Scientific Session 2	
12:00 pm	<i>Lunch</i>	Sendero Ballroom
1:00 pm	Poster Session	Pavilion Court
1:30 pm	Large Animal Diagnostic Imaging Society (LADIS) Scientific Session 1	
3:00 pm	<i>Break with Exhibitors</i>	Pavilion I - III
3:30 pm	LADIS Scientific Session 2	
5:00 pm	<i>Adjourn for the Day</i>	

**RO**

8:00 am	<u>Radiation Oncology Keynote Address</u> Dr. Phillip Devlin, Radiation Oncologist from Brigham and Women's Hospital	Enchantment A - D
10:30 am	<i>Break with Exhibitors</i>	Pavilion I - III
11:00 am	VRTOG Society Meeting	
12:00 pm	<b>Lunch/Welcome New Diplomates/RO Business Meeting</b> Get buffet lunch at Sendero Ballroom, then take it to Enchantment A - D	
1:30 pm	Radiation Oncology Scientific Session 3 <b>Round Table Discussion--TBA</b>	
3:30 pm	<i>Adjourn for the Day (VRTOG/RO)</i>	

**Monday, October 10, 2011**

8:30 am – 5:00 pm **Interventional Radiology Laboratory: Tracheal and Urethral Stenting**  
Sponsored by Infiniti Medical  
**Off-Site Location**

**Tuesday, October 11, 2011**

7:00 am	<i>Registration opens</i>	Pavilion Landing
8:00 am	<u>Special Guest Speaker</u> <b>Innovation and Veterinary Medicine: Interventional Radiology as a Template for Change and What This Means to You</b> Dr. Jeffrey Solomon	Pavilion IV - VI
9:00 am	<u>ACVR Forum</u> <b>Current Trends in and Uses of CT in Veterinary Medicine</b> A Roundtable Discussion	
9:00 am	<b>Lumbosacral Disease</b> Dr. Jeryl Jones	
10:00 am	<i>Break</i>	
10:15 am	<b>Abdominal Disease</b> Dr. Gabrielle Seiler	
11:15 am	<b>Respiratory Tract Imaging</b> Dr. Robert O'Brien	
12:15 pm	<i>Lunch</i>	Back of Pavilion IV - VI
1:15 pm	<b>Dynamic Vascular Imaging</b> Dr. Allison Zwingenberger	
2:15 pm	<b>Detector Design</b> Dr. Tobias Schwartz	
3:15 pm	<i>Break</i>	
3:30 pm	<b>Large Animal Imaging</b> Dr. Peter Scrivani	
4:30 pm	<b>Question and Answer Panel</b>	
5:00 pm	<i>Adjourn for the Day</i>	

**Wednesday, October 12, 2011**

- 7:00 am     *Registration opens*     Pavilion Landing
- 7:00 am     Veterinary Ultrasound Society Meeting     Pavilion IV - VI
- 8:00 am     **2011 ACVR Meeting Opening Welcome**  
Dr. Jay Stefanacci, Program Chair
- 8:15 am     **ACVR Presidential Address**  
Dr. Val Samii
- 8:45 am     Resident Authored Paper Award
- 9:00 am     ACVR Keynote Address  
**ACVR 2011: Time to Kick the Tires**  
Dr. Donald Thrall
- 10:00 am     *Break with Exhibitors*     Pavilion I - III
- 10:30 am     **Radiology Scientific Session (Moderator: Dr. Allison Zwingenberger)**
- 10:30 am     **The Influence of Feeding Position on Esophageal Motility and Gastroesophageal Reflux in Dogs with Geriatric Onset Laryngeal Paralysis Polyneuropathy (GOLPP).**  
A.M. Adrian<sup>1</sup>, B. Stanley<sup>1</sup>, M. Fritz<sup>1</sup>, J. Hauptman, J.Kinns<sup>1,1</sup>SAS, Michigan State University, VTH, East Lansing, Michigan 48824, USA.
- 10:42 am     **Vertebral Heart Scores in Chondrodystrophic and Brachycephalic Breeds.**  
K. Jepsen-Grant, L.R. Johnson, R.E. Pollard, University of California-Davis School of Veterinary Medicine, California, 95616.
- 10:54 am     **Imaging Characteristics of Intrathoracic Histiocytic Sarcoma in Dogs.**  
S. Tsai, J. Sutherland-Smith, K. Burgess, R. Ruthazer, A. Sato. Tufts Cummings School of Veterinary Medicine, Massachusetts, 01536.
- 11:06 am     **Comparison Between Automatic Approach of the Vertebral Heart Size and Normalized Cardiac Area to Assess Left Atrial Enlargement in Poodles with Mitral Insufficiency.**  
G.P.R. Banon, A.C.B.C. Fonseca Pinto, G.J.F. Banon, C.O. Baroni, G.T. Goldfeder, A. Pellegrino. School of Veterinary Medicine and Animal Science, University of São Paulo, Brazil, 05508 270.
- 11:18 am     **Reducing Susceptibility Artifacts in Magnetic Resonance Images of The Post-Operative Canine Stifle.**  
F.H. David, J. Grierson, C. R. Lamb. The Royal Veterinary College University of London, Hertfordshire, AL9 7TA, UK.

**Wednesday, October 12, 2011, continued**

- 11:30 am **Computed Tomographic Signs of Lung Lobe Torsion in Dogs.**  
M.R. Gutman, P.V. Scrivani, M.S. Thompson, K.R. Winegardner, N.L. Dykes, D. Schmidt. Cornell University, College of Veterinary Medicine, Hospital for Animals, NY 14853.
- 12:00 pm *Lunch* Sendero Ballroom
- 1:00 pm Ultrasound Keynote Address  
**Advanced and Interventional Equine Sonography**  
Dr. Natasha Werpy
- 2:00 pm **Ultrasound Scientific Session 1 (Moderator: Dr. Kristina Miles)**
- 2:00 pm **Safety Of Contrast Enhanced Ultrasound in Dogs and Cats.**  
G.S. Seiler<sup>1</sup>, J. Brown<sup>1</sup>, J.A. Reetz<sup>2</sup>, O. Taeymans<sup>3</sup>, M. Bucknoff<sup>3</sup>, F. Rossi<sup>4</sup>, S. Ohlerth<sup>5</sup>, D. Alder<sup>5</sup>, N. Rademacher<sup>6</sup>, W.T. Drost<sup>7</sup>, R. Pollard<sup>8</sup>, O. Travetti<sup>9</sup>, P. Pey<sup>9</sup>, J. Saunders<sup>9</sup>, M. Shanaman<sup>10</sup>, C. Oliveira<sup>10</sup>, R.T. O'Brien<sup>10</sup>, L. Gaschen<sup>6</sup>. <sup>1</sup>North Carolina State University, NC 27607, <sup>2</sup>University of Pennsylvania, PA 19104, <sup>3</sup>Tufts University, MA 01536, <sup>4</sup>Clinica Veterinaria dell'Orologio, Italy 40037, <sup>5</sup>University of Zurich, Switzerland 8057, <sup>6</sup>Louisiana State University, LA 70803, <sup>7</sup>The Ohio State University, OH 43210, <sup>8</sup>University of California Davis, CA 95616, <sup>9</sup>Ghent University, Belgium 9820, <sup>10</sup>University of Illinois, IL 61802.
- 2:12 pm **Comet-Tail Artifacts in Normal Dogs and Dogs with Cardiogenic Pulmonary Edema.**  
N. Rademacher, R. Pariaut, J. Pate, C. Saelinger, L. Gaschen. Louisiana State University, School of Veterinary Medicine, Baton Rouge, LA.
- 2:30 pm *Break with Exhibitors* Pavilion I - III
- 3:00 pm **Ultrasound Scientific Session 2 (Moderator: Dr. Silke Hecht)**
- 3:00 pm **Contrast Harmonic Ultrasonography of the Normal and Diseased Feline Pancreas.**  
N. Rademacher, F. Gaschen, A. Royal, M. Kearney, L. Gaschen. Louisiana State University School of Veterinary Medicine, Louisiana, 70803.
- 3:12 pm **Association Between Hyperechoic Splenic Speckles and Stripes with Several Medical Conditions in 22 Dogs.**  
A.V. Caceres. University of Pennsylvania, Clinical Studies Department, Radiology Section, PA, 19104.
- 3:24 pm **Color and Power Doppler Ultrasonography for Characterization of Splenic Masses in Dogs.**  
J.L. Sharpley<sup>1</sup>, A.J. Marolf<sup>1</sup>, J.K. Reichle<sup>2</sup>, A. Bachand<sup>1</sup>, E.K. Randall<sup>1</sup>. <sup>1</sup>Colorado State University, College of Veterinary Medicine and Biomedical Sciences, Fort Collins, CO. 80523, and <sup>2</sup>Animal Surgical and Emergency Center, Los Angeles, CA. 90025.



## THE INFLUENCE OF FEEDING POSITION ON ESOPHAGEAL MOTILITY AND GASTROESOPHAGEAL REFLUX IN DOGS WITH GERIATRIC ONSET LARYNGEAL PARALYSIS POLYNEUROPATHY (GOLPP).

A.M. Adrian<sup>1</sup>, B. Stanley<sup>1</sup>, M. Fritz<sup>1</sup>, J. Hauptman, J.Kinns<sup>1,1</sup>SAS, Michigan State University, VTH, East Lansing, Michigan 48824, USA.

**Introduction/Purpose:** It has been shown that esophageal dysmotility is present in dogs with geriatric onset laryngeal paralysis polyneuropathy (GOLPP) syndrome. In addition to esophageal dysmotility, gastroesophageal reflux (GER) has been recorded in 62% of dogs with GOLPP syndrome when imaged in lateral recumbency. Esophageal motility has traditionally been assessed using esophagram evaluation with the dog in right lateral recumbency. It has recently been shown that esophageal transit time is delayed in normal dogs when in lateral compared to sternal recumbency. It is likely that esophageal transit patterns are also altered by feeding position in dogs with abnormal esophageal motility, and evaluation in lateral recumbency may misinterpret the degree of dysfunction present. The incidence of GER in a more natural standing or incline plane position in these dogs is also not known. Further it is a common clinical recommendation for dogs with esophageal dysmotility to be fed on an incline plane, with their thoracic limbs raised, though the degree to which this alters motility is unknown. This study therefore aimed to evaluate the effect of feeding position on esophageal transit time and gastroesophageal motility in affected animals.

**Methods:** Study esophagrams were obtained in random order in right lateral recumbency, standing, and on an incline plane. Positioning for standing and incline plane esophagrams was achieved using a custom built stanchion. A standardized slurry was fed and each bolus of food was followed from the pharynx to the stomach using video-fluoroscopy. The transit time from the pharynx to the thoracic inlet, the pharynx to the carina, the carina to the stomach and the total transit time were measured. The incidence and subjective severity of GER was recorded. Subjective scores of esophageal dysmotility were recorded based on a previously established scale.

**Results:** There is a significant influence of the feeding position on the esophageal function between the lateral and standing positions in dogs affected by GOLPP ( $P=0.0012$ ), except for the esophageal function from the level of the carina to the stomach. However no significant difference of the feeding position on the esophageal function between the standing and incline position ( $P=0.99$ ) was found. The feeding position has no influence on the subjective score of esophageal dysmotility, however does have a significant effect on the incidence of GER.

**Discussion/Conclusion:** The study shows an influence of the feeding position on esophageal motility between lateral recumbency and a standing position. No difference was found for the transit time from the carina to the stomach. This correlates with the innervation of the pararecurrent nerve, which is effected in dogs with GOLPP. Based on this study there is no advantage of feeding a dog with GOLPP in an incline plane compared to a standing position.

## VERTEBRAL HEART SCORES IN CHONDRODYSTROPHIC AND BRACHYCEPHALIC BREEDS.

K. Jepsen-Grant, L.R. Johnson, R.E. Pollard, University of California-Davis School of Veterinary Medicine, California, 95616.

**Introduction/Purpose:** The Vertebral Heart Score (VHS) measurement has been used to provide an objective assessment of heart size by expressing cardiac size in terms of vertebral body length. Several studies have shown differences in the range of VHS among various dog breeds. This study was designed to establish VHS measurements for chondrodystrophic and/or brachycephalic breeds.

**Methods:** Dogs from select breeds that did not have a heart murmur or gallop and had 2- view thoracic radiographs lacking subjective evidence of cardiomegaly were evaluated in random order. VHS and thoracic dimensions were measured from right lateral and dorsoventral radiographs using electronic calipers. VHS was compared among breeds using analysis of variance. A 2 sample t-test was used to compare breed specific VHS measurements to the reported value of normal dogs ( $9.7 \pm 0.5$ )

**Results:** Dogs evaluated included 30 Pugs, 18 Pomeranians, 30 Yorkshire Terriers, 29 Dachshunds, 30 Bulldogs (including French and English), 30 Shih Tzus, 18 Lhasa Apsos, and 19 Boston Terriers fitting the inclusion criteria. Mean VHS was significantly different among many breeds examined. VHS measurements for Pugs ( $10.7 \pm 0.9$ ), Pomeranians ( $10.5 \pm 0.9$ ), Bulldogs ( $12.7 \pm 1.7$ ) and Boston Terriers ( $11.7 \pm 1.4$ ) were significantly increased compared to the reported normal value.

**Discussion/Conclusion:** VHS measurements can be used to objectively determine heart size in dogs however breed specific standards must be used to account for disparities in breed conformation.

## **IMAGING CHARACTERISTICS OF INTRATHORACIC HISTIOCYTIC SARCOMA IN DOGS.**

S. Tsai, J. Sutherland-Smith, K. Burgess, R. Ruthazer, A. Sato. Tufts Cummings School of Veterinary Medicine, Massachusetts, 01536.

**Introduction/Purpose:** The distribution of lesions in dogs with thoracic histiocytic sarcoma has not previously been described. Diagnostic imaging plays an important role in the diagnosis and staging of histiocytic sarcoma. Distinguishing histiocytic sarcoma from other thoracic neoplasms is important both for more accurate diagnosis and prognosis, as well as to aid in recommending appropriate therapy and further imaging for staging. Our hypothesis was that the most common presentation of thoracic histiocytic sarcoma is one or more caudoventrally located pulmonary masses.

**Methods:** Two board certified radiologists retrospectively reviewed thoracic images from dogs identified with thoracic histiocytic sarcoma between 2004 and 2010. Diagnoses were confirmed with cytology or histology (tissue biopsy or necropsy). Images were evaluated for pulmonary masses, pulmonary nodules, abnormal pulmonary patterns, pleural effusion, and lymphadenopathy. Pulmonary masses were further characterized based on lung lobe of origin, and lymphadenopathy was further characterized by location (sternal, cranial mediastinal, tracheobronchial) and severity. The images were evaluated independently by the two observers, and interobserver agreement on the features above was determined by calculation of the kappa statistic. Both observers recorded additional descriptive information from the computed tomography (CT) studies: masses and enlarged lymph nodes were categorized as homogeneous or heterogeneous, and the degree of enhancement was recorded as mild, moderate, marked, or nonenhancing. Masses were further categorized as having well defined or poorly defined margins, as well as whether they surrounded a bronchus.

**Results:** Thirty-nine dogs were identified, of which 36 had three view thoracic radiographs and 13 had thoracic CT studies. The most common findings were intrathoracic lymphadenopathy (identified by the first and second observers in 82.1% and 87.2% of dogs, respectively) and pulmonary masses (74.4% and 82.1%). Right middle lung lobe masses were significantly more common than masses in any other lung lobe ( $P < 0.0013$ ), with the majority of masses generally having a ventral distribution. Sternal and tracheobronchial lymphadenopathy were significantly more common than cranial mediastinal lymphadenopathy ( $P$  values of 0.0002 and 0.012, respectively). Interobserver agreement regarding distribution of lymphadenopathy and pulmonary masses was good ( $\kappa = 0.64$  and 0.75, respectively).

**Discussion/Conclusion:** The most striking finding in this study was that half of all pulmonary masses were located in the right middle lung lobe with other locations distributed fairly evenly among the remaining lung lobes (with the exception of the accessory lung lobe). This finding provides a characteristic distribution of histiocytic sarcoma that can aid in distinguishing this disease from primary lung tumors. The majority of masses on CT were noncavitated, surrounded a bronchus, were poorly margined, and exhibited mild to moderate heterogeneous contrast enhancement.

## COMPARISON BETWEEN AUTOMATIC APPROACH OF THE VERTEBRAL HEART SIZE AND NORMALIZED CARDIAC AREA TO ASSESS LEFT ATRIAL ENLARGEMENT IN POODLES WITH MITRAL INSUFFICIENCY.

G.P.R. Banon, A.C.B.C. Fonseca Pinto, G.J.F. Banon, C.O. Baroni, G.T. Goldfeder, A. Pellegrino. School of Veterinary Medicine and Animal Science, University of São Paulo, Brazil, 05508 270.

**Introduction/Purpose:** Left atrial enlargement (LAE) is the earliest and most consistent radiographic finding of mitral regurgitation. According to the vertebral heart size (VHS) method, the maximal cardiac short axis is measured in the central third region, which might not include LAE. Normalized cardiac area (NCA), however, considers the contours of cardiac silhouette. The aim of this study was to compare the efficacy of VHS and NCA in radiographic diagnosis of LAE.

**Methods:** Thoracic radiographs of Poodles were allotted to five groups: (I) normal cardiopulmonary structures ( $n=18$ ), (IIa) mild ( $n=4$ ), (IIb) moderate ( $n=7$ ), (IIc) severe ( $n=28$ ) and (IId) absent ( $n=17$ ) LAE. These LAE were confirmed by echocardiography to be caused by mitral insufficiency. Measurements were performed by one experienced veterinary radiologist in right lateral view, using computing techniques that permit to obtain automatically the VHS and NCA results. For VHS and NCA measurements in each group, the mean, the standard deviation (SD) and 95% confidence interval ( $CI_{(\mu, 0.95)}$ ) were calculated. The VHS and NCA means for group I were compared with respective means of three other groups with LAE by using Student's unpaired t test. The kappa test was used to test the agreement between VHS or NCA and echo in heart enlargement diagnosis. Pearson correlation coefficients ( $R$ ) were measured to evaluate the linear relationship between VHS or NCA and Ao/LA ratio. All analyses were carried out at the 5% significance level.

**Results:** In groups I, IIa, IIb and IIc, respectively, the VHS had a mean  $\pm$  SD of  $9.9 \pm 0.5v$ ,  $10.4 \pm 0.4v$ ,  $10.6 \pm 0.6v$  and  $12 \pm 1.4v$ , and a  $CI_{(\mu1, 0.95)}=[9.7; 10.1]$ ,  $CI_{(\mu2a, 0.95)}=[9.8; 10.9]$ ,  $CI_{(\mu2b, 0.95)}=[10; 11.2]$  and  $CI_{(\mu2c, 0.95)}=[11.5; 12.6]$ . In groups I, IIa, IIb and IIc, respectively, the NCA had a mean  $\pm$ SD of  $18.9 \pm 1.8v^2$ ,  $20.6 \pm 1.5v^2$ ,  $22.3 \pm 3.3v^2$  and  $28.6 \pm 6.5v^2$ , and a  $CI_{(\mu1, 0.95)}=[18; 19.7]$ ,  $CI_{(\mu2a, 0.95)}=[18.2; 22.9]$ ,  $CI_{(\mu2b, 0.95)}=[19.3; 25.4]$  and  $CI_{(\mu2c, 0.95)}=[26; 31.1]$ . For the VHS and NCA means, there were significant differences between the following groups: I and IIa ( $P < 0.05$  and  $P < 0.05$ ); I and IIb ( $P < 0.05$  and  $P = 0.001$ ), and I and IIc ( $P < 0.001$  and  $P < 0.001$ ). The values of kappa showed a moderate ( $\kappa = 0.46$  and  $\kappa = 0.45$ ) strength of agreement, respectively, between VHS or NCA and echo. The correlation coefficients ( $R = -0.66$  and  $R = -0.65$ ) showed that there was a significant linear relationship ( $P < 0.001$ ), respectively, between VHS or NCA and Ao/LA ratio.

**Discussion/Conclusion:** The automatic approach proved adequate for an easy practical application. The determination of NCA includes all the data carried out by VHS and enjoys some few advantages in terms of accuracy to establish LAE.

**Acknowledgement:** The authors would like to thank Fapesp for financial support.

## REDUCING SUSCEPTIBILITY ARTIFACTS IN MAGNETIC RESONANCE IMAGES OF THE POST-OPERATIVE CANINE STIFLE.

F.H. David, J. Grierson, C. R. Lamb. The Royal Veterinary College University of London, Hertfordshire, AL9 7TA, UK.

**Introduction/Purpose:** Magnetic resonance (MR) images of the canine stifle are adversely affected by susceptibility artifacts associated with metallic implants. The Tibial Plateau Leveling Osteotomy (TPLO) implant produces artifacts that obscure most stifle anatomy. Tibial Tuberosity Advancement (TTA) and Extra-capsular Stabilization (ECS) implants produce less extensive artifacts that may allow the cruciate ligaments and medial meniscus to be evaluated satisfactorily. The purpose of the present study was to determine to what extent susceptibility artifacts could be reduced by modifications to MR sequences.

**Methods:** Three cadaver limbs with a TPLO, TTA or ECS implant were imaged at 1.5T. Series of proton density and T2-weighted images were acquired in both sagittal and dorsal planes with a changing variable, and ranked by a blinded observer according to the size of susceptibility artifact. Images were obtained with different combinations of frequency-encoding gradient (FEG) orientation, fat shift (FS) direction, and stifle flexion or extension. The highest ranked combination of these variables was then used for images obtained with different echo spacing (ES) (12, 16, 20, 24 ms) and readout bandwidth (BW) (51, 66, 82 kHz). Paired data were tested using the Wilcoxon signed-ranks test. ES and BW data were tested using Friedman's test.

**Results:** The most significant effects on image ranking were observed for FS ( $p=0.005$ ), stifle flexion ( $p=0.01$ ), and BW ( $p=0.0001$ ). For TPLO and TTA implants, highest ranked images were obtained with the stifle flexed, lateromedial FEG, and medial FS for dorsal images, and craniocaudal FEG and caudal FS for sagittal images. For the ECS implant, highest ranked images were obtained with the stifle extended, a proximodistal FEG and proximal FS for dorsal images, and craniocaudal FEG and cranial FS for sagittal images. There was a trend for higher image ranking with smaller ES ( $p=0.2$ ). Wider BW was associated with reduced susceptibility artifact ( $p=0.001$ ).

**Discussion/Conclusion:** Susceptibility artifacts in MR images of post-operative canine stifles may be reduced significantly by adjustments to technique. As expected based on previous studies, aligning the FEG perpendicular to the long axis of the implants reduced the susceptibility artifact associated with TPLO and TTA implants; however, the complex lobed shape of the artifact contributed variability to results, and in some instances parts of the stifle joint were better visualized with the FEG parallel to the implants and tibia. Stifle flexion tended to move the artifact associated with TPLO and TTA away from critical structures, which improved images despite this placing the long axis of these implants at an oblique angle the main magnetic field ( $B_0$ ) when artifacts are usually reported to be smaller when metallic implants are parallel to  $B_0$ . Smaller ES tends to reduce size of susceptibility artifacts and enables shorter scan times. Wider bandwidth significantly reduced the susceptibility artifact. A potential drawback of wide bandwidth is decreased signal to noise ratio; however, this was not perceived with the bandwidths values used in this study.

## **COMPUTED TOMOGRAPHIC SIGNS OF LUNG LOBE TORSION IN DOGS.**

M.R. Gutman, P.V. Scrivani, M.S. Thompson, K.R. Winegardner, N.L. Dykes, D. Schmidt. Cornell University, College of Veterinary Medicine, Hospital for Animals, NY 14853.

**Introduction/Purpose:** Several case reports are available that describe the radiographic and computed tomography (CT) signs, and frequency of signs, of lung-lobe torsion in dogs. Although some of the patterns of signs are fairly indicative of lung-lobe torsion, other findings are common to many diseases and the diagnosis of lung-lobe torsion therefore remains challenging. Lung-lobe torsion is relatively rare and the number of reported cases is low, which may give a false impression of the frequency of certain signs or may not describe the full range of possible findings. The aims of this study are to describe the CT signs of lung-lobe torsion in an additional group of dogs to better estimate frequency of signs, and to identify new signs if possible.

**Methods:** For this case report, the sample population included all dogs that underwent thoracic CT at the Cornell University Hospital for Animals between July 1999 and February 2009, and were diagnosed with lung-lobe torsion during surgery or necropsy. Surgery was performed within at least 2 days of CT. The medical record was reviewed for patient signalment, duration, and type of clinical signs, surgical or necropsy diagnosis, location of lung-lobe torsion, and other surgical or post mortem finding. Thoracic CTs were examined for the following signs: pleural fluid, lung attenuation, lobe size, abnormal position of lung lobe, abrupt ending bronchus, emphysema, and pneumothorax.

**Results:** Lung-lobe torsion was diagnosed in 7 dogs including 3 neutered males, 2 intact males, and 2 neutered females. The mean age was 6 years (range, 3mo. to 10 years). Breeds included 1 Italian Greyhound, 1 Pug, 1 Chihuahua, and 1 Pekingese, as well as 3 mixed breeds. All 7 dogs had pleural fluid and increased lung attenuation. Similar to previous reports, a pattern of an enlarged, consolidated lung lobe with a narrowed or abruptly terminating bronchus was identified in 3/7 dogs. Of these, 2/3 had emphysematous accumulations. In 4/7 dogs, the common pattern of lung lobe torsion, including an abruptly terminating bronchus and emphysematous accumulation, was not seen and lung lobe torsion was not diagnosed pre-operatively.

**Discussion/Conclusion:** Lung-lobe torsion is a rare diagnosis, and accurate diagnosis of this disease is imperative as surgery is curative. Understanding the frequency of certain signs in a larger number of dogs is important. The results of this study add to what is previously reported. Some of the more specific signs may be insensitive as they are infrequent. Diagnosis of this disease remains challenging due its variable appearance. The various pitfalls of its diagnosis will be discussed.

## **SAFETY OF CONTRAST ENHANCED ULTRASOUND IN DOGS AND CATS.**

G.S. Seiler<sup>1</sup>, J. Brown<sup>1</sup>, J.A. Reetz<sup>2</sup>, O. Taeymans<sup>3</sup>, M. Bucknoff<sup>3</sup>, F. Rossi<sup>4</sup>, S. Ohlerth<sup>5</sup>, D. Alder<sup>5</sup>, N. Rademacher<sup>6</sup>, W.T.Drost<sup>7</sup>, R. Pollard<sup>8</sup>, O. Travetti<sup>9</sup>, P. Pey<sup>9</sup>, J. Saunders<sup>9</sup>, M. Shanaman<sup>10</sup>, C. Oliveira<sup>10</sup>, R.T. O'Brien<sup>10</sup>, L. Gaschen<sup>6</sup>. <sup>1</sup>North Carolina State University, NC 27607, <sup>2</sup>University of Pennsylvania, PA 19104, <sup>3</sup>Tufts University, MA 01536, <sup>4</sup>Clinica Veterinaria dell'Orologio, Italy 40037, <sup>5</sup>University of Zurich, Switzerland 8057, <sup>6</sup>Louisiana State University, LA 70803, <sup>7</sup>The Ohio State University, OH 43210, <sup>8</sup>University of California Davis, CA 95616, <sup>9</sup>Ghent University, Belgium 9820, <sup>10</sup>University of Illinois, IL 61802.

**Introduction/Purpose:** Microbubble ultrasound contrast media increase the sensitivity and specificity of ultrasound imaging and are increasingly used in veterinary imaging. No complications in dogs or cats have been reported in the literature, however the true occurrence of adverse events is unknown. Accurate information about potential risks is important when educating pet owners and veterinarians about this diagnostic method. The purpose of this study was to perform a representative multicenter survey on adverse effects observed after contrast-enhanced ultrasound (CEUS).

**Methods:** Multiple imaging centers were invited to participate in this study. Investigators were asked to retrospectively search the medical records and enter data of all dogs and cats that had received CEUS. The survey collected demographic patient data, information about pre-existing conditions, indications, contrast agent type, dose and route of administration, occurrence of immediate and late adverse reactions including death within 24 hours, diagnosis and known survival time after the contrast study. Investigators were also asked to enter data of a control group of patients that had ultrasound without CEUS for the same or similar indications. Descriptive statistics were performed using statistical software (SAS®v.9.2). Risk ratios were calculated compared with the control group.

**Results:** Information about 627 dogs and 101 cats was collected in this survey. CEUS was performed in 480 animals (403 dogs, 77 cats), 248 were controls (224 dogs, 24 cats). All CEUS examinations included intravenous bolus injections of contrast medium; five different contrast agents were used. Of the dogs receiving CEUS, 4 (0.99%) were reported to have potential adverse reactions, 3 within 1 hour of CEUS, and 1 within 24 hours. Reactions included vomiting (3), and collapse (1). All reactions were single transient episodes that did not require treatment. None of the cats had adverse reactions. Death within 24 hours was reported in 24/480 (5%) animals receiving CEUS and 14/248 (5.6%) control animals. This results in a risk ratio for dying within 24 hours of CEUS of 0.89 (95% CI=0.47-1.68) compared with the control group (p=0.7).

**Discussion/Conclusion:** CEUS was determined to be a safe imaging method in dogs and cats; the rate of potential adverse reactions was lower compared with other contrast studies commonly used in veterinary diagnostic imaging. None of the adverse reactions were severe. The relative risk of dying after CEUS was not significantly different from a control group.

## COMET-TAIL ARTIFACTS IN NORMAL DOGS AND DOGS WITH CARIOGENIC PULMONARY EDEMA.

N. Rademacher, R. Pariaut, J. Pate, C. Saelinger, L. Gaschen. Louisiana State University, School of Veterinary Medicine, Baton Rouge, LA.

**Introduction/Purpose:** Pulmonary edema is the most common complication of congestive heart failure in dogs. Interstitial pulmonary edema, which usually precedes more severe alveolar edema, may not be radiographically detectable. In human medicine, transthoracic ultrasonography is used to detect narrow repetition artifacts, or comet-tail artifacts, that indicate the presence of edema in the lung. The hypothesis of this study is that comet-tail artifacts can be identified using ultrasonography in dogs with cardiogenic pulmonary edema, and that these artifacts occur in greater numbers and are more widely distributed in dogs with congestive heart failure than in normal dogs.

**Methods:** Transthoracic ultrasonography was performed in a normal group of clinically healthy dogs and dogs with heart failure with radiographic and echocardiographic signs of congestive heart failure. Physical examination, two-view thoracic radiographs, two-dimensional and Doppler transthoracic echocardiogram and heartworm antigen test were performed on all dogs. During ultrasonography, dogs were gently restrained in a standing or seated position. The thorax was divided into 4 quadrants on each side, and video clips and still images of each quadrant were recorded. Distribution, characteristics and number of comet-tails were determined using Qlab software (Philips Healthcare, Bothell, WA). Statistical analysis was performed using SAS software version 9.1.3 (SAS Institute, Cary, NC).

**Results:** 31 dogs were recruited in the normal group and 9 dogs were included in the heart failure group. Transthoracic ultrasonography was easily and quickly performed on all dogs, with an average examination time of ten minutes or less. Comet-tails were detected in 32% of the normal dogs, with a mean of 2 per dog. No statistical association was found between the variables age, sex, side and distribution using a phi correlation coefficient. Subjectively, in dogs with cardiogenic pulmonary edema, comet-tails occurred in greater numbers and were more widely distributed. In severe cases, comet-tail artifacts were so numerous that they became confluent and obscured the borders of the pleura. The presence of artifacts was consistent with the distribution of edema on radiographs.

**Discussion/Conclusion:** Artifacts are rare and isolated in normal dogs, but numerous and widely distributed in dogs with congestive heart failure, as has been described in human patients. Further studies are needed to determine if the number and distribution of comet-tail artifacts in dogs with pulmonary edema correlates with the severity of clinical and radiographic signs. Thoracic ultrasonography is a fast, easy, and effective method to characterize pulmonary edema in dogs with mitral valve disease. It may provide additional information in combination with traditional diagnostic tests for the assessment of dogs with heart failure, the most important being the detection of early signs of heart failure and monitoring of the response to treatment.

## **CONTRAST HARMONIC ULTRASONOGRAPHY OF THE NORMAL AND DISEASED FELINE PANCREAS.**

N. Rademacher, F. Gaschen, A. Royal, M. Kearney, L. Gaschen. Louisiana State University School of Veterinary Medicine, Louisiana, 70803.

***Introduction/Purpose:*** The ante mortem diagnosis of feline pancreatic diseases is difficult, as clinical abnormalities and routine non-invasive diagnostic tests are unreliable. B-mode ultrasound (US) is very sensitive in detecting abnormalities of the pancreas but differentiation of various diseases is difficult. Contrast harmonic imaging is being increasingly used as an advanced approach for the clinical assessment of liver, splenic and kidney disease in small animals and humans. Contrast harmonic ultrasound improves the detection of tissue perfusion as well as organ and lesion vascular patterns. The purpose of this study is to quantify normal perfusion dynamics of the feline pancreas and detect abnormal patterns in cats with pancreatic disease.

***Methods:*** Nine normal cats and 8 cats with signs of pancreatic disease were selected based on physical examination, abdominal ultrasound, and blood work consisting of CBC, chemistry panel and fPLI. A contrast study was performed twice after injecting 0.1 ml of Definity® (Bristol-Myers Squibb, New York) contrast medium i.v. followed by 2 ml heparinized saline flush. Data analysis was performed using time-intensity curves created by Q-lab advanced ultrasound quantification software version 6.0 (Philips Ultrasound, Bothel, WA). The following was compared between normal and abnormal cats: peak pixel intensity, time to peak wash in rates, arrival time. Statistical analysis was performed using SAS software version 9.1.3 (SAS Institute, Cary, NC).

***Results:*** Subjectively, a difference was seen between the 2 groups of cats with heterogeneous contrast enhancement noted in all diseased cats with increased pixel intensity in the majority of cats. Homogeneous early, mild to moderate enhancement was seen as the normal pattern in the feline pancreas. All diseased cats had elevation of fPLI and changes of the pancreas on ultrasound. Three cats had neoplastic lesions associated with the pancreas (2 neuroendocrine tumors and one sarcoma). No statistical significant difference was found in any of the parameters in between groups.

***Discussion/Conclusion:*** Significant differences were observed in perfusion patterns between normal cats and cats with pancreatic disease. Contrast enhanced ultrasound is a feasible and effective method for the evaluation of pancreatic diseases in cats. This method may have future potential for improving diagnosing feline pancreatitis and differentiating neoplastic and benign diseases.

## **ASSOCIATION BETWEEN HYPERECHOIC SPLENIC SPECKLES AND STRIPES WITH SEVERAL MEDICAL CONDITIONS IN 22 DOGS.**

A.V. Cáceres. University of Pennsylvania, Clinical Studies Department, Radiology section, PA, 19104.

**Introduction/Purpose:** Hyperechoic speckles and lines throughout the spleen were occasionally identified on abdominal ultrasonography in dogs. The cause and significance of this finding have not been reported. The purpose of this study was to correlate their presence with medical conditions in dogs.

**Methods:** A prospective study of patients having ultrasonographic findings of diffuse hyperechoic splenic speckles and stripes was performed. Clinical and laboratory data from affected patients was reviewed to determine final diagnosis based on blood work and clinical history.

**Results:** Dogs age ranged from 3 to 19 years. Thirteen different breeds were affected. Eleven (50%) of the dogs were diagnosed with Cushing's Syndrome (CS), eight (36%) with Diabetes Mellitus (DM), four (18%) with chronic steroid use, two (9%) with Immune Mediated Hemolytic Anemia (IMHA), one of each (4%) with hepatic carcinoma, hepatic adenoma with fibrosis, hypercholesterolemia-hypertriglyceridemia. Five (23%) of the dogs had concurrent DM and CS and one (4%) of the dogs had concurrent IMHA and CS. After adding the CS and chronic steroid use groups the number increased to fifteen (68%). Necropsy performed in four dogs found diffuse hemosiderosis and multifocal siderofibrotic plaques in all dogs, parenchyma mineralization in two dogs and tunica media-intima mineralization in two dogs.

**Discussion/Conclusion:** Similar ultrasonographic findings in humans were found to represent siderofibrotic plaques,<sup>1</sup> perivascular fibrosis<sup>2</sup> and tunica media calcification (Monckeberger's arteriosclerosis).<sup>3</sup> Calcification of the tunica intima and media has been associated with CS and DM in humans.<sup>4</sup> Hyperechoic speckles and stripes in the spleen are occasionally identified in dogs and when seen, it is most commonly associated with CS, DM and chronic steroid use, less frequently is seen in patients with liver disease and IMHA. This ultrasonographic finding should raise a red flag for the above mentioned medical conditions.

### References

1. Bhatt S, Simon R, Dogra VS. Gamna-gandy bodies: Sonographic features with histopathologic correlation. J Ultrasound Med. 2006 Dec;25(12):1625-9.
2. Gillott TJ, Mantle M, Rai A. Splenic perivascular fibrosis as an ultrasound finding. J R Soc Med. 1999 Oct;92(10):532-3.
3. Parks A, Russ P, Bieker T, Stamm ER. Monckeberg's arteriosclerosis of the liver and spleen demonstrated by ultrasound. JDMS. 2001 July/August;17(4):225-9.
4. Takemura A, Iijima K, Ouchi Y. Molecular mechanism of vascular aging: Impact of vascular smooth muscle cell calcification via cellular senescence. Clin Calcium. 2010 Nov;20(11):1646-55.

## COLOR AND POWER DOPPLER ULTRASONOGRAPHY FOR CHARACTERIZATION OF SPLENIC MASSES IN DOGS.

J.L. Sharpley<sup>1</sup>, A.J. Marolf<sup>1</sup>, J.K. Reichle<sup>2</sup>, A. Bachand<sup>1</sup>, E.K. Randall<sup>1</sup>. <sup>1</sup>Colorado State University, College of Veterinary Medicine and Biomedical Sciences, Fort Collins, CO. 80523, and <sup>2</sup>Animal Surgical and Emergency Center, Los Angeles, CA. 90025.

**Introduction/Purpose:** Splenic masses are a common ultrasonographic finding in dogs. Benign and malignant splenic masses can have similar B-mode imaging features, making ultrasound sensitive but not specific in their diagnosis. The goal of this study was to find color and/or power Doppler characteristics of vasculature within and adjacent to a splenic mass which would distinguish a benign versus malignant lesion. The hypothesis was that malignant splenic masses will have altered vascular patterns compared with benign masses.

**Methods:** This was a prospective study of dogs with an ultrasound finding of a splenic mass at least 2 cm in any dimension. Color and power Doppler cineloops evaluating the vasculature within the mass and in adjacent normal splenic parenchyma were obtained in sagittal and transverse imaging planes using a standardized protocol. Cineloops were reviewed independently by one board-certified radiologist and one resident unaware of the final diagnosis. If a discrepancy occurred, cineloops were re-evaluated adding a second board-certified radiologist to reach a consensus opinion. Categories of evaluation included presence of peritoneal effusion, presence of a large aberrant or tortuous vessel within the mass, relative blood flow within the mass compared with normal parenchyma, and path of vessels in the adjacent parenchyma entering into the mass. All patients had histopathologic or definitive cytologic diagnosis of the mass. Fisher's exact test was used to investigate potential associations between vascular patterns of splenic masses and malignancy.

**Results:** Twenty-six dogs were included. There were 10 malignant masses (hemangiosarcoma, lymphoma, malignant histiocytosis, high grade sarcoma, mast cell tumor, malignant neoplasia of splenic stroma) and 16 benign lesions (hematoma, lymphoid hyperplasia, extramedullary hematopoiesis, no cytologic abnormalities). Peritoneal effusion was significantly associated with malignancy ( $p=0.0038$ ). Presence of an aberrant or tortuous vessel within the mass was borderline significant ( $p=0.0549$ ). There was no significant difference in any of the color or power Doppler blood flow evaluations.

**Discussion/Conclusion:** Ultrasonographic findings of a splenic mass and peritoneal effusion may indicate malignancy. The presence of an aberrant vessel within a splenic mass could suggest malignancy, however further investigation to determine true significance is needed. Color and power Doppler evaluation of blood flow of splenic masses cannot distinguish between benign and malignant lesions.

## **ULTRASOUND-GUIDED STANDING CERVICAL CENTESIS IN THE HORSE TO OBTAIN CEREBROSPINAL FLUID.**

A. Pease, A. Behan, G. Bohart. Michigan State University, College of Veterinary Medicine, East Lansing, MI. 48824 USA.

**Introduction/Purpose:** Horses with intracranial lesions and severe ataxia are not good anesthesia candidates; however, only one method to obtain cerebrospinal fluid (CSF) from the cervical region in a standing horse has been reported using a dorsal approach into the cerebellomedullary cistern. This method is not routinely performed due to the difficulty for sample acquisition and potential of damaging the spinal cord. Ultrasound-guided centesis of the CSF between C1 and C2 using a lateral approach has not been previously described and provides a method to observe needle placement to minimize the risk of spinal cord damage. Our hypothesis was that standing cervical centesis could be performed in horses without complication.

**Methods:** Eleven neurologically normal horses and 2 horses with neurologic disease were used in this study. The 2 neurologic horses included one with a suspected intracranial lesion and one horse that had weakness in the pelvic limbs and was confirmed EPM positive. Horses were sedated using 0.01-0.02 mg/kg of detomidine hydrochloride intravenously followed approximately 3 minutes later by 0.06 mg/kg (approximately 30 mL) of morphine sulfate intravenously. A 10 MHz, microconvex, curvilinear ultrasound probe was used to identify the subarachnoid space and spinal cord between C1 and C2 using a lateral approach with the probe oriented dorsal to ventral. With ultrasound guidance, an 18-gauge 3.5 inch (8.9 cm) needle was introduced ventral to the ultrasound probe and directed dorsally into the dorsal aspect of the subarachnoid space in all horses. Ten milliliters of CSF were obtained and submitted for analysis. Horses were then observed for 15 minutes to 48 hours after the procedure for signs of neck pain, reluctance to move or change in mentation. These findings were recorded in all horses if observed.

**Results:** In all 13 horses, no adverse reactions were observed during the procedure or after the acquisition of the sample. When the sample was obtained, gentle suction was needed since the fluid did not flow freely. Two of the first three normal horses in this study had moderate red blood cell contamination in the CSF (940 and 612 RBC/ $\mu$ L). Patient motion and redirection of the needle appears to influence the presence of RBCs in the sample. In the remaining horses, one horse sample had 11 RBC/ $\mu$ L and the remaining 8 samples had less than 4 RBC/ $\mu$ L with 5 samples having 0 RBC/ $\mu$ L. The other CSF parameters measured included the specific gravity that was 1.005 in all horses, microprotein ranging from 30-104 mg/dL, 0-3 nucleated cells/ $\mu$ L and a PCV of less than 2%. The total procedure time was less than 2 minutes from the introduction of the needle to removal of the needle after the acquisition of fluid.

**Discussion/Conclusion:** Ultrasound-guided centesis between C1 and C2 is a rapid procedure that causes minimal to no reaction in standing, sedated horses. The use of ultrasound to guide a standing cervical centesis of the subarachnoid space using a lateral approach between C1 and C2 provides an additional route to obtain CSF for analysis in the equine patient.

## **IN VIVO EVALUATION OF THE ACOUSTOELASTIC STRAIN GAUGE IN THE NORMAL CANINE GASTROCNEMIUS TENDON.**

M. Ellison<sup>1</sup>, H. Kobayashi<sup>2</sup>, F Delaney<sup>1</sup>, K. Danielson<sup>1</sup>, R. Vanderby<sup>2</sup>, P. Muir<sup>1</sup>, L.J. Forrest<sup>1</sup>. University of Wisconsin-Madison <sup>1</sup>School of Veterinary Medicine, Department of Surgical Sciences, and <sup>2</sup>School of Medicine and Public Health, Department of Orthopedic and Rehabilitation, Wisconsin, 53706.

**Introduction/Purpose:** Acoustoelastic strain gauge (ASG) is an ultrasound-based tissue evaluation technique that relates the change in echo intensity observed during relaxation or stretching of tendons to the tissue's mechanical properties. ASG has been proven to accurately model strain and stiffness within tendons *in vitro*. The purpose of this study is to evaluate normal canine gastrocnemius tendons and determine repeatability of ASG *in vivo*.

**Methods:** Ten dogs less than 4 years old presenting for elective spay/neuter with normal orthopedic exams were recruited. Patients were sedated and restrained in right lateral recumbency. Two observers obtained cine loops of the mid portion of the each gastrocnemius tendon while the tarsus was being extended. ASG was used to calculate a stiffness-gradient for each pixel within the middle third of the imaged tendon.

**Results:** Mean of the average and mean of the SD of the stiffness-gradients for each tendon was 0.0144 (95% CI 0.0121-0.0167) and 0.0053 (95% CI 0.0043-0.0063), respectively. Mean difference in the average stiffness-gradients and mean difference in the SD of the stiffness-gradients when comparing observers was -0.0021 (95% CI -0.0057-0.0014) and -0.0005 (95% CI -0.0017-0.0007) and when comparing right and left limbs -0.0011 (95% CI -0.0042-0.0020) and -0.0008 (95% CI -0.0018-0.0003).

**Discussion/Conclusion:** The average and SD of the stiffness-gradients are consistent with expected mechanical properties for normal tendon. The  $\leq 15\%$  mean difference between observers and between limbs demonstrates precision using ASG to measure these parameters in normal canine gastrocnemius tendon *in vivo*.

Funding for this project was provided by the ACVR Ultrasound Society.

## **ULTRASONOGRAPHIC FINDINGS IN CANINE SCHISTOSOMIASIS.**

R.S. Sayre<sup>1</sup>, M.A. Bishop<sup>1</sup>, K.A. Spaulding<sup>2</sup>. <sup>1</sup>Department of Small Animal Clinical Sciences, College of Veterinary Medicine, Texas A&M University, TX 77843.

<sup>2</sup>Department of Large Animal Clinical Sciences, College of Veterinary Medicine, Texas A&M University, TX 77843.

**Introduction/Purpose:** *Heterobilharzia americana* is a trematode and the causative agent of Canine Schistosomiasis. Infection in the dog may be asymptomatic or can include a variety of non-specific clinical problems including chronic or intermittent diarrhea, weight loss, and or hepatic disease and dysfunction. The aim of this study was to report the ultrasound findings associated with this disease.

**Methods:** Medical records from Texas A&M University's College of Veterinary Medicine were reviewed from 2003 – 2011. Criteria for inclusion included canine cases that underwent abdominal ultrasound and had a confirmed diagnosis of *Heterobilharzia americana* by either histopathology, sodium chloride sedimentation, or fecal PCR. The signalment, bodyweight, and ultrasonographic findings were reviewed. All data was checked for normal distribution using a Shapiro-Wilk normality test and data was compared using an unpaired t test for normally distributed data and a Mann-Whitney test for non-parametric data. Alpha was set at 0.05.

**Results:** There were 16 cases that met the criteria. Cases included 9 different breeds. These dogs had a mean (SD) age of 6.5 (4.3) years and a mean (SD) body weight of 27.0 (11.1) kg. There were a total of 10 males (7 intact) and 6 females (1 intact). Of these dogs, 9/16 had abnormal findings on their abdominal ultrasound. Three dogs had only hepatic changes, 1 dog had intestinal only findings and the remaining 5 dogs had changes in both their gastrointestinal tract as well as their liver. One dog had similar changes in the pancreas. One dog had peritoneal effusion consistent with an exudate. Findings in the liver included a heterogeneous appearance with subtle hypoechoic small nodules and/or hyperechoic pinpoint foci with shadowing that exhibited a twinkle artifact and one dog had a diffusely hyperechoic liver. GI findings included a marked hyperechoic appearance to the submucosal layer with hyperechoic stippled appearance that shadowed and exhibited a twinkle artifact that periodically extended into the muscularis layer.

**Discussion/Conclusion:** Canine Schistosomiasis is being recognized with increased frequency in the southern part of the US. This disease may affect multiple abdominal organs. Characteristic sonographic findings found in varying degrees have been found in the liver, intestinal tract and pancreas. The ultrasonographic appearance may aid in the diagnosis and treatment of this disease.

## **INTEGRATING MULTIMEDIA SOFTWARES AND 3D CT VOLUME RENDERING IN SMALL ANIMAL ABDOMINAL ULTRASOUND TEACHING.**

d'Anjou M.-A.<sup>1</sup>, Piche N.<sup>2</sup>, de Guise J.<sup>3</sup> <sup>1</sup>Department of Clinical Sciences, Faculté de médecine vétérinaire, Université de Montréal, St-Hyacinthe, Canada. <sup>2</sup>The Object Research System, Montreal, Canada. <sup>3</sup>Laboratoire de recherche en imagerie et orthopédie, ETS and CRCHUM, Montreal, Canada.

**Introduction/Purpose:** Ultrasonography (US) has become readily available to veterinary practitioners, increasing the need for proper teaching of its fundamental concepts and technique. Understanding US images and identifying normal anatomy represent initial challenges that require substantial practice in live patients. The identification of specific 3D structures in 2D US images necessitates thorough understanding of anatomical spatial relationships and proper probe positioning. The purpose of this project was to develop tutorials integrating multimedia softwares and 3D CT volume rendering to facilitate abdominal US learning for veterinary students and small animal practitioners.

**Methods/Results:** Abdominal structures of an intact female, 2-yr old Beagle dog were ultrasounded<sup>1,2</sup> smoothly and repeatedly generating 1-2 min loops that were recorded as uncompressed .AVI files. Immediately after, the dog was imaged in dorsal recumbency with a 16-slice CT scanner<sup>3</sup> (pre- contrast, and at 10 and 30 seconds post-iodinated contrast injection; 1.25mm slice thickness). From CT images, abdominal organs and vessels were segmented manually and semi-automatically<sup>4</sup> and surface meshes were created, with individual color and transparency. Movies and still images demonstrating anatomical relationships through variations in viewing angle and transparency were created. Convex and linear US probes with their scanning field were illustrated<sup>5</sup> and imported into Photoshop CS5 Extended. In Photoshop, US probes were placed as 3D layers on top of 3D-CT rendered images of the dog in dorsal recumbency. Then, US video loops were synchronized with the movement of the corresponding US probes in the patient. This was repeated individually for all structures of the abdomen, using different probes and 3D-CT images highlighting specific structures. Movies were exported from Photoshop (30fps), then narrated and animated in Camtasia Studio 7<sup>6</sup>. Tutorials for each structure teaching spatial anatomy and US examination were exported in .FLV format and diffused initially to students through a Flash player. These tutorials were then implemented as pre-US lab formation for practitioners.

**Discussion/Conclusion:** Integrating multimedia tools and 3D CT volume rendering can complement US teaching, by helping apprentices better understand the relationships between 3D anatomical structures and US anatomy, as well as providing technical guidelines for proper US examination.

---

<sup>1</sup> ATL HDI 5000, convex 5-8 MHz, Mississauga, ON, Canada.

<sup>2</sup> Esaote MyLab Twice, convex 4-8 MHz and linear 10-15 MHz, Georgetown, ON, Canada.

<sup>3</sup> GE LightSpeed 16, Mississauga, ON, Canada.

<sup>4</sup> ORS Visual, The Object Research System, Montreal, QC, Canada.

<sup>5</sup> Google SketchUp 8, <http://sketchup.google.com/intl/en/index.html>

<sup>6</sup> [www.techsmith.com/camtasia/](http://www.techsmith.com/camtasia/)

## THE USE OF POWERPOINT CUSTOM ANIMATION FEATURES TO SIMULATE ULTRASONOGRAPHIC EXAMINATIONS.

M.B. Whitcomb. Department of Surgical & Radiological Sciences, University of California, Davis, 95616.

**Introduction/Purpose:** Instruction of ultrasonography is on the rise, both in veterinary school and at continuing education courses. The ability of today's ultrasound machines to store digital video-clips has enhanced our ability to provide meaningful educational experiences in the lecture setting, but the observer is often left to guess how the image was acquired. Ultrasound is a dynamic imaging modality and is highly reliant on transducer position; however, proper technique is difficult to simulate on slide presentations, especially when transducer movement is required to evaluate a specific structure. The use of PowerPoint<sup>a</sup> Custom Animation features to produce effective 2-D simulations of ultrasound examinations, using the horse as a model, is presented.

**Methods:** Digital photos of ultrasound transducers were taken from multiple angles and imported into photo editing software.<sup>b</sup> The background was removed from each photo, leaving only the transducer visible, and the image stored as a .png file to preserve background transparency. Photos of equine limbs, or entire horses, with and without pathology were altered in similar fashion to remove distracting background imagery. A photo of the area to be scanned was then inserted into a PowerPoint slide, after which an appropriate transducer image was inserted and positioned at the "start" of the exam, i.e. proximal metacarpus for evaluation of the flexor tendons. A motion path was then assigned to the transducer image using PowerPoint Custom Animation (CA) features by clicking "add effect," then "motion paths," then "draw custom path," then "freeform" and drawing the intended path of transducer movement on the slide relative to the anatomic region. A corresponding video-clip of the ultrasound exam was inserted into the same slide and set to "play" using "movie actions" in the CA menu box. The movie was then altered to "start with previous" so that the ultrasound video-clip began playing with the onset of transducer movement, thereby simulating the examination. Finally, the timing of the transducer's motion path was adjusted according to the video-clip's duration using the timing option in the CA menu box.

**Results:** Two-dimensional, real-time simulations of ultrasound exams of nearly all equine musculoskeletal and abdominal structures have been created using this technique. Examinations with straightforward paths are easiest to simulate. The addition of the "spin" effect (under the "emphasis" submenu in CA) into transducer movements has been especially useful when an angle change is required to illustrate proper technique, such as when illustrating "on beam, off beam" effects or during evaluation of curved structures such as the biceps tendon or fetlock region.

**Discussion/Conclusion:** The incorporation of motion paths into slide presentations has greatly improved the author's ability to provide ultrasonographic instruction for veterinary students and graduate veterinarians. In contrast to 3D animation and modeling, this technique requires little to no advanced training and can be easily adopted for use in other applications, such as small animal ultrasonographic instruction.

<sup>a</sup> [www.office.microsoft.com/en-us](http://www.office.microsoft.com/en-us); <sup>b</sup> Adobe Photoshop, [www.adobe.com](http://www.adobe.com)

## **MAGNETIC RESONANCE IMAGING FINDINGS ASSOCIATED WITH LATERAL CEREBRAL VENTRICULOMEGALY IN ENGLISH BULLDOGS.**

C.T. Ryan<sup>1</sup>, E.N. Glass.<sup>2</sup>, G. Seiler<sup>3</sup>, A.L. Zwingenberger<sup>4</sup>, W. Mai<sup>1</sup>. <sup>1</sup>University of Pennsylvania, PA 19104 <sup>2</sup>Red Bank Veterinary Hospital, NJ 07724, <sup>3</sup>North Carolina State University, NC 27695 <sup>4</sup>University of California-Davis, CA 95616.

**Introduction/Purpose:** Multiple congenital or development anomalies associated with the central nervous system have been reported in English Bulldogs. In previous studies this breed was shown to have significantly larger cerebral ventricles compared to beagles. It is thought that developmental mesencephalic aqueduct stenosis associated with fusion of the rostral colliculi is a common reason for congenital obstructive hydrocephalus. Cerebral ventriculomegaly in bulldogs has also been associated with an abnormal septum pellucidum and atrophy with thinning of the corpus callosum (CC). Brief reference has also been made to the presence of a persistent craniopharyngeal canal in English Bulldogs. The purpose of this study was to identify and describe prevalence and MRI characteristics of these anomalies and their association with presence and degree of cerebral ventriculomegaly.

**Methods:** Medical records from several university veterinary teaching hospitals and a private referral veterinary hospital were searched for English Bulldogs who underwent MRI exam of the brain during the period 2003-2010. All dogs were evaluated for presence and degree of lateral cerebral ventriculomegaly (quantified as relative ventricular area, RVA), presence and appearance of the septum pellucidum, thinning of the CC, fusion of the rostral colliculi and presence of a persistent craniopharyngeal canal. Dogs were also divided into two groups consisting of those with normal MRIs and those with obvious intracranial lesions for statistical comparison.

**Results:** Fifty English Bulldogs were included. Forty-eight dogs had some degree of lateral cerebral ventriculomegaly. Twenty-three had intra-cranial lesions other than enlargement of the lateral cerebral ventricles. Presence of lateral ventriculomegaly was not significantly associated with presence of another intra-cranial lesion. The septum pellucidum was variable, ranging from intact to incomplete or completely absent. RVA was significantly larger in dogs with incomplete or absent septum pellucidum. The CC was subjectively thinned in all but three dogs, two of which had normal lateral ventricles. A weak trend existed for progressive thinning of the CC as relative ventricular area increased. Fusion of the rostral colliculi was not found in any dog. A persistent craniopharyngeal canal was identified in one dog.

**Discussion/Conclusion:** Lateral cerebral ventriculomegaly is a common finding in English Bulldogs with or without other intra-cranial lesions. Although postulated as potentially causing aqueductal stenosis, fusion of the rostral colliculi was not identified in any dog and is unlikely to be a common etiology leading to obstructive hydrocephalus in this breed. Presence of a large craniopharyngeal canal is a rare finding in English Bulldogs which is easily visualized with MRI and has unknown clinical significance at this time.

**Thursday, October 13, 2011 (ACVR and RO simultaneous sessions)**

**ACVR**

- 7:00 am      *Registration opens*      Pavilion Landing
- 7:00 am      Society of Veterinary Nuclear Medicine Meeting      Pavilion IV - VI
- 8:00 am      Nuclear Medicine Roundtable Discussion:  
**Feline Hyperthyroidism—Diagnosis and Treatment...Where Are We?**  
Panelists: Dr. Greg Daniel  
                 Dr. Peter Scrivani  
                 Dr. Seth Wallack  
                 Dr. David Herring
- 9:30 am      **Nuclear Medicine Scientific Session (Moderator: Dr. Clifford Berry)**
- 9:30 am      **The Effect of Ketoconazole Administration on Brain Accumulation of Technetium-99m-Sestamibi in Wild-Type ABCB1 Dogs.**  
J.C. Coelho, D. Reyes-Gastelum. College of Veterinary Medicine, Michigan State University, East Lansing, MI 48824.
- 9:42 am      **Optimal Timing of Blood Sample Collection for Determining GFR in the Cat Using Plasma Clearance of <sup>99m</sup>Tc-DTPA.**  
G.B. Daniel, R. Tyson, D.C. Grant, W.H. Eyestone SR Werre. Virginia-Maryland Regional College of Veterinary Medicine. Blacksburg, VA 24061.
- 9:54 am      **Evaluation of the Biliary and Brain Distribution of <sup>99m</sup>Tc-sestamibi in ABCB1 Normal Dogs Before and After Treatment with Spinosad.**  
C.S. MacKay, J.S. Mattoon, G.D. Roberts, R.L. Tucker, T.R. Morimoto, K.L. Mealey. Washington State University, Pullman, WA 99164.
- 10:06 am      **Distribution of 2-Deoxy-2-[18F] Fluoro-D-Glucose (<sup>18</sup>F) in the Coeloma of Normal Bald Eagles.**  
F. Morandi,<sup>1</sup> M.P. Jones,<sup>1</sup> J.S. Wall,<sup>2</sup> M.J. Long,<sup>2</sup> A.C. Stuckey,<sup>2</sup> A.K. LeBlanc.<sup>1,2</sup> University of Tennessee, <sup>1</sup>College of Veterinary Medicine, <sup>2</sup>Graduate School of Medicine, Molecular Imaging and Translational Research Program; Knoxville, TN, 37996.
- 10:18 am      **Hematologic Sparing of Samarium-153-DOTMP, a Novel Bone-Seeking Radiopharmaceutical Agent for the Treatment of Bone Tumors.**  
K.A. Selting<sup>1</sup>; J.C. Lattimer<sup>1</sup>; A.R. Ketring<sup>2</sup>; J. Bryan<sup>1</sup>, D. Crump<sup>3</sup>; J. Simon<sup>3</sup>; R.K. Frank<sup>3</sup>; C.J. Henry<sup>1,4</sup>. 1. Veterinary Medicine and Surgery, University of Missouri, Columbia, MO. 2. Research Reactor, University of Missouri, Columbia, MO. 3. IsoTherapeutics Group LLC, Angleton, TX. 4. Department of Internal Medicine, Division Hematology/Oncology, School of Medicine, University of Missouri, Columbia, MO.
- 10:30 am      *Break with Exhibitors*      Pavilion I - III

**Thursday, October 13, 2011, continued (ACVR and RO simultaneous sessions)**

**ACVR**

11:00 am	Meet the New Diplomates	
12:00 pm	<i>Lunch</i>	Sendero Ballroom
1:00 pm	Image Interpretation Session	Pavilion IV - VI
2:30 pm	<i>Break with Exhibitors</i>	Pavilion I - III
3:00 pm	ACVR Business Meeting	Pavilion IV - VI
5:00 pm	<i>Adjourn for the Day</i>	
5:00 pm	LADIS Meeting	Pavilion IV - VI

## THE EFFECT OF KETOCONAZOLE ADMINISTRATION ON BRAIN ACCUMULATION OF TECHNETIUM-99M-SESTAMIBI IN WILD-TYPE ABCB1 DOGS.

J.C. Coelho, D. Reyes-Gastelum. College of Veterinary Medicine, Michigan State University, East Lansing, MI 48824.

**Introduction/Purpose:** Ketoconazole, an antifungal agent widely used in veterinary medicine is, along with many other drugs, a substrate for the transmembrane protein pump, P-glycoprotein (P-gp). P-glycoprotein is a product of the ABCB1 gene (formerly known as MDR1 gene). In the endothelial cells of the brain's capillaries, P-gp is thought to significantly contribute to the transport of numerous drugs to the outside of the brain. Mutation of the ABCB1 gene in dogs results in a defective blood-brain-barrier that does not promptly transport drugs that are P-gp substrates, resulting in neurotoxicity from otherwise standard therapeutic doses. Similar to endogenous (ABCB1 gene mutation), exogenous (pharmacological P-gp inhibition) factors may result in increased brain concentration of P-gp substrate drugs. Thus, concurrent administration of ketoconazole with other P-gp substrate drugs may result in impaired transport of these drugs through the blood-brain-barrier and consequently increase the risk of central nervous system side effects. The goal of this study is to determine the effect of the administration of ketoconazole on brain accumulation of a radiolabeled P-gp substrate, technetium-99m-sestamibi. Technetium-99m-sestamibi is not known to cause neurologic signs and it was used solely to quantify brain radioactivity. The hypothesis of this study is that the administration of ketoconazole to ABCB1 gene wild-type dogs significantly increases brain accumulation of technetium-99m-sestamibi.

**Methods:** Six healthy adult dogs wild-type for the ABCB1 gene were used in this study. Each dog served as its own control. Scintigraphy was performed with and without administration of ketoconazole. Ketoconazole (8-22 mg/Kg PO q12h x 11 doses) was administered to each dog for 5 days and in the morning of the day scintigraphy was performed. Ventral, 60 seconds, static images of the brain were obtained at 10 min intervals from 5 min up to 125 min after intravenous injection of approximately 8 mCi of technetium-99m-sestamibi. Brain radioactivity was determined over time, using ratios of mean counts per pixel of regions of interest drawn on the brain and neck muscle.

**Results:** The study showed that the administration of therapeutic dosages of ketoconazole to ABCB1 wild-type dogs results in significantly increased brain accumulation of technetium-99m-sestamibi within 125 minutes after its administration.

**Discussion/Conclusion:** The administration of therapeutic doses of ketoconazole resulted in significant inhibition of P-gp at the blood-brain-barrier in ABCB1 wild-type dogs. Concurrent administration of ketoconazole with other P-glycoprotein substrate drug(s) is likely to result in increased brain accumulation of these drugs. In the case of drugs that exert their toxicity in the central nervous system, neurotoxicity may ensue. Based on imaging studies, mathematical models may be developed in the future to try to determine doses of P-glycoprotein substrate drugs that can be concurrently administered to dogs without causing neurotoxicity.

## OPTIMAL TIMING OF BLOOD SAMPLE COLLECTION FOR DETERMINING GFR IN THE CAT USING PLASMA CLEARANCE OF $^{99m}\text{Tc}$ -DTPA.

G.B. Daniel, R. Tyson, D.C. Grant, W.H. Eyestone SR Werre. Virginia-Maryland Regional College of Veterinary Medicine. Blacksburg, VA 24061.

**Introduction/Purpose:** Glomerular filtration rate (GFR) is an important index of renal function.  $^{99m}\text{Tc}$ -DTPA can be used to estimate GFR via imaging or plasma clearance techniques. The plasma clearance techniques determine renal clearance by dividing the injected dose of  $^{99m}\text{Tc}$ -DTPA by the area under the plasma disappearance curve (AUC). Accuracy of this technique is dependent on the AUC measurement. Multiple blood samples are required to construct a plasma disappearance curve. In general, the greater the number of blood samples (i.e. data points), the more accurate the plasma disappearance curves. Taking multiple blood samples is problematic in the cat. A minimum of 4 data points is required to fit a 2-compartment model. The purpose of this study was to determine optimal timing of these 4 blood samples.

**Methods:** Six male cats had  $^{99m}\text{Tc}$ -DTPA plasma clearance studies performed at three different times. Eight blood samples were collected at 5, 15, 30, 45, 60, 90, 120, and 180 minutes following injection of  $2.49 \pm 0.24$  (Mean  $\pm$  SD) mCi of  $^{99m}\text{Tc}$ -DTPA. The plasma activity data was fitted using a two-compartment model. A least-squares approximation was used to determine the coefficients of the bi-exponential function. The AUC was determined using the following formula:  $A\alpha_a + B\alpha_b$ , where A and B are the Y-intercept of the fast and slow compartments and  $\alpha_a$  and  $\alpha_b$  are the slopes from the respective compartments.

The AUC using all 8 data points was used as the standard for comparison. The AUC and GFR were calculated for each of 18 combinations of 4 data points and were compared to the respective standard using Bland-Altman Plots. The differences in GFRs from that of the standard were determined by mixed model ANOVA.

**Results:** The GFR using 8 data points was  $2.47 \pm 0.29$  ml/min/kg (Mean  $\pm$  SD). The 4-point plasma disappearance curves utilizing samples taken at 5, 15, 120, 180 minutes produced areas under the curves closest to those of the 8-point standards. The GFRs estimated from the same four points were also closest to the GFR calculated using all 8 points. There was no significant difference in the GFRs calculated from the 4-point (5, 15, 120, 180 minutes) versus 8-point plasma disappearance curves.

**Discussion/Conclusion:** GFRs calculated from a 4-point plasma disappearance curve (5, 15, 120, 180 minutes) of  $^{99m}\text{Tc}$ -DTPA are not different than GFRs measured from an 8-point curve. Collection of 4 blood samples in this time frame is practical and may provide a clinically useful method to estimate GFR in the cat.

## EVALUATION OF THE BILIARY AND BRAIN DISTRIBUTION OF <sup>99m</sup>Tc-SESTAMIBI IN ABCB1 NORMAL DOGS BEFORE AND AFTER TREATMENT WITH SPINOSAD.

C.S. MacKay, J.S. Mattoon, G.D. Roberts, R.L. Tucker, T.R. Morimoto, K.L. Mealey. Washington State University, Pullman, WA 99164.

**Introduction/Purpose:** Recently, the FDA issued a warning stating that the concurrent use of spinosad and ivermectin (at extra-label doses) can result in neurologic toxicity, with symptoms resembling those observed with ivermectin intoxication. The mechanism of this toxicity has not been elucidated, but knowing that ivermectin is a substrate of the membrane transporter P-glycoprotein, we hypothesized that the toxicity observed with the co-administration of spinosad and ivermectin results from inhibition of P-glycoprotein by spinosad. Using the radiolabeled P-glycoprotein substrate <sup>99m</sup>Tc-Methoxy-Isobutyl-Isonitrile (sestamibi), we studied the effect of spinosad on P-glycoprotein function. Our hypothesis was that the distribution of <sup>99m</sup>Tc-sestamibi activity would be significantly different in the study dogs after administration of spinosad. Specifically, we expected increased activity of <sup>99m</sup>Tc-sestamibi within the brain tissue and decreased activity of <sup>99m</sup>Tc-sestamibi within the gallbladder of study dogs after spinosad administration compared to that observed in untreated dogs.

**Methods:** Six dogs, each serving as their own control, were divided into treatment and control groups. Treatment dogs received spinosad at the manufacturer's recommended dose 48 hours prior to being imaged with <sup>99m</sup>Tc-sestamibi while control dogs were imaged without prior administration of spinosad. Scintigraphic images of the head and abdomen were obtained on both imaging days for all dogs. Gallbladder:Liver (G:L) and Brain:Neck Musculature (B:M) ratios of <sup>99m</sup>Tc-sestamibi were calculated and compared between groups.

**Results:** No significant difference in G:L (P=0.2754) or B:M (P=1.0) ratios were found between groups.

**Discussion/Conclusion:** Results provide evidence that, 48 hours after dosing, spinosad does not inhibit P-glycoprotein function. Further investigation is necessary to elucidate the mechanism of reported toxic interaction between spinosad and ivermectin.

## DISTRIBUTION OF 2-DEOXY-2-[<sup>18</sup>F] FLUORO-D-GLUCOSE (<sup>18</sup>FDG) IN THE COELOMA OF NORMAL BALD EAGLES.

F. Morandi,<sup>1</sup> M.P. Jones,<sup>1</sup> J.S. Wall,<sup>2</sup> M.J. Long,<sup>2</sup> A.C. Stuckey,<sup>2</sup> A.K. LeBlanc.<sup>1,2</sup> University of Tennessee, <sup>1</sup>College of Veterinary Medicine, <sup>2</sup>Graduate School of Medicine, Molecular Imaging and Translational Research Program; Knoxville, TN, 37996.

**Introduction/Purpose:** Positron Emission Tomography (PET) with 2-deoxy-2-[<sup>18</sup>F]fluoro-D-glucose (<sup>18</sup>FDG) has become increasingly more widespread in veterinary medicine. Studies establishing the normal <sup>18</sup>FDG distribution have to date been performed in cats,<sup>1</sup> dogs<sup>2,3</sup> and Hispaniolian Amazon Parrots.<sup>4</sup> Because of many anatomical and physiological variations among bird species, it is important to determine the <sup>18</sup>FDG distribution in individual species before employing this imaging modality for the diagnosis of disease.

**Methods:** Seven adult, normal bald eagles (*Haliaeetus leucocephalus*) weighing 4,011±459 grams underwent whole-body PET/CT imaging with <sup>18</sup>FDG (3.4±0.5 mCi, 125.2±19.3 MBq, mean±SD) using a 64-slice PET/CT scanner (Siemens mCT, Siemens Molecular Imaging, Knoxville, TN) under general anesthesia. After the transmission non-contrast CT scan was completed, the following scans were acquired: 1) 60 minutes dynamic PET scan of the celomic cavity, starting immediately after <sup>18</sup>FDG injection; 2) whole-body static PET scan at steady state, 60 minutes after <sup>18</sup>FDG injection; 3) whole body contrast-CT (iohexol 240 mgI/mL, 1mL/lb IV). After reconstruction, images were analyzed using dedicated software (Inveon Research Workplace, Siemens Preclinical Solutions USA, Inc.). In addition to qualitative image evaluation, regions of interest (ROIs) were drawn over the ventricular myocardium, liver, spleen, proventriculus, cloaca, kidneys, and lungs on both dynamic and static PET images. Standardized uptake values (SUV) were calculated using standard formula.<sup>1</sup>

**Results:** The kidneys had the most intense uptake of <sup>18</sup>FDG, followed by cloaca and intestinal tract; liver activity was mild and slightly more intense than spleen; proventricular activity was always present, while little to no activity identified in the ventricular wall. Activity in the myocardium was always present and variable among birds. The lungs showed no visibly discernible activity. Mean±SD SUVs calculated using representative ROIs at 60 minutes were as follows: myocardium 1.6±0.2 (transverse plane) and 1.3±0.3 (sagittal plane); liver 1.1±0.1; spleen 0.9±0.1; proventriculus 1.0±0.1; cloaca 4.4±2.7; right kidney 17.3±1.0; left kidney 17.6±0.3; right and left lungs both 0.3±0.02.

**Discussion/Conclusion:** This study established the pattern of uptake of <sup>18</sup>FDG in the coeloma of adult eagles, providing a baseline for comparison for future research.

### References:

1. LeBlanc AK et al. *Vet Radiol Ultrasound* 2009;50:436-441.
2. LeBlanc AK et al. *Vet Radiol Ultrasound* 2008;49:182-188.
3. Lee MS et al. *Vet Radiol Ultrasound* 2010;51:670-673.
4. Souza MJ et al. *Vet Radiol Ultrasound* 2011;52:340-344.

## **HEMATOLOGIC SPARING OF SAMARIUM-153-DOTMP, A NOVEL BONE-SEEKING RADIOPHARMACEUTICAL AGENT FOR THE TREATMENT OF BONE TUMORS.**

K.A. Selting<sup>1</sup>; J.C. Lattimer<sup>1</sup>; A.R. Ketring<sup>2</sup>; J. Bryan<sup>1</sup>, D. Crump<sup>3</sup>; J. Simon<sup>3</sup>; R.K. Frank<sup>3</sup>; C.J. Henry<sup>1,4</sup>. 1. Veterinary Medicine and Surgery, University of Missouri, Columbia, MO. 2. Research Reactor, University of Missouri, Columbia, MO. 3. IsoTherapeutics Group LLC, Angleton, TX. 4. Department of Internal Medicine, Division Hematology/Oncology, School of Medicine, University of Missouri, Columbia, MO.

**Introduction/Purpose:** Primary and metastatic bone cancer are significant sources of morbidity and mortality in dogs. Samarium(Sm)-153-EDTMP has been used to treat bone cancer pain, but exposure of normal marrow by radiation causes prolonged and sometimes pronounced myelosuppression which can delay chemotherapy and other treatments. Sm-153-DOTMP uses a superior chelator relative to other available constructs. Our objective was to assess degree of myelosuppression following treatment of dogs with spontaneous bone tumors with Sm-153-DOTMP and compare this to historical data for Sm-153-EDTMP.

**Methods:** Dogs with spontaneously-occurring bone cancer (8 osteosarcoma, 2 metastatic carcinoma and 1 metastatic multilobular tumor of bone) were recruited from the hospital population at the University of Missouri Veterinary Medical Teaching Hospital. Each dog was evaluated with blood count, biochemical profile, urinalysis, and technetium-99m-MDP skeletal scintigraphy. Dogs were treated with 1 (n=7) or 2 (n=4) mCi/kg Sm-153-DOTMP intravenously and monitored using weekly blood counts. Gamma scintigraphy was acquired post injection for most cases. Myelosuppression was compared to historical data from dogs treated with Sm-153-EDTMP.

**Results:** Treatment was well tolerated. There was excellent correlation between pretreatment technetium and post-treatment Sm-153-DOTMP scintigraphy. Region of interest ratios of uptake between tumor and contralateral normal bone ranged from 12.6-45.7 and ratio of tumor to adjacent bone ranged from 8.6-24.8. At 1 mCi/kg (n=7) and in 1 dog treated at 2 mCi/kg, no dog experienced a dose-limiting hematologic toxicity. Asymptomatic grade 3 and 4 myelosuppression were seen in 3 dogs treated at 2 mCi/kg. Sm-153-DOMTP was less myelosuppressive than Sm-153-EDTMP.

**Discussion/Conclusion:** Given the favorable toxicity profile, Sm-153-DOTMP in combination with chemotherapy should be explored for treatment of bone cancer.

Research Support : NCI R43CA150601

**Thursday, October 13, 2011 (ACVR and RO simultaneous sessions)**

**RO**

- 7:00 am **NO** VRTOG/RO Meeting
- 8:00 am **VRTOG/RO Scientific Session 1** Enchantment A - D  
**(Moderator: Dr. Sheri Siegel)**
- 8:00 am **A Retrospective Study of a Novel Palliative Radiotherapy Protocol for Nasal Tumors in Dogs and Cats.**  
L.A. Askin, A.F.Pruitt. North Carolina State University-College of Veterinary Medicine, North Carolina, 27606.
- 8:21 am **Cyberknife Radiosurgery for Irradiation of Non-Lymphomatous Nasal Tumors in Dogs and Cats.**  
SC Charney,<sup>1</sup> SA Glasser,<sup>1</sup> NG Dervisis,<sup>2</sup> MR Witten,<sup>1</sup> SN Ettinger,<sup>1</sup> JM Berg,<sup>1</sup> RJ Joseph.<sup>1</sup> <sup>1</sup>Animal Specialty Center, Yonkers, NY 10701. <sup>2</sup>Michigan State University College of Veterinary Medicine, Lansing, MI 48824.
- 8:42 am **Early Detection of Nasal Tumor Recurrence Following Megavoltage Irradiation.**  
S.M. Cook, L. Donnelly, K.A. Selting, D. Bommarito, J.C. Lattimer. University of Missouri College of Veterinary Medicine, Missouri, 65211.
- 9:03 am **Administration of Atracurium for Stereotactic Radiation Therapy of the Thoracic Cavity.**  
J.T. Custis, J.F. Harmon, S.M. LaRue. Colorado State University Animal Cancer Center (CSU ACC), Colorado, 80523.
- 9:24 am **Normal Tissue Response to the Addition of Toceranib Phosphate (Palladia<sup>®</sup>) to External Beam Radiation Therapy Utilized in the Treatment of Canine Nasal Carcinoma.**  
T.J. Ehling, M.K. Klein. Southwest Veterinary Oncology, Arizona, 85705.
- 9:45 am **Influence of Palliative Radiation Therapy on Vascularity of Spontaneous Tumors in Dogs.**  
G.S. Seiler<sup>1</sup>, A.F. Pruitt<sup>1</sup>, M.K. Boss<sup>1</sup>, L. Lan<sup>2</sup>, D.E. Thrall<sup>1</sup>. <sup>1</sup>North Carolina State University, NC 27607, <sup>2</sup>Duke University, NC 27705.
- 10:06 am **Radiation Therapy for Control of Infiltrative Lipomas and Liposarcomas, a Retrospective Study.**  
J. Fidel, R. Sellon, B. Wheeler, R.K. Houston. Washington State University, Washington, 99164-6610.
- 10:30 am *Break with Exhibitors* Pavilion I - III

**Thursday, October 13, 2011, continued (ACVR and RO simultaneous sessions)**

**RO**

11:00 am	<b>VRTOG/RO Scientific Session 2 (Moderator: Dr. Sheri Siegel)</b>	
11:00 am	<b>Optic Chiasm Imaging for Stereotactic Radiation Planning.</b> <u>L. Griffin</u> , E. Randall, J. Custis, M. Nolan, D. Zwang, S. Kraft and S. LaRue. Fint Animal Care Center, Colorado State University, Colorado, 80524.	
11:21 am	<b>Radiographic Lymphography in the Dog Using Iodized Oil.</b> <u>M.N. Mayer</u> , T.I. Silver, C.K. Grier, J.M. Anthony. University of Saskatchewan, SK, S7N 5B4.	
11:42 am	<b>A Survey of Veterinary Radiation Facilities in the United States During 2010.</b> <u>J. Farrelly</u> <sup>1</sup> , M.C. McEntee. <sup>2</sup> <sup>1</sup> The Animal Medical Center, New York, NY 10065, <sup>2</sup> Cornell University Hospital for Animals, Ithaca, NY 14853.	
12:00 pm	<i>Lunch</i>	Sendero Ballroom
1:00 pm	Image Interpretation Session	Pavilion IV - VI
2:30 pm	<i>Break with Exhibitors</i>	Pavilion I - III
3:00 pm	ACVR Business Meeting	Pavilion IV - VI
5:00 pm	<i>Adjourn for the Day</i>	
5:00 pm	LADIS Meeting	Pavilion IV - VI

## **A RETROSPECTIVE STUDY OF A NOVEL PALLIATIVE RADIOTHERAPY PROTOCOL FOR NASAL TUMORS IN DOGS AND CATS.**

L.A. Askin, A.F.Pruitt. North Carolina State University-College of Veterinary Medicine, North Carolina, 27606.

***Introduction/Purpose:*** To determine the response to treatment and survival in dogs and cats with nasal tumors treated with a cyclical hypofractionated palliative radiotherapy regimen.

***Methods:*** A retrospective study of dogs and cats with nasal tumors treated with a novel palliative radiotherapy scheme called the “quad shot” adapted from human medicine at NCSU-VTH between June 2006 and September 2010. The quad shot consisted of 4 fractions of 4 Gy, given twice a day at least 6 hours apart, for 2 days. It was recommended the course of radiation be repeated at 4 weeks and 8 weeks if at least stable disease was achieved.

***Results:*** Forty-nine dogs and 9 cats received at least one course of the quad shot palliative protocol. The overall median survival time was 172 days. The median survival for dogs alone receiving at least one course of therapy was 172 days. The median survival for cats alone receiving at least one course of therapy was 95 days. Thirty-three dogs received all three courses with a median survival of 199 days.

***Discussion/Conclusion:*** The palliative radiation protocol described is a safe and effective palliative treatment option for nasal tumors in dogs and cats with minimal toxicity, a good response rate, and potentially long term survival.

## **CYBERKNIFE RADIOSURGERY FOR IRRADIATION OF NON-LYMPHOMATOUS NASAL TUMORS IN DOGS AND CATS.**

SC Charney,<sup>1</sup> SA Glasser,<sup>1</sup> NG Dervisis,<sup>2</sup> MR Witten,<sup>1</sup> SN Ettinger,<sup>1</sup> JM Berg,<sup>1</sup> RJ Joseph.<sup>1</sup> <sup>1</sup>Animal Specialty Center, Yonkers, NY 10701. <sup>2</sup>Michigan State University College of Veterinary Medicine, Lansing, MI 48824.

***Introduction/Purpose:*** Radiation therapy is often used for the treatment of nasal tumors in dogs and cats. Conventional radiation therapy requires the use of multiple fractions over many weeks to minimize damage to normal tissue. The CyberKnife® Radiosurgery System<sup>a</sup> (CyberKnife) is a frameless stereotactic radiosurgery system that uses multiple non-isocentric, non-coplanar beams to deliver single fraction or hypofractionated radiation with sub-millimeter accuracy. The large number of beams combined with continual image guidance throughout treatment results in a high degree of conformality and steep dose gradients.

CyberKnife couples an orthogonal pair of x-ray cameras to a dynamically manipulated robot-mounted linear accelerator that guides the therapy beam to the treatment target. CyberKnife uses skeletal landmarks or implanted fiducial markers to track the treatment target during planning and treatment delivery. Proprietary inverse planning software is used to create a treatment plan.

The purpose of the study was to evaluate the clinical outcome of dogs and cats with non-lymphomatous nasal tumors treated with CyberKnife radiation therapy.

***Methods:*** Dogs and cats with non-lymphomatous nasal tumors treated at Animal Specialty Center with hypofractionated CyberKnife radiosurgery were eligible for inclusion in the study. In addition, a follow-up time of at least one year was required for inclusion. Survival time was evaluated using Kaplan-Meier survival curves. Factors including species, age, breed, tumor type, stage, tumor size, dose of radiation, and heterogeneity index were analyzed for prognostic significance.

***Results:*** Twenty-four dogs and cats with non-lymphomatous nasal tumors were included. Overall median survival time was 381 days. No statistically significant prognostic factors were identified. Acute side effects were rare and if identified were mild. Late side effects included one dog with an oro-nasal fistula.

***Discussion/Conclusion:*** These results indicate that the CyberKnife radiosurgery for non-lymphomatous nasal tumors provides comparable outcomes to conventional radiation with fewer required fractions and fewer acute side effects.

<sup>a</sup> Accuray, Inc., Sunnyvale, CA

## **EARLY DETECTION OF NASAL TUMOR RECURRENCE FOLLOWING MEGAVOLTAGE IRRADIATION.**

S.M. Cook, L. Donnelly, K.A. Selting, D. Bommarito, J.C. Lattimer. University of Missouri College of Veterinary Medicine, Missouri, 65211.

***Introduction/Purpose:*** Nasal tumors in dogs are commonly treated with radiation therapy, and median survival times vary among tumor types and among various case series. Despite an initial metastatic rate of 0-12% and eventual metastatic rate of up to 45%, most dogs succumb to locoregional recurrence. The purpose of this study was to document sites of recurrence as detected by regularly planned CT scans.

***Methods:*** This retrospective study evaluated records of dogs treated at the University of Missouri with megavoltage irradiation between 2000 and 2009. Owners were routinely instructed to return for CT scan evaluation every 3 months following the completion of radiation therapy. Cases were included if repeated CT scans were performed and progression-free survival (PFS) could be determined. The nasal cavity was divided into 7 regions based on anatomic landmarks, and location of tumor recurrence was documented.

***Results:*** Thirty dogs met the criteria for inclusion. Median age was 9 years (range 4-14) and weight was 24 kg (range 3-45). Median total delivered dose was 55 Gy (range 44-69) in 18-21 fractions (median 18). Median PFS was 234 days (range 110-1193). Median survival time was 610 days (range 229-1740). Eight dogs underwent rhinotomy for excision of recurrent tumor, and two dogs received additional radiation therapy for recurrent disease. Epistaxis was the most common clinical sign reported at the time of recurrence (18/30 dogs); however, two patients had no clinical signs when the repeat CT was performed. The most frequent sites of tumor recurrence were between the canine tooth root and the orbit, and between the orbit and cribriform plate.

***Discussion/Conclusion:*** Routine evaluation via CT scan to monitor clinical progress of canine nasal tumors makes it possible to detect early recurrence. This can allow intervention with additional treatment modalities such as re-irradiation or surgical excision. Understanding patterns of tumor recurrence can guide initial treatment planning to improve dosimetry.

## **ADMINISTRATION OF ATRACURIUM FOR STEREOTACTIC RADIATION THERAPY OF THE THORACIC CAVITY.**

J.T. Custis, J.F. Harmon, S.M. LaRue. Colorado State University Animal Cancer Center (CSU ACC), Colorado, 80523.

**Introduction/Purpose:** Stereotactic radiation therapy (SRT) utilizes patient immobilization, image guidance, and intensity modulated delivery to achieve ablative radiation doses within the tumor, while preferentially sparing the surrounding normal tissues. The impact of tumor motion, secondary to respiration, must be considered for lesions located within the thoracic cavity. Given that the feasibility of stereotactic radiation therapy is dependent upon minimizing the volume of normal tissues within the planned target volume (PTV), efforts to induce paralysis of the diaphragm and eliminate respiration and respiratory induced tumor motion were evaluated.

**Methods:** Patients were positioned within a rigid, indexed whole body cradle. Pre and post-contrast computed tomography scans (CT) were obtained of the thoracic cavity by suspending mechanical ventilation at maximum expiration for the brief duration of the scan. An individual SRT plan was generated utilizing computer based, inverse radiation therapy planning. At the time of SRT delivery, atracurium was administered intravenously following the induction of general anesthesia. Upon achieving and maintaining paralysis of the diaphragm, mechanical ventilation was suspended briefly at maximum expiration. Kilovoltage radiographs (kVR) and kilovoltage cone beam computed tomography scans (kV CBCT) were obtained and matched to digitally reconstructed radiographs (DRR) generated from the original planning CT. Upon verification of tumor alignment via the on-board imaging (OBI), the process of suspending mechanical ventilation was repeated for the delivery of each individually and dynamically modulated field. Each SRT plan was delivered once daily for three to five total days depending upon the individual prescription. The administration of additional atracurium was based upon the response to peripheral nerve stimulation.

**Results:** Four patients with tumors within the thoracic cavity (three mediastinal masses; one recurrent pulmonary adenocarcinoma with sternal lymph node metastasis) were administered atracurium in an effort to eliminate respiration during the delivery of daily SRT. In all four patients, apnea was induced and successfully maintained throughout the administration of each individual SRT field. During the delivery of SRT under apneic conditions, none of the tumors were subjected to appreciable respiratory motion. All four patients recovered fully from general anesthesia without experiencing any adverse effects.

**Discussion/Conclusion:** Administration of atracurium was well tolerated and without evidence of complication. By inducing diaphragmatic paralysis and allowing for the controlled suspension of mechanical ventilation, there is potential for improving the SRT dose coverage to intrathoracic tumors, while decreasing the volume of treated normal tissue as compared to free breathing.

## **NORMAL TISSUE RESPONSE TO THE ADDITION OF TOCERANIB PHOSPHATE (PALLADIA®) TO EXTERNAL BEAM RADIATION THERAPY UTILIZED IN THE TREATMENT OF CANINE NASAL CARCINOMA.**

T.J. Ehling, M.K. Klein. Southwest Veterinary Oncology, Arizona, 85705.

**Introduction/Purpose:** A study is currently underway to identify the activity of toceranib phosphate alone or as a radiation-sensitizing agent in the treatment of canine nasal carcinoma. Primary activity of toceranib against nasal carcinoma has been documented. In vitro data indicates that toceranib is an effective radiosensitizer. Whether the addition of toceranib to external beam radiation therapy will potentiate the radiation side effects is unknown.

**Methods:** Toceranib phosphate is administered to patients at an initial dose of 3.0-3.25 mg/kg every other day. Patients within the radiation arm of the study receive radiation to a total dose of 42 Gy (10 fractions of 420 cGy) administered over 2 weeks.

**Results:** At this time 8 patients have completed the radiation portion of the protocol. Mean VRTOG grading of side effects associated with this combination protocol are 0.44 for skin, 1.6 for mucus membranes and 0.25 for ocular. Maximal grade for skin was 2. Maximal mucus membrane grade was 3. Maximal ocular grade was 3. No central nervous system side effects have been noted to date.

**Discussion/Conclusion:** Based on the limited amount of data available at this time, the radiation side effects do not appear to be higher in grade than those previously reported.

## **INFLUENCE OF PALLIATIVE RADIATION THERAPY ON VASCULARITY OF SPONTANEOUS TUMORS IN DOGS.**

G.S. Seiler<sup>1</sup>, A.F. Pruitt<sup>1</sup>, M.K. Boss<sup>1</sup>, L. Lan<sup>2</sup>, D.E. Thrall<sup>1</sup>. <sup>1</sup>North Carolina State University, NC 27607, <sup>2</sup>Duke University, NC 27705.

**Introduction/Purpose:** Radiation therapy (RT) is used frequently to treat cancer in dogs and humans. Traditionally, damage to the DNA of tumor cells has been considered the major effect of radiation treatment. However, there is increasing evidence that tumor endothelial cells are also an important target of RT. The effect of radiation on tumor vessels is poorly understood. The purpose of this study was to characterize changes in tumor vascularity after short course hypofractionated palliative RT using contrast enhanced ultrasound imaging (CEUS).

**Methods:** Dogs with spontaneous tumors undergoing palliative RT were included if the tumor was amenable to ultrasound imaging. Tumors were irradiated with a total dose of 16 Gy, given in twice daily fractions of 4 Gy over 2 days 6 hours apart and repeated approximately one month later. CEUS imaging was performed before and immediately (10 minutes) after the first and third fraction, and 30 days later before and after the first fraction. Microbubble contrast medium (Targestar-P<sup>TM</sup>, Targeson Inc, San Diego, CA) was injected intravenously at a dose of 0.025ml/kg, and the tumor was imaged for 60 seconds. Video clips of tumor enhancement were recorded digitally and exported for evaluation with dedicated contrast analysis software (Qontrast, Esaote S.p.A. Genova, Italy). Regions of interest (ROI) were drawn around the entire tumor and the subcutaneous tissue adjacent to the tumor and perfusion parameters were calculated. Statistics were performed using SAS@v.9.2 software.

**Results:** Ten dogs were imaged. Six had a sarcoma (two osteosarcoma, four undifferentiated soft tissue sarcoma) and four had a carcinoma (two prostate, one thyroid and one anal sac). Increased tumor vascularity was observed in 9/10 (90%) of tumors after the first fraction, in 3/9 (33.3%) after the third, and in 3/5 (60%) after the first fraction of the 30 day treatment. Similar, but less pronounced changes were seen in the surrounding subcutaneous tissues. The difference in the magnitude of vascularity change was not statistically significant ( $P=0.54$ ) but the direction of change was ( $P=0.02$ ).

**Discussion/Conclusion:** The results indicate that 4Gy of radiation can cause an immediate increase in tumor blood flow. The number of tumor types and tumor heterogeneity resulted in poor statistical power to detect absolute changes in tumor perfusion. However, the change towards increased vascularity was statistically significant. While the mechanism of this increased vascularity is unclear, this finding is in accordance with reports of increased tumor oxygenation shortly after radiation treatment in therapy responders, but not in non-responders. A better understanding of the effect of radiation treatment on tumor blood vessels may be useful for prognosis and selection of appropriate treatment protocols.

## **RADIATION THERAPY FOR CONTROL OF INFILTRATIVE LIPOMAS AND LIPOSARCOMAS, A RETROSPECTIVE STUDY.**

J. Fidel, R. Sellon, B. Wheeler, R.K. Houston. Washington State University, Washington, 99164-6610.

**Introduction/Purpose:** Infiltrative lipoma is a low grade tumor which, theoretically would not respond well to radiation therapy (RT). However, the one previous report of radiation of infiltrative lipomas in the veterinary literature (McEntee M.C. 2000) had prolonged survival noted (median of 40 months). This study was undertaken to see if these results could be confirmed.

**Methods:** Cases were identified from the radiation therapy data base and the problem list base, at Washington State University. All cases had been diagnosed with either an infiltrative lipoma or liposarcoma and had received RT as a part of treatment. Information gathered from the medical record included age, sex, breed, color, tumor location, treatment protocol, and pathology. Follow-up was attained in all but one case through phone calls and emails with referring veterinarians or clients.

**Results:** A total of 18 cases were found from 1999 to present including one cat with a vaccine associated tumor. Of the dogs, 8 were Labradors and 6 of these were yellow in color. The remaining dogs were golden retriever (3), Australian shepherd type (3), and boxer, English springer spaniel, Rottweiler (1 each). Median age was 7 years (range 3-13). Six of the tumors were designated as liposarcomas and one of these was low grade. Locations were shoulder or axilla (7), muscles of the upper hind leg (5), tarsus (1), lower forelimb (2), and neck, mandible, tongue (1 each). Two dogs had gross disease present at the time of radiation and all others had cytoreductive surgery prior to RT. Three patients received coarse fractionated RT (3 x 8 Gy) the remainder received fine fractionated (18 x 3 Gy). In 17 patients with follow information available only 4 had tumor recurrence, one infiltrative lipoma returned at 18 months, 2 axillary liposarcomas recurred at 8 and 16 months and the cat amputated for a hind leg liposarcoma had tumor recurrence at 7 months. Four patients died of other tumors and 2 were lost to follow up. Median survival of all patients was 24 months. Diagnosis of liposarcoma gave a significantly shorter survival ( $P = .0154$ ) but survivals were still long with a median 16 months versus 68 months for infiltrative lipoma.

**Discussion/Conclusion:** Infiltrative lipomas are well controlled with radiation therapy and due to the young age and prolonged survival of many of the dogs, finely fractionated protocols are desirable. Yellow Labradors may have a propensity for development of tumors of fat origin.

## **OPTIC CHIASM IMAGING FOR STEREOTACTIC RADIATION PLANNING.**

L. Griffin, E. Randall, J. Custis, M. Nolan, D. Zwang, S. Kraft and S. LaRue. Fint Animal Care Center, Colorado State University, Colorado, 80524.

**Introduction/Purpose:** The optic chiasm during fractionated radiation therapy is very forgiving to small doses delivered over multiple treatments. As such it will often not be contoured or have constraints placed on it during planning. However, in stereotactic radiation (SRT) where large doses of radiation are delivered in 1-5 fractions there is the potential for inducing optic neuritis and/or neuropathy. In human patients undergoing radiation therapy, radiation induced optic neuritis/neuropathy (RION) is a not uncommon complication during treatment for sellar and parasellar brain tumors, often leading to discomfort, blurred vision, loss of depth perception and possibly blindness. The length of tract involved, as well as the total overall dose are contributing factors.

With the increasing popularity of using SRT for radiation treatment in veterinary medicine it is essential that we are able to precisely localize the optic chiasm in order to accurately determine the dose to the nerve tracts.

CT scans are routinely used for radiation planning as they are able to quantify the heterogeneity of various tissues. Unfortunately imaging of the central nervous system tends to be fairly non-specific in comparison an MRI.

The purpose of this study is to use CT/MRI fusions in order to accurately localize the optic chiasm prior to creating a radiation plan for stereotactic radiation therapy. CT and MR studies will then be independently evaluated to determine if the chiasm and nerve can be accurately contoured using CT alone.

**Methods:** All dogs were anesthetized and had a pre and post contrast CT scan with 2mm slices taken in a 512X512 pixel window. Dogs were positioned in sternal recumbency and had their head and necks immobilized using a vaculock neck pillow, carbon fiber bite block stand, bite block and face mask. Following the CT scan dogs were transported while under anesthetic to the MRI machine and positioning was repeated. An MRI of the volume of interest (ie. Centered over the pituitary fossa) was taken in 2mm slices in T1 pre and post contrast, T2 and T2\*. Following imaging the 2mm post contrast CT and the 2mm T1 post contrast MRI were imported into the Varian Eclipse Treatment Planning System and fused. For treatment purposes the optic chiasm was contoured using both the CT and MR images. At later, independent sessions, the chiasm was contoured using only the CT scan and then only the MR. The contoured volumes were then compared to the original volume obtained from the fused images.

**Results:** CT and MRI studies can be accurately fused. Localization of the nerve and chiasm will be discussed.

**Discussion/Conclusion:** Given the sensitivity of the optic nerve to large doses of radiation, it is vital that accurate contouring is performed when creating a plan for stereotactic radiation.

## **RADIOGRAPHIC LYMPHOGRAPHY IN THE DOG USING IODIZED OIL.**

M.N. Mayer, T.I. Silver, C.K. Grier, J.M. Anthony. University of Saskatchewan, SK, S7N 5B4.

**Introduction/Purpose:** Unlike water-soluble contrast agents, iodized oil contrast material is retained within lymph nodes for several weeks to months following lymphography. Potential applications of this property include visualization of lymph nodes on kVp portal imaging for radiation patient positioning and assessment of interfractional node position changes. Our objective was to establish a clinically useful technique for radiographic lymphography of superficial lymph nodes and vessels in the dog using an iodized oil contrast agent.

**Methods:** 16 healthy research dogs were studied. Indirect lymphography was attempted using submucosal infusion at the level of the rostral maxilla, sublingual infusion, intramammary infusion, intradermal infusion in the ventrodorsal thoracic and abdominal regions and between the toe webs, and infusion into the digital pads. Direct lymphography was attempted using lymphatic vessels associated with the dorsal common digital veins, the collateral ulnar vein at the level of the elbow joint and the tail vein, as well as using the lymphatic vessels draining the mammary glands.

**Results:** Submucosal infusion of contrast into the labial aspect of the rostral maxilla reliably demonstrated the ipsilateral mandibular and retropharyngeal lymph nodes. Intradermal infusion in the ventrolateral thoracic and abdominal regions reliably demonstrated the axillary and superficial inguinal lymph nodes, while intradermal infusion between the toe webs of the paw demonstrated the superficial cervical (manus) and the popliteal and ipsilateral medial iliac lymph nodes (pes). Contrast infusion into a lymphatic vessel on the dorsal aspect of the paw demonstrated the superficial cervical lymph node (manus) and popliteal and ipsilateral medial iliac lymph nodes (pes), and intranodal infusion into the popliteal lymph node demonstrated the ipsilateral medial iliac lymph nodes. The superficial inguinal lymph nodes did not receive contrast material from the popliteal lymph nodes in any dog. Surgical catheterization of a lymphatic vessel on the dorsal aspect of the manus and pes was easily accomplished. The iodized oil was present in lymph nodes at 1 and 2 months after injection in 6 of the 6 dogs imaged at these timepoints. Approximately one-half of dogs that received intradermal infusions developed nonpainful swelling at the injection sites 14 to 28 days post injection. The swelling resolved within 7 to 10 days with no treatment.

**Discussion/Conclusion:** Indirect lymphography provides reliable radiographic visualization of the mandibular, retropharyngeal, superficial inguinal and axillary lymph nodes, while both direct and indirect methods can be used for the popliteal, medial iliac and superficial cervical lymph nodes. While direct lymphography is a more invasive technique, a higher rate of complications is associated with indirect methods.

## **A SURVEY OF VETERINARY RADIATION FACILITIES IN THE UNITED STATES DURING 2010.**

J. Farrelly<sup>1</sup>, M.C. McEntee.<sup>2</sup> <sup>1</sup>The Animal Medical Center, New York, NY 10065,  
<sup>2</sup>Cornell University Hospital for Animals, Ithaca, NY 14853.

**Introduction/Purpose:** The survey of veterinary radiation therapy facilities performed in 2001 by McEntee<sup>1</sup> was repeated for the calendar year 2010 to determine changes in the type of radiation equipment available, radiation protocols, case load, tumor types irradiated, and other details of the practice of radiation oncology.

**Methods:** The survey was updated to reflect changes in technology since the original study and was performed using an on-line survey website<sup>a</sup>. Invitations for the survey were sent and data collected using this website.

**Results:** A total of 52 sites were identified. The overall response rate is 63% (33/52 responded). Responders included 11 (33%) academic institutions, and 22 (67%) private practice external beam radiation facilities. Of respondents American College of Veterinary Radiology boarded radiation oncologists direct 100% of the radiation facilities at academic institutions and 20/22 (91%) of the private practice facilities. The majority of facilities (31/33, 94%) report having a linear accelerator with one facility having an orthovoltage radiation unit and two a cobalt unit in addition to a linear accelerator. One third (11/33) of facilities upgraded their equipment within the past five years. Nine sites reported having access to IMRT and 9 to radiosurgery equipment. Patient load information was available from 22 sites (42% of the radiation facilities surveyed), and based on the responses 2410 dogs and 680 cats were irradiated in 2010.

**Discussion/Conclusion:** Based on this survey there has been a substantial change in the types of equipment available at veterinary radiation facilities since 2001.

a Survey Monkey® [www.surveymonkey.com](http://www.surveymonkey.com)

1 McEntee, MC A survey of veterinary radiation facilities in the United States during 2001 Vet Radiol Ultrasound 2004;45:476–479.

**Friday October 14, 2011 (ACVR and RO simultaneous sessions)**

**ACVR**

- 7:00 am CT/MRI Society Meeting Pavilion IV - VI
- 7:30 am *Registration opens* Pavilion Landing
- 8:00 am CT/MRI Society Keynote Address  
**Applications of MRI in Human Orthopedic Sports Medicine**  
Charles P. Ho, PhD, MD, Director of Imaging Research, Steadman Philippon Research Institute, Vail, CO
- 9:00 am **CT/MRI Scientific Session 1 (Moderator: Dr. John Hathcock)**
- 9:00 am **Correlation of MRI Findings and Neurological Status in Great Danes with Cervical Spondylomyelopathy.**  
J. Gadbois, L. Blond, G. Beauchamp, J. Parent, Département de Sciences Cliniques, Faculté de Médecine Vétérinaire, Université de Montréal, St-Hyacinthe, Québec, Canada J2S 7C6.
- 9:12 am **Computed Tomographic Appearance of Equine Sinonasal Neoplasia and Comparison to Radiographic Findings.**  
D.D. Cissell<sup>1</sup>, E.R. Wisner<sup>1</sup>, J.F. Textor<sup>1</sup>, F.C. Mohr<sup>1</sup>, P.V. Scrivani<sup>2</sup>, A.P. Théon<sup>1</sup>.  
<sup>1</sup>School of Veterinary Medicine, University of California, Davis, CA 95616 and <sup>2</sup>College of Veterinary Medicine, Cornell University, Ithaca, NY 14853.
- 9:24 am **Dynamic CT Comparison of the Lumbosacral Region in Working German Shepherd Dogs (with and without Lumbosacral Disease) Versus Racing Greyhound Dogs (without Lumbosacral Disease).**  
Hartman AC\*, Worth AJ\*, Bridges JP, Blume L, Thompson DJ, Cogger N\*. \*Centre for Service and Working Dog Health, IVABS, Massey University, Palmerston North, NZ.
- 9:36 am **Cranial Thoracic Spinal Stenosis in Large Breed Dogs.**  
P.J. Johnson<sup>1</sup>, L. De Risio<sup>1</sup>, J.F. McConnell<sup>2</sup>, A.H. Sparkes<sup>1</sup>, R. Dennis<sup>1</sup>, A. Holloway<sup>1</sup>.<sup>1</sup> Animal Health Trust, Kentford, Newmarket, UK. <sup>2</sup> University of Liverpool Faculty of Veterinary Science, Liverpool, UK.
- 9:48 am **Imaging of the Canine Heart Using Non ECG-Gated 16 and ECG-Gated 64 Detector Computed Tomography.**  
D. Saulnier<sup>1</sup>, R. Tyson<sup>1</sup>, G.B. Daniel<sup>1</sup>, C. Ricco<sup>1</sup>, A. Lantis<sup>1</sup>, D. Entrikin<sup>2</sup>. <sup>1</sup>VA-MD Regional College of Veterinary Medicine, Department of Small Animal Clinical Sciences, Blacksburg, VA, 24061. <sup>2</sup>Wake Forest Baptist Medical Center, Department of Radiology, Winston Salem, NC, 27157.
- 10:00 am **Magnetic Resonance Imaging of the Canine Cranial Abdomen: Quantitative and Qualitative Evaluation of Various Imaging Sequences.**  
R. Manley, A.R. Matthews, F. Morandi, G.A. Henry, G. Conklin, K. Haifley. University of Tennessee College of Veterinary Medicine, Knoxville TN, 37996.

**Friday October 14, 2011, continued (ACVR and RO simultaneous sessions)**

**ACVR**

- 10:12 am      **Effect of Reconstruction Algorithm on Quantitative Analysis of Pulmonary Computed Tomography in Cats.**  
H. Polf, J. Polf, M. Fabiani. Texas Gulf Coast Veterinary Specialists, Houston, TX, 77027.
- 10:24 am      **Magnetic Resonance Imaging in Foals with Infectious Arthritis.**  
L. Gaschen, A. LeRoux, J. Trichel, G. Middleton, L. Riggs, H.H. Bragulla, N. Rademacher, D. Rodriguez. Department of Veterinary Clinical Sciences, Louisiana State University, Baton Rouge, USA.
- 10:30 am      *Break with Exhibitors* Pavilion I - III
- 11:00 am      **CT/MRI Scientific Session 2 (Moderator: Dr. Shannon Holmes)**
- 11:00 am      **Assessment of Extrahepatic Portosystemic Shunts Using Computed Tomography Angiography After Cellophane Band Attenuation.**  
N.C. Nelson, L.L. Nelson. Department of Small Animal Clinical Sciences, Michigan State University, East Lansing, MI, 48824.
- 11:12 am      **Computed Tomographic Features of Canine Segmental Caudal Vena Cava Aplasia.**  
T. Schwarz<sup>1</sup>, F. Rossi<sup>2</sup>, B. Åblad<sup>3</sup>, M.W. Beal<sup>4</sup>, J. Kinns<sup>4</sup>, G.S. seiler<sup>5</sup>, J.F. McConnel<sup>6</sup>, H. McAllister<sup>7</sup>, M. Costello<sup>8</sup>. <sup>1</sup>Royal (Dick) School of Veterinary Studies, UK EH10 4RP; <sup>2</sup>Clinica Veterinaria dell'Orologio, Italy, 40037; <sup>3</sup>Blue Star Animal Hospital, Sweden 41707; <sup>4</sup>Michigan State University, MI 48824; <sup>5</sup>North Carolina State University, NC 27606; <sup>6</sup>University of Liverpool, UK GL2 7JN; <sup>7</sup>University of Dublin, Ireland 4; <sup>8</sup>Diagnostic Imaging Service, UK GL2 7JN.
- 11:24 am      **Computed Tomographic Arthrography of the Canine Elbow.**  
A. Gendler, N.S. Keuler, S. Schaefer. University of Wisconsin-Madison School of Veterinary Medicine, Department of Surgical Sciences, Wisconsin, 53706.
- 11:36 am      **Evaluation of Ideal Limb Position for High Field Magnetic Resonance Imaging of the Equine Digit.**  
D.D.Cissell, M. Spriet. School of Veterinary Medicine, University of California, Davis, CA.
- 11:48 am      **Computed Tomography of Pleural Masses and Nodules in Six Dogs and One Cat.**  
J.A.Reetz, E.L. Buza, E. Krick. University of Pennsylvania School of Veterinary Medicine, Philadelphia, Pennsylvania, 19104.
- 12:00 pm      *Lunch* Sendero Ballroom

**Friday October 14, 2011, continued (ACVR and RO simultaneous sessions)**

**ACVR**

1:00 pm

**Poster Session with Authors**

Pavilion Court

**MRI Appearance of Progressive Ethmoid Hematoma in Four Horses.**

F.A. Castro<sup>1</sup>, E. Parente<sup>2</sup>, M. Leitch<sup>2</sup>, W. Mai<sup>1</sup>. <sup>1</sup>University of Pennsylvania, Ryan Veterinary Hospital, Philadelphia, PA 19104. <sup>2</sup>University of Pennsylvania, New Bolton Center, Kennett Square, PA 19348.

**Ultrasonographic Identification of Undescended Testes in Dogs and Cats.**

A Felumlee,<sup>1</sup> JK Reichle,<sup>1</sup> D Penninck,<sup>2</sup> A Dietze Yeager,<sup>3</sup> L Zekas,<sup>4</sup> J Goggin,<sup>5</sup> J Lowry.<sup>6</sup> 1. Animal Surgical & Emergency Center, West LA CA 90025; 2. Cummings School of Veterinary Medicine at Tufts University, North Grafton MA 01536; 3. Cornell University Hospital for Animals, Ithaca NY 14850; 4. Ohio State University College of Veterinary Medicine, Columbus OH 43210; 5. Metropolitan Veterinary Radiology, Ltd., Montclair NJ 07042; 6. Mountain Veterinary Imaging, Ft Collins CO 80526.

**CT And MRI Study of Equine Epiphyseal Development Towards Understanding Osteochondritis Dissecans (OCD).**

P. Fontaine<sup>†</sup>, L. Blond<sup>†</sup>, K Alexander<sup>†</sup>, E-N. Carmel<sup>†</sup> and S. Laverty<sup>†</sup>  
<sup>†</sup> Département de sciences cliniques, Faculté de Médecine Vétérinaire, Université de Montréal, Québec.

**MR Characterization of Vertebral Endplate Changes in the Dog.**

Karine Gendron<sup>1</sup>, Marcus Doherr<sup>1</sup>, Patrick Gavin<sup>2</sup>, Johann Lang<sup>1</sup>. <sup>1</sup> University of Bern, Switzerland, <sup>2</sup> MR Vets, Inc, Ponderay, ID 83852.

**Radiographic and Magnetic Resonance Imaging of the Equine Foot: A Focus on the Sole.**

I.N.M. Grundmann, W.T. Drost, L.J. Zekas, J.K. Belknap, R.B. Garabed, S.E. Weisbrode, M.V. Knopp, J. Maierl. The Ohio State University, OH 43210, Ludwig-Maximilians University, Munich 80539, Germany.

**Agreement Between T2 and Haste (Half-Fourier-Acquisition Single-Shot Turbo Spin-Echo) Sequences in the Evaluation of Intervertebral Disc Disease in Dogs.**

J.M. Mankin, S. Hecht, W.B. Thomas. Department of Small Animal Clinical Sciences, University of Tennessee College of Veterinary Medicine, Knoxville, TN 37996-4544.

**Airspace Disease in Dogs Detected During Computed Tomography.**

N.Holmes<sup>1</sup>, P.Scrivani<sup>1</sup>, M.Thompson<sup>1</sup>, N.Dykes<sup>1</sup>, J.Gerdin<sup>2</sup>, T.Southard<sup>2</sup>. <sup>1</sup>Department of Clinical Sciences, <sup>2</sup>Department of Biomedical Sciences, Cornell University College of Veterinary Medicine, Ithaca, NY 14853.

**Imaging Findings in Dogs with Caudal Intervertebral Disc Herniation.**

C.M. Lawson, J.K. Reichle, T. McKlveen, M.O. Smith. Animal Surgical & Emergency Center, Los Angeles, California 90025.

Friday October 14, 2011, continued (*ACVR and RO simultaneous sessions*)

**ACVR**

**Feasibility of Computed Tomography in Conscious Canine Patients with Pelvic Fracture.**

Kichang Lee<sup>1</sup>, Jimo Chung<sup>1</sup>, Jinwon Kim<sup>1</sup>, Haebeom Lee<sup>1</sup>, Minsu Kim<sup>1</sup>, Namsoo Kim<sup>1</sup>, Hock Gan Heng<sup>2</sup>, Jacob J Rohleder<sup>2</sup>, James F Naughton<sup>2</sup>. <sup>1</sup> Chonbuk National University, Chonbuk Animal Medical Center, Jeonju, 561-756 Republic of Korea and <sup>2</sup>Purdue University, Department of Veterinary Clinical Sciences, West Lafayette, IN 47907.

**Magnetic Resonance Imaging of Canine Mast Cell Tumors.**

E. Pokorny, S. Hecht, P.A. Sura, A.K. LeBlanc, J. Phillips. Department of Small Animal Clinical Sciences, University of Tennessee College of Veterinary Medicine, Knoxville, TN 37996.

**Sonographic Appearance and Average Size of the Normal Feline Spleen.**

<sup>1</sup>R.S. Sayre, <sup>2</sup>K.A. Spaulding. <sup>1</sup>Department of Small Animal Clinical Sciences, College of Veterinary Medicine, Texas A&M University, TX 77843. <sup>2</sup>Department of Large Animal Clinical Sciences, College of Veterinary Medicine, Texas A&M University, TX 77843.

**Visceral Fat Measured with CT Correlates with Adverse Cardiac Changes in Obese Dogs.**

T.I. Silver, J. Adolphe, L.P. Weber. WCVU, University of Saskatchewan, SK, S7N 5B4.

**Estimation of Feline Renal Volume Using Computed Tomography and Ultrasound.**

S.A. Logsdon, R. Tyson, G.B. Daniel, S.R. Werre. VA-MD Regional College of Veterinary Medicine, Blacksburg, VA 24061.

1:30 pm **Large Animal Diagnostic Imaging Society (LADIS) Scientific Session 1 (Moderator: Dr. Bunita Eichelberger)**

1:30 pm **Spontaneous Echocardiographic Contrast in Horses: Incidence and Significance.**

N. W. Rantanen. Fallbrook, CA 92088.

1:48 pm **Elastographic Evaluation of Normal Tendons and Ligaments of the Equine Distal Forelimb.**

G.S. Seiler, M. Lustgarten, W.R. Redding. North Carolina State University, NC 27607.

2:06 pm **Effects of Alpha-2 Adrenergic Agonist Sedation on the Ultrasonographic Evaluation of Gastrointestinal Motility in the Adult Horse.**

D.A. Neelis, R.L. Tucker, J.S. Mattoon, G.D. Roberts. Washington State University, WA, 99163.

**Friday October 14, 2011, continued (ACVR and RO simultaneous sessions)**

**ACVR**

- 2:24 pm **Simulated Occupational Personnel Scatter Radiation Exposure for Radiography of the Equine Stifle.**  
R. Tyson, D.C. Smiley, R.S. Pleasant, G.B. Daniel. Virginia-Maryland Regional College of Veterinary Medicine. Blacksburg, VA 24061.
- 2:42 pm **Magnetic Resonance and Radiographic Diagnosis of Osseous Resorption at the Attachment of the Distal Sesamoidean Impar Ligament on the Distal Phalanx in the Horse.**  
A.C. Young, A.N. Dimock, S.M. Puchalski, M. Spriet. University of California, Davis, CA 95616.
- 3:00 pm *Break with Exhibitors* Pavilion I - III
- 3:30 pm **LADIS Scientific Session 2 (Moderator: Dr. Lisa Neuwirth)**
- 3:30 pm **Characterization of the Pulmonary System in Alpacas without Thoracic Disease Using Computed Tomography.**  
SB Cooley, SM Stieger-Vanegas. Department of Clinical Sciences, College of Veterinary Medicine, Oregon State University, Oregon, 97333.
- 3:48 pm **Comparison of MRI and Computed Tomography Arthrography for Identification of Pathologic Change in the Equine Stifle.**  
N.M. Werpy\*, C.P. Ho\*\*, C.E. Kawcak\*. \*Colorado State University, CO, 80523; \*\*Steadman Philippon Research Institute CO, 81658.
- 4:06 pm **Evaluation of an FSE T2 Weighted Sequence with Varying Echo Time to Reverse the Magic Angle Effect in the Collateral Ligaments of the Distal Interphalangeal Joint in Horses.**  
N.M. Werpy\*, C.P. Ho\*\*, E.B. Garcia\*\*\* C.E. Kawcak\*. \*Colorado State University, CO, 80523; \*\*Steadman Philippon Research Institute, CO, 81658; \*\*\*Louisiana State University, LA, 70803.
- 4:24 pm **Magnetic Resonance Imaging Characteristics of Confirmed Navicular Bursa Adhesions and Response to Treatment.**  
M. E. Holowinski, M. Solano, J. Garcia-Lopez, L. Maranda, Tufts Cummings School of Veterinary Medicine, MA, 01536.
- 4:42 pm **Clinical Significance and Prognosis of DDFT Lesions Assessed Overtime Using Standing Equine MRI.**  
M.Vanel\*, J.Olive\*, S.GoldΦ, ‡R.D.Mitchell, δL.Walker. \*University of Montreal, Saint-Hyacinthe, QC, Canada; ΦB.W. Furlong and Associates, Oldwick, NJ; ‡Fairfield Equine Associates, Newtown, CT; δCalifornia Equine Orthopedics, San Marcos, CA.
- 5:00 pm *Adjourn for the Day*

## **CORRELATION OF MRI FINDINGS AND NEUROLOGICAL STATUS IN GREAT DANES WITH CERVICAL SPONDYLOMYELOPATHY.**

J. Gadbois, L. Blond, G. Beauchamp, J. Parent, Département de Sciences Cliniques, Faculté de Médecine Vétérinaire, Université de Montréal, St-Hyacinthe, Québec, Canada J2S 7C6.

**Introduction/Purpose:** Great Dane is one of the breeds commonly affected with cervical spondylomyelopathy (CSM). There is scarce information regarding magnetic resonance imaging (MRI) findings, their progression and clinical relevance in CSM-affected Great Danes. The purpose of this study is to describe MRI features of Great Danes affected with CSM and evaluate the correlation with the neurological status and its progression over time, to ascertain if MRI findings could predict clinical outcome.

**Methods:** Medical records of Great Danes diagnosed with CSM and treated medically were reviewed. Results of neurological examinations and high field MRI of the cervical spine were reviewed. The owners were contacted for an additional follow-up examination at least 6 months following the first MRI study. Morphologic and morphometric evaluation of all MR images was done. The relationship between neurological status, MRI findings and clinical outcome was then statistically assessed ( $p < 0.05$ ).

**Results:** Fourteen CSM-affected Great Danes were included in this study, all with MRI abnormalities. Multiple extradural compressive spinal cord lesions were observed in all dogs, affecting mainly C4-C5, C5-C6 and C6-C7 intervertebral spaces. Magnetic resonance abnormalities by order of frequency included: articular facet enlargement (13), intervertebral foraminal stenosis (12), intervertebral disk degeneration (12), extradural synovial cysts (11), intervertebral disk protrusion (10), intramedullary hyperintensity on T2-weighted images (10), ligamentum flavum hypertrophy (8), and syringomyelia (2). There was a positive association between neurological status and severity of spinal cord compression ( $p=0.003$ ). The neurological status was significantly worse when the number of sites of spinal cord compression increased ( $p=0.01$ ), when there were articular facet changes ( $p=0.008$ ) and with presence of foraminal stenosis ( $p=0.03$ ). Only a higher ratio of the height of spinal cord over the height of vertebral canal on sagittal images was significantly associated with a worsened long term clinical progression ( $p < 0.05$ ). Five dogs had MRI re-evaluation; there was no significant difference with the initial MRI findings.

**Discussion/Conclusion:** In a population of CSM-affected Great Danes, the severity of spinal cord compression on MRI is significantly correlated to the neurological status. Other MRI findings such as the number of compression sites, articular facet changes or foraminal stenosis all negatively correlated with the neurological status. The present study has also shown that some parameters of the morphometric evaluation could be used to predict the clinical outcome of CSM-affected Great Danes.

## **COMPUTED TOMOGRAPHIC APPEARANCE OF EQUINE SINONASAL NEOPLASIA AND COMPARISON TO RADIOGRAPHIC FINDINGS.**

D.D. Cissell<sup>1</sup>, E.R. Wisner<sup>1</sup>, J.F. Textor<sup>1</sup>, F.C. Mohr<sup>1</sup>, P.V. Scrivani<sup>2</sup>, A.P. Théon<sup>1</sup>.

<sup>1</sup>School of Veterinary Medicine, University of California, Davis, CA 95616 and <sup>2</sup>College of Veterinary Medicine, Cornell University, Ithaca, NY 14853.

**Introduction/Purpose:** Neoplasia of the nasal cavity and paranasal sinuses comprises 2-19% of equine sinonasal disorders diagnosed at referral equine hospitals. Other causes of space occupying masses of the nasal cavities and paranasal sinuses may be difficult to differentiate from neoplasia due to similar clinical, radiographic, and endoscopic features. The purpose of this report is to describe the pertinent CT imaging features of sinonasal neoplasia in horses. A secondary objective is to compare CT findings to those of skull radiographs.

**Methods:** The computed tomographic (CT) features of tumors involving the nasal cavity and/or paranasal sinuses of 15 horses were reviewed retrospectively. When available, radiographs were also reviewed and compared to CT findings.

**Results:** The 15 tumors included 5 neuroendocrine tumors / neuroblastomas, 2 undifferentiated carcinomas, 2 myxosarcomas, and 1 each of nasal adenocarcinoma, hemangiosarcoma, chondroblastic osteosarcoma, anaplastic sarcoma, myxoma, and ossifying fibroma. All of the tumors except the ossifying fibroma were iso- or hypoattenuating relative to masseter muscle. Thirteen of fifteen tumors exhibited moderate or marked osteolysis of adjacent cortical bone. Ten horses had moderate or marked involvement of the cribriform plate and 6 had clear intracranial extension of the mass. CT features were compared to radiographic findings for 10 horses. A mass or mass effect was observed in 10/10 radiographic studies and mass involvement of the caudal and rostral maxillary sinuses was correctly identified in most horses. Radiographs were least sensitive for identifying mass involvement of the sphenopalatine sinus, cranium, and retrobulbar space. Radiographs also underestimated potential features of malignancy, such as severity of osteolysis and osseous production.

**Discussion/Conclusion:** CT features of equine sinonasal neoplasia include iso- or hypoattenuating, homogeneous soft tissue masses with poorly defined margins and moderate to marked osseous destruction. Radiographs are a useful screening tool for identification of sinonasal masses, but CT provides greater information regarding mass extent, features of malignancy, and important prognostic indicators e.g. intracranial invasion.

## **DYNAMIC CT COMPARISON OF THE LUMBOSACRAL REGION IN WORKING GERMAN SHEPHERD DOGS (WITH AND WITHOUT LUMBOSACRAL DISEASE) VERSUS RACING GREYHOUND DOGS (WITHOUT LUMBOSACRAL DISEASE).**

Hartman AC\*, Worth AJ\*, Bridges JP, Blume L, Thompson DJ, Cogger N\*. \*Centre for Service and Working Dog Health, IVABS, Massey University, Palmerston North, New Zealand.

**Introduction/Purpose:** Lumbosacral (LS) degeneration is a common career-limiting disease of working German Shepherd Dogs (GSD). Previous studies have shown the significance of the facet angle difference between L6/7 and the LS junction and sacral laminar overhang between GSD and other breeds. Recently there has been a focus on the L7/S1 intervertebral foramen and surgical procedures have been advocated which address static and/or dynamic nerve root compression. This study was designed to establish the significance of L7/S1 foraminal narrowing and to help determine any anatomical predisposing factors to LS degeneration in the GSD as compared to the Greyhound (GH).

**Methods:** Nine working police GSD and 11 racing GH dogs with no historical or neurological signs of LS disease and 6 working police GSD with signs of LS disease are included in this study. A CT was performed in flexed, neutral and extended LS positions with quantitative assessment of motion, facet angle, L7 and sacral laminar overhang, LS disk pivot point, and foraminal volume. Statistical analysis was performed.

**Results:** The difference in facet angle between the L6/7 and L7/S1 articulations was similar in unaffected GSD and GH (mean difference = 14). The difference in angle was higher in the affected GSD (mean difference = 33) as compared to unaffected GSD. There was no significant difference in the longitudinal range of motion of the LS functional unit between groups, although there was a trend for the GH to be able to extend more, although flex less, than the GSD.

An elongated sacral lamina is highly associated with reduced longitudinal extension of the LS functional unit, often found in the GSD. The L7 caudal laminar overhang, seen more significantly in the GSD, appears to be associated with this reduced motion. The extended foraminal volumes are smaller in GSD as compared to GH. This loss of volume is primarily in the caudal aspect of the foramen.

**Discussion/Conclusion:** The difference in transverse facet angle between LS and L6/7 is much larger in the affected GSD as compared to the unaffected GSD and GH. This is likely a significant predisposing factor for LS disease in GSD and may be valuable for screening working dogs with further study. The sacral lamina appears to interfere with the L7 caudal lamina in GSD with sacral laminar overhang and limits the ability to extend in the longitudinal plane. Foraminal volume is smaller during extension in the GSD as compared to the GH, primarily in the caudal foramen although no significant difference is noted in the affected GSD as compared to the unaffected.

## **CRANIAL THORACIC SPINAL STENOSIS IN LARGE BREED DOGS.**

P.J. Johnson<sup>1</sup>, L. De Rasio<sup>1</sup>, J.F. McConnell<sup>2</sup>, A.H. Sparkes<sup>1</sup>, R. Dennis<sup>1</sup>, A. Holloway<sup>1</sup>. <sup>1</sup> Animal Health Trust, Kentford, Newmarket, UK. <sup>2</sup> University of Liverpool Faculty of Veterinary Science, Liverpool, UK.

**Introduction/Purpose:** Developmental stenosis of the cranial thoracic spinal canal has been suggested to occur in large breed dogs, and is documented in the Dogue de Bordeaux (DdB). The purposes of the study were to investigate developmental cranial thoracic stenosis (CTS) further by calculation of reference data in large breed dogs and to determine whether morphometric and/or subjective criteria could be used to characterise CTS.

**Methods:** Magnetic Resonance Imaging (MRI) studies of large breed dogs (>20kg) which included transverse images of the 1<sup>st</sup> to 5<sup>th</sup> thoracic vertebrae were evaluated for the period 2001-2011. A single, blinded observer graded the morphological appearance of the vertebral canal and spinal cord as grade 0 controls (no bony stenosis), grade 1 moderately stenotic (stenosis without cord compression) or grade 2 severely stenotic (stenosis with cord compression). Morphometric analysis consisted of cross-sectional area measurements of the vertebral canal at mid-vertebral and intervertebral disc levels to form the canal-area ratio (CAR) and of the spinal cord and vertebral canal at the intervertebral disc level to form the cord-canal ratio (CCR). Normal reference ranges were calculated for CAR and CCR and agreement between the subjective grading and objective data was evaluated. The signalment, neurological presentation and morphological features of CTS were documented.

**Results:** Seventy-seven MRI studies of the cranial thoracic spine were included. Fifty-eight were graded as controls (grade 0) and 19 as moderately or severely stenotic (grade 1 or 2 respectively). Statistically there was a significant difference in CAR and CCR values at different thoracic vertebral sites and between breeds in the control group. CAR discriminated better between the control and stenosis cases than CCR. When comparing the ratios with the subjective grading system CCR had poor agreement even with the use of breed specific reference ranges whereas CAR had substantial agreement when breed specific reference ranges were utilized. CTS was recognized in predominantly young (most < 3 years old) dogs. Breeds affected included the DdB, Neapolitan mastiff, Bullmastiff, Chow Chow, St Bernard, Staffordshire Bull terrier, German Shepherd Dog, Rottweiler and Doberman. Vertebral morphological changes included enlarged pedicles, facet hypertrophy, altered vertebral body shape and dorsal lamina cleft formation. In 10/19 of the dogs, CTS was the only spinal abnormality. Eight of these dogs had pelvic limb ataxia and postural reaction deficits and two were neurologically normal. 9/19 cases had concurrent neurological disease of which cervical stenotic myelopathy was the most common.

**Discussion/Conclusion:** Within the control group there was significant variation between breeds and between sites. Ideally, breed-specific reference ranges should be generated for the ratios at each vertebral site. CAR gave a better discrimination between the control and stenosis cases and had better agreement with the subjective grading system than CCR. CTS should be a differential diagnosis in young large breed dogs that present with pelvic limb neurological dysfunction. CTS may be subclinical and should be considered in dogs with cervical stenotic myelopathy.

## **IMAGING OF THE CANINE HEART USING NON ECG-GATED 16 AND ECG-GATED 64 DETECTOR COMPUTED TOMOGRAPHY.**

D. Saulnier<sup>1</sup>, R. Tyson<sup>1</sup>, G.B. Daniel<sup>1</sup>, C. Ricco<sup>1</sup>, A. Lantis<sup>1</sup>, D. EntriKin<sup>2</sup>. <sup>1</sup>VA-MD Regional College of Veterinary Medicine, Department of Small Animal Clinical Sciences, Blacksburg, VA, 24061. <sup>2</sup>Wake Forest Baptist Medical Center, Department of Radiology, Winston Salem, NC, 27157.

***Introduction/Purpose:*** ECG-gated multidetector computed tomography (MDCT) is an imaging modality widely utilized for the evaluation of cardiac pathology in human patients. However, there has been little research of MDCT cardiac imaging in veterinary patients. Presently, ECG-gating is an expensive upgrade for MDCT, which few veterinary institutions currently possess. The purpose of this study was to compare image quality between a 16 non ECG-gated and 64 ECG-gated MDCT for clinically important veterinary cardiac anatomy in dogs.

***Methods:*** In a double crossover design, six purpose-bred dogs were scanned using 16 non ECG-gated and 64 ECG-gated MDCT. A standardized anesthetic protocol, designed to induce bradycardia (mean HR 45 bpm  $\pm$  12.6) was used. For each study, a pre and post contrast scan was performed. Post contrast scans were obtained after intravenous injection of 0.45 ml/kg of non-ionic iodinated contrast medium (370 mgI/ml) using a pressure injector at a rate of 0.8 ml/sec. Five sequential post-contrast scans through the heart were performed for each patient when utilizing the 16 non ECG-gated MDCT, in an attempt to obtain a motion free series of images of the heart. Mean scan time following the initiation of contrast administration was 91.2s. Scan initiation time was chosen to optimize contrast density and homogeneity within the right and left heart. For each scan, assessment of cardiac morphology was performed by evaluating a group of cardiac structures using a 5-point scale. From this, a quality score (QS) was derived for each individual scan. The maximum QS for each patient's study on the 16 non ECG-gated MDCT was compared to the 64 ECG-gated MDCT using a paired student t-test. Similar comparisons were made using the median and minimum QS.

***Results:*** The maximum QS of the 16 non ECG-gated and 64 ECG-gated studies were not significantly different ( $p < 0.05$ ). The median and minimum QS from each patient's study for the 16 non ECG-gated scans were statistically lower than the 64 ECG-gated MDCT ( $p < 0.05$ ).

***Discussion/Conclusion:*** A 16 non ECG-gated MDCT scanner can produce cardiac images which are of similar quality, based on clinically important veterinary cardiac anatomy, to those of a 64 ECG-gated MDCT. Cardiac motion negatively impacts image quality in studies acquired without ECG-gating. However, this can be overcome by performing multiple sequential scans through the heart.

## **MAGNETIC RESONANCE IMAGING OF THE CANINE CRANIAL ABDOMEN: QUANTITATIVE AND QUALITATIVE EVALUATION OF VARIOUS IMAGING SEQUENCES.**

R. Manley, A.R. Matthews, F. Morandi, G.A. Henry, G. Conklin, K. Haifley. University of Tennessee College of Veterinary Medicine, Knoxville TN, 37996.

**Introduction/Purpose:** Artifacts, especially motion secondary to respiration, are a major limitation of abdominal magnetic resonance imaging (MRI). Technical advances in hardware and software and the implementation of faster sequences have allowed the acquisition of MR images that have short acquisition times and greatly reduce artifact secondary to motion, while concurrently providing excellent anatomic detail. The study objective was to quantitatively and qualitatively compare selected MR sequences for imaging of the canine cranial abdomen.

**Methods:** Sixteen MR sequences were evaluated in 10 normal dogs including sequences designed to minimize artifacts, such as breath-holding and respiratory navigation, as well as traditional spin echo sequences. Subjective evaluation of specific organs and overall sequence quality was performed by 4 observers independently. Common artifacts were identified and their effects on the specific organs were subjectively graded. For a quantitative comparison, signal-to-noise ratio (SNR) and contrast-to-noise ratio (CNR) were calculated for each sequence.

**Results:** The sequence with the overall highest mean diagnostic quality score was the dorsal T2 turbo spin echo (TSE) with breath-holding; however, only one observer ranked this the most diagnostic study. The dorsal T2 half Fourier acquisition single shot turbo spin echo (HASTE) with respiratory navigation was selected as the sequence with the highest diagnostic quality by two observers while the transverse T1 gradient echo (GRE) with breath-holding was chosen by one observer. The sequence with the lowest mean diagnostic quality score was the dorsal T2 fast spin echo (FSE), and was selected by 2 observers as the least diagnostic sequence. The sequence with the highest SNR for all evaluated organs was the sagittal T1 spin echo. The SNR/CNR did not correlate with the subjective assessment of overall diagnostic quality for the majority of the sequences evaluated ( $p < 0.05$ ).

**Discussion/Conclusion:** While the observed diagnostic quality did not correlate with the SNR or CNR, the MR sequences utilizing motion-minimizing techniques such as breath-holding and respiratory navigation were considered to have the highest diagnostic quality by our observers, and should be considered as part of a canine abdominal MR protocol.

## **EFFECT OF RECONSTRUCTION ALGORITHM ON QUANTITATIVE ANALYSIS OF PULMONARY COMPUTED TOMOGRAPHY IN CATS.**

H. Polf, J. Polf, M. Fabiani. Texas Gulf Coast Veterinary Specialists, Houston, TX, 77027.

**Introduction/Purpose:** Quantitative computed tomography (CT) of the lungs is a valuable diagnostic tool to evaluate pulmonary disease in humans. The purpose of this study was to evaluate the histogram properties of computed tomographic images of the lungs of normal cats, evaluate mean lung attenuation of normal cats, and evaluate the effect of reconstruction algorithm on the appearance of the histogram and the mean lung attenuation. The null hypothesis was that the CT reconstruction algorithm would have no effect on histogram properties or mean lung attenuation.

**Methods:** *Animals* – Twenty-one cats both from the institution's blood donor colony and employee volunteer pets were imaged. Normality of the lungs was determined based on lack of history of respiratory disease, physical exam, complete blood count, chemistry panel, and negative heartworm antigen and antibody, and negative FeLV and FIV tests. A board certified radiologist blinded to the identity of the cats reviewed the CT images to determine if the images of the lungs were normal. *CT image acquisition* – Cats were anesthetized, intubated, and positioned in dorsal recumbency. CT data were acquired using a General Electric Light Speed 4-slice machine using a helical technique with slice thickness of 2.5 mm and collimator pitch of 1.5. Technique was 120 kVp with 190 mAs. Images were reconstructed using a lung, edge and detail reconstruction algorithm. Matrix size was 512 x 512. CT images were analyzed at lung settings (window width, 1500; window level -600). *Data analysis* – CT Images were segmented using Segmenting Assistant plug-in for Image J image analysis program from the NIH. Pixels with Hounsfield unit (HU) values of less than -998 and greater than -254 were set to zero. Histograms of voxel frequency for each CT number were created using the segmented data. Mean lung attenuation or density was calculated.

**Results:** Ten cats were considered normal. For normal cats, the average attenuation of the lung tissue using the lung algorithm was -874 HU +/- 6 HU. Analysis of variance was performed to determine the effect of reconstruction algorithm on mean lung attenuation measurements for all cats. A significant difference (1% significance level) was found in lung attenuation measurements between lung and edge and lung and detail algorithms. No significant difference was found in mean lung attenuation when comparing edge and detail algorithms. Kurtosis and skewness of the histogram was affected by reconstruction algorithm.

**Discussion/Conclusion:** Reconstruction algorithm can have a significant effect on lung attenuation measurements and histogram appearance and should be kept constant when comparing lung attenuation and histogram properties in cats.

## **MAGNETIC RESONANCE IMAGING IN FOALS WITH INFECTIOUS ARTHRITIS.**

L. Gaschen, A. LeRoux, J. Trichel, G. Middleton, L. Riggs, H.H. Bragulla, N. Rademacher, D. Rodriguez. Department of Veterinary Clinical Sciences, Louisiana State University, Baton Rouge, USA.

**Introduction/Purpose:** MRI findings have not been reported to assess foals with joint effusion, infectious arthritis, and osteomyelitis of the distal extremities. The purpose of this study is to describe MRI findings in foals with non-infectious and infectious arthritis and to correlate these findings with currently accepted diagnostic tests. We hypothesize that abnormalities in the articular cartilage and bone of the epiphysis, metaphysis and physis can be diagnosed better with MRI than radiography.

**Methods:** Client-owned foals younger than four months of age that presented with joint effusion, pain and swelling affecting the fetlock, carpus and/or tarsus were included in the study. Joint fluid analysis, digital radiographic and MRI examinations were performed in each foal. Foals were categorized into two groups, septic and non-septic arthritis, based on joint fluid analysis. The following pulse sequences were performed on each affected joint: Sagittal T2W, STIR, 3D RSSG Water Excitation and PD, transverse PD and T2W and dorsal T2W pulse sequences.

**Results:** A total of 28 joints were examined in six septic, three non-septic and one control foal ranging in age from 1.5 to 16 weeks. A total of 14 septic joints and seven non-septic joints were examined in nine foals. Nineteen osseous lesions in six septic joints were detected with MRI and only four of these lesions were detected radiographically. T2W, STIR and PD pulse sequences demonstrated 19 hyperintense osseous lesions with a hypointense halo in six different joints in four of the six septic foals, but not in those with non-septic arthritis nor in the control. All except for one lesion was hyperintense on additional 3D RSSG Water Excitation pulse sequences and the contrast with the signal void of the surrounding bone made them stand out more than on other pulse sequences. Four lesions were epiphyseal, four metaphyseal, five physeal, five in cuboidal bones and one lesion was detected in articular cartilage. The three foals with non-septic arthritis showed no bone lesions in MRI or radiographically. Four of the six foals with septic arthritis had to be euthanized due to the severity of the disease. These foals had a minimum of one to maximal six MRI osseous lesions per joint, whereas two of the surviving septic arthritis foals had no bone lesions.

**Discussion/Conclusion:** MRI appears to be better than radiography in the detection of osseous lesions in foals diagnosed with infectious arthritis. Hyperintense T2W, STIR, PD and 3D RSSG Water Excitation osseous lesions were the most common abnormalities in septic joints. Foals with infectious arthritis are more likely to have heterogeneous signals in the synovial fluid compared to those with non-septic arthritis. Assessment of cartilage damage with MRI warrants further investigation and comparisons with histology. The results of this study warrant further investigation as to the predictive value of the presence of osteomyelitis detected in MRI and prognosis. Osteomyelitis may be clinically indistinguishable from septic arthritis and pre-intervention MRI may be a future screening test for early disease.

## **ASSESSMENT OF EXTRAHEPATIC PORTOSYSTEMIC SHUNTS USING COMPUTED TOMOGRAPHY ANGIOGRAPHY AFTER CELLOPHANE BAND ATTENUATION.**

N.C. Nelson, L.L. Nelson. Department of Small Animal Clinical Sciences, Michigan State University, East Lansing, MI, 48824.

**Introduction/Purpose:** Extrahepatic portosystemic shunts (EHPSS) are congenital, anomalous vessels joining the portal and systemic venous circulations. Different surgical treatments of EHPSS have been described, but circumferential cellophane band placement has been recently advocated as a method of attenuation. These bands result in local inflammation and fibrosis, leading to gradual shunt attenuation. The purpose of this study was to describe the degree of shunt attenuation by cellophane bands as assessed by computed tomography (CT) angiography, and to assess changes in hepatic and portal vein size after surgical intervention.

**Methods:** 18 dogs with extrahepatic portosystemic shunts were recruited. CT angiography was performed on the dogs prior to surgical intervention, then again between six months and one year after surgery. The location of cellophane band placement was recorded and the degree of shunt closure was measured on CT images. The hepatic volumes were measured from CT images and divided by volume of the second lumbar vertebra (to account for differences in patient size over time). The diameter of the portal vein was measured and divided by the aortic diameter. A paired t-test compared the portal vein:aorta ratio and hepatic volume:vertebra volume between pre- and post-operative CT examinations.

**Results:** Hepatic:vertebrae and portal vein:aorta ratios increased significantly between pre- and post-operative examinations. The cellophane band completely attenuated or nearly completely attenuated (<2.5 mm residual shunt diameter) the shunt vessel in 16/18 dogs. The cellophane band was not ideally positioned in 6/18 dogs. In these dogs, either anastomosing vessels still connected portal and systemic venous circulation or small tributary vessels (usually from the left side of the stomach) were seen to enter the shunt distal to the site of attenuation. One dog developed acquired portosystemic shunts. Cystolith analysis was performed on calculi identified on computed tomography studies in three dogs and confirmed ammonium urate composition.

**Discussion/Conclusion:** Cellophane bands cause near complete or complete shunt attenuation in most dogs and result in relative increases in hepatic volume and portal vein diameter. Proper placement of the cellophane is important to prevent persistent communication between venous and portal circulations, but increases in hepatic volume and portal vein size occurred even in cases with poor band placement. Urate cystoliths are identifiable on computed tomography.

## **COMPUTED TOMOGRAPHIC FEATURES OF CANINE SEGMENTAL CAUDAL VENA CAVA APLASIA.**

T. Schwarz<sup>1</sup>, F. Rossi<sup>2</sup>, B. Åblad<sup>3</sup>, M.W. Beal<sup>4</sup>, J. Kinns<sup>4</sup>, G.S. seiler<sup>5</sup>, J.F. McConnel<sup>6</sup>, H. McAllister<sup>7</sup>, M. Costello<sup>8</sup>. <sup>1</sup>Royal (Dick) School of Veterinary Studies, UK EH10 4RP; <sup>2</sup>Clinica Veterinaria dell'Orologio, Italy, 40037; <sup>3</sup>Blue Star Animal Hospital, Sweden 41707; <sup>4</sup>Michigan State University, MI 48824; <sup>5</sup>North Carolina State University, NC 27606; <sup>6</sup>University of Liverpool, UK GL2 7JN; <sup>7</sup>University of Dublin, Ireland 4; <sup>8</sup>Diagnostic Imaging Service, UK GL2 7JN.

**Introduction/Purpose:** Absence of the prerenal segment of the abdominal caudal vena cava (CVC) has been reported as a very rare congenital anomaly in the dog since the mid 19<sup>th</sup> century, but much more frequently in the last decade, due to increased use of advanced imaging techniques such as ultrasound, computed tomography (CT) and magnetic resonance imaging. The condition has been linked with severe complications such as thrombosis and with other vascular anomalies such as portosystemic shunts. Purpose of this study was to review the clinical data and CT features of canine segmental caudal vena cava aplasia.

**Methods:** A retrospective study was performed reviewing CT archives of multiple institutions for dogs with segmental CVC aplasia. Inclusion criteria included a diagnostic quality CTA study, supportive diagnostic and follow-up information. Abdominal vessels were reviewed for size, shape, location and course including tributaries and branches and classified as normal, abnormal or shunt vessels.

**Results:** Ten dogs with segmental CVC aplasia were identified. In all dogs post renal caval blood was shunted to either a right or left azygos vein, with 8 different angiographic patterns. Affected dogs were predominantly female and young. Additional portocaval or portoazygos shunt vessels were identified in 5 cases. CT angiography (CTA) depicted details of abdominal vessels including thrombus formation in one dog.

**Discussion/Conclusion:** Canine segmental CVC aplasia is frequently associated with portosystemic shunts and rarely with thrombosis. The shunt vessels can connect to the prehepatic CVC intra- or extrahepatically, or they can feed into the CVC-azygos shunt vessel, partially or completely. CTA is an excellent tool to demonstrate the complex vascular anatomy and to guide treatment planning for portosystemic shunts and thrombolytic therapy.

## **COMPUTED TOMOGRAPHIC ARTHROGRAPHY OF THE CANINE ELBOW.**

A. Gendler, N.S. Keuler, S. Schaefer. University of Wisconsin-Madison School of Veterinary Medicine, Department of Surgical Sciences, Wisconsin, 53706.

**Introduction/Purpose:** Assessment of the articular cartilage of the elbow is an important aspect of the clinical evaluation of elbow joint dysfunction. Osteochondral lesions of the human elbow are commonly evaluated with computed tomographic arthrography (CTA). To date, no investigation has been conducted to evaluate CTA of the canine elbow joint. The purpose of this investigation was to determine if positive contrast CTA of the canine elbow would accurately and precisely depict articular cartilage thickness and establish the optimal contrast concentration.

**Methods:** Thirty-two canine cadaver elbows were examined with a multidetector CT scanner (0.625 mm slice thickness, bone algorithm) before and after intra-articular administration of iohexol at one of three different concentrations (150 mg I/ml, 75 mg I/ml or 37.5 mg I/ml). Articular cartilage thickness was measured on both the CTA images and corresponding histologic specimens. CTA derived cartilage thickness data was compared to the reference standard by way of Bland-Altman analysis. The bias and standard deviation of different groups were compared with paired student t-tests and/or ANOVA (analysis of variance). Levene's median test was conducted to determine the level of measurement precision.

**Results:** The mean difference (bias  $\pm$  SD) between the CTA and histomorphologic measurements of the articular cartilage thickness was 0.18 mm  $\pm$  0.11 in the dorsal plane and 0.19 mm  $\pm$  0.09 in the sagittal planar image reformations. The mean bias and precision of CTA measurements made in the sagittal or dorsal reformations were not significantly different ( $p = 0.76$ ) from one another. The mean difference (bias  $\pm$  SD) between the CTA and histomorphologic measurements was 0.17 mm  $\pm$  0.11, 0.23 mm  $\pm$  0.09, and 0.18 mm  $\pm$  0.07 for the elbows that contained 150 mg I/ml, 75 mg I/ml and 37.5 mg I/ml contrast medium concentrations, respectively. CTA measurements from elbows with 75 mg I/ml (mean 0.54 mm, bias 0.22 mm) were significantly larger ( $p < 0.0001$ ) and had greater bias ( $p = 0.0002$ ), when compared to the other contrast medium groups. There was no significant difference in CTA measurement precision between different contrast medium concentrations.

**Discussion/Conclusion:** CTA allowed excellent visualization of the thin articular cartilage of the normal canine elbow and provided high cartilage measurement precision regardless of CT image plane, contrast medium concentration or anatomic zone. Articular cartilage thickness values were consistently overestimated on CTA images compared to the reference standard and this may have resulted from cartilage shrinkage during histologic preparation or be due to the spatial resolution limits of the imaging system.

## EVALUATION OF IDEAL LIMB POSITION FOR HIGH FIELD MAGNETIC RESONANCE IMAGING OF THE EQUINE DIGIT.

D.D.Cissell, M. Spriet. School of Veterinary Medicine, University of California, Davis, CA

**Introduction/Purpose:** Magic angle effect has been reported to create increased signal intensity in the equine deep digital flexor tendon (DDFT) and collateral ligaments of the distal interphalangeal joint (CL-DIPJ) associated with limb position during high field magnetic resonance (MR) imaging. There has been no attempt to describe the ideal limb position during high field MRI to avoid artifactual hyperintensity due to the magic angle effect. We hypothesize that signal intensity in the DDFT and CL-DIPJ is affected by position of the digit in both the sagittal and dorsal planes.

**Methods:** The right thoracic limb of a horse was imaged post-mortem in right lateral recumbency in a 1.5T MR unit. A jig was used to standardize limb position. The limb was initially positioned with the metacarpus and digit parallel to the axis of the main magnetic field ( $B_0$ ). For subsequent series of images, the metacarpus was maintained parallel to  $B_0$  in the dorsal plane. The orientation of the digit relative to  $B_0$  in the sagittal plane was varied by extending and flexing the metacarpophalangeal joint (MCPJ) to achieve angles of -20, -10 (dorsal to  $B_0$ ), 10, and 20 (palmar to  $B_0$ ) degrees relative to  $B_0$ . The limb was then repositioned by raising the carpus relative to the digit, changing the angle of the digit and metacarpus relative to  $B_0$  in the dorsal plane by 10 degrees (tilt). Sagittal, transverse, and dorsal plane T1-weighted spin echo images of the distal extremity were acquired for each position. Each series of images were evaluated subjectively and objectively for signal intensity in the DDFT and CL-DIPJ.

**Results:** Hyperintensity was observed in the distal DDFT upon extension of the MCPJ and was similar at -10 and -20 degrees. Signal intensity in the DDFT was subjectively intermediate-hypointense with the digit parallel to  $B_0$  and uniformly hypointense on flexion of the DDFT. Signal intensity in the DDFT in the -10 degree position in the sagittal plane was 2.0 times greater than in the parallel position. Conversely, hyperintensity was observed in the CL-DIPJ upon flexion of the MCPJ in the 10 and 20 degree positions. The CL-DIPJ were uniformly hypointense when the digit was parallel to  $B_0$  and upon extension of the MCPJ. Signal intensity in the CL-DIPJ in the 10 degree position in the sagittal plane was ~3.5 times greater than in the parallel position. Tilt of the limb resulted in asymmetrical signal intensity in the CL-DIPJ, but had no effect on the DDFT. Tilt caused hyperintensity in the lateral collateral ligament that was greatest in the parallel and -10 degree positions where it caused a difference of 1.8 and 2.1 times the signal intensity compared to the no tilt positions, respectively.

**Discussion/Conclusion:** Angulation of the digit in the sagittal plane is the main cause of the magic angle effect in the DDFT on high field MR images. Angulation in the sagittal and dorsal planes both affect the signal intensity of the CL-DIPJ. Flexion of the MCPJ prevents the occurrence of the magic angle effect in the DDFT but leads to occurrence of the artifact in the CL-DIPJ. Ideally, the digit of the horse should be aligned parallel to  $B_0$  in both the sagittal and dorsal planes to avoid misinterpretation due to the magic angle effect.

## COMPUTED TOMOGRAPHY OF PLEURAL MASSES AND NODULES IN SIX DOGS AND ONE CAT.

J.A.Reetz, E.L. Buza, E. Krick. University of Pennsylvania School of Veterinary Medicine, Philadelphia, Pennsylvania, 19104.

**Introduction/Purpose:** Pleural space masses and nodules have rarely been described on computed tomography (CT) and have only been described in cases of neoplasia. The purpose of this study was to describe the CT findings and diagnoses in 7 cases with pleural masses and nodules of both neoplastic and non-neoplastic origin.

**Methods:** CT examinations performed at our institution in six dogs and one cat between May 2008 and March 2011 identified pleural masses and/or nodules. All cases had the lesions diagnosed by histopathology (6 dogs) or cytology (1 cat). The CT examinations were reviewed for presence, location, and appearance of pleural space mass(es) and/or nodule(s), as well as presence, distribution and appearance of pleural thickening and presence of any additional intra-thoracic or extra-thoracic lesions. Contrast enhancement of the pleural lesions (n=6) was evaluated for homogeneity or heterogeneity.

**Results:** All cases had lesions along the costal pleura; other sites of pleural involvement included mediastinal (n = 4), diaphragmatic (n = 2), visceral pleura (n = 1) and cupula pleura (n = 1). Two cases had broad-based, plaque-like pleural masses, both of which were diagnosed with neoplasia (pleural carcinoma, metastatic thymoma). Two cases had well-defined pleural nodules and nodular pleural thickening, one of which had mesothelial hypertrophy and the other had metastatic hemangiosarcoma. Three cases had ill-defined pleural nodules to nodular pleural thickening, one of which had metastatic pulmonary carcinoma, while the other two had bacterial infection with secondary mesothelial proliferation (n = 2), fibrinous pleuritis (n= 1) and severe mediastinal pleuritis/mediastinitis (n= 2). Five of 7 cases had additional sites of focal, multifocal or diffuse smooth and/or irregular pleural thickening. All cases except one had additional lesions identified on CT besides those in the pleural space. Contrast enhancement of pleural lesions was most often homogeneous. Some of the pleural lesions were only delineated from surrounding pleural effusion on post-contrast images.

**Discussion/Conclusion:** CT was useful in identifying and characterizing pleural space lesions and could be used to guide further diagnostic procedures such as thoracoscopy or exploratory thoracotomy. Post-contrast CT was helpful in delineating more subtle pleural lesions from pleural effusion. Due to the small number of cases and varying diagnoses, conclusions regarding specific CT features to distinguish neoplastic from non-neoplastic diseases could not be made. Both processes should be considered in the differential diagnoses for pleural space masses and nodules found on thoracic CT.

## **MRI APPEARANCE OF PROGRESSIVE ETHMOID HEMATOMA IN FOUR HORSES.**

F.A. Castro<sup>1</sup>, E. Parente<sup>2</sup>, M. Leitch<sup>2</sup>, W. Mai<sup>1</sup>. <sup>1</sup>University of Pennsylvania, Ryan Veterinary Hospital, Philadelphia, PA 19104. <sup>2</sup>University of Pennsylvania, New Bolton Center, Kennett Square, PA 19348.

**Introduction/Purpose:** Paranasal sinus conditions are common in horses and include sinusitis, cysts, progressive ethmoid hematoma and neoplastic conditions. Radiology is the most commonly used imaging modality but interpretation is complicated by the superimposition of complex anatomical structures and the uniform soft tissue opacity seen in the affected area with most disease processes. Computed tomography is becoming more widely available and frequently used for sinus evaluation eliminating the problem of superimposition experienced with radiography. Still, a number of sinus conditions present as uniform soft tissue attenuating structures and CT lacks specificity. No information is available about the MRI appearance of most disease processes of the equine paranasal sinuses. The purpose of this study was to describe the MRI features of progressive ethmoid hematoma in 4 horses.

**Methods:** The MRI database of the large animal hospital of the University of Pennsylvania was searched between August 2005 and March 2011 for horses undergoing skull MRI in which a sinus mass lesion was identified and had been previously diagnosed or later confirmed surgically as progressive ethmoid hematoma. MRI exams were performed using a 0.28 T permanent magnet (Vet-MR Grande, Esaote, Florence, Italy). Clinical presentation, results of physical exam, endoscopic and radiographic examinations were retrieved from the medical records.

**Results:** Four patients were identified (3 castrated males, 1 female). Age ranged from 7 to 10 years. Radiographic findings included soft tissue opacities or masses in the affected paranasal sinuses or ethmoid turbinate region in all cases and fluid lines in two cases. MRI findings included rounded encapsulated masses with well-defined margins that originated from the ethmoid region or the right maxillary sinuses. The masses displayed heterogeneous signal intensity on T1- and T2-weighted images, but were overall more hypointense on T2-w images. Hypointense signal was seen on Gradient-Echo images indicating blood content. No significant contrast enhancement post-gadolinium administration was seen in any case. Fluid accumulation that was uniformly hypointense to adjacent mucosa on T1-w and hyperintense on T2-w images was seen in the sinuses adjacent to the masses in all cases and enhancement of the mucosa surrounding the fluid was seen in two cases.

**Discussion/Conclusion:** The MRI findings allowed the characterization of the masses as ethmoid hematomas based on location, lack of contrast-enhancement, hypointense signal on GRE sequence and the heterogeneous intensity on T1w and T2w images that is compatible with the variable age of the hematoma and different types of hemoglobin by-products present in different regions of the mass. It also permitted the differentiation of mass from fluid accumulated in the sinus and revealed the extent of sinus cavities involved, thereby providing more detailed information than radiography.

## **ULTRASONOGRAPHIC IDENTIFICATION OF UNDESCENDED TESTES IN DOGS AND CATS.**

A Felumlee,<sup>1</sup> JK Reichle,<sup>1</sup> D Penninck,<sup>2</sup> A Dietze Yeager,<sup>3</sup>

L Zekas,<sup>4</sup> J Goggin,<sup>5</sup> J Lowry.<sup>6</sup> 1. Animal Surgical & Emergency Center, West LA CA 90025; 2. Cummings School of Veterinary Medicine at Tufts University, North Grafton MA 01536; 3. Cornell University Hospital for Animals, Ithaca NY 14850; 4. Ohio State University College of Veterinary Medicine, Columbus OH 43210; 5. Metropolitan Veterinary Radiology, Ltd., Montclair NJ 07042; 6. Mountain Veterinary Imaging, Ft Collins CO 80526.

**Introduction/Purpose:** Inability to locate one or both testes may delay the time of castration and require additional time under general anesthesia attempting to locate the teste(s), sometimes with negative results. The goal of this study is to review the ultrasonographic (US) findings of canine and feline patients with undescended testes and compare the US location to the surgical findings.

**Methods:** Cases were requested via e-mailing ACVR members. Requirements included breed; whether surgery had been attempted prior to US exam; dates of birth, US exam, and subsequent surgery; ultrasonographic and surgical descriptions of the location of the testes; type of US machine and transducer probe/frequency used; and histopathology of the testes, if performed.

**Results:** Four feline patients (2 domestic shorthairs, 1 domestic longhair, 1 Scottish Fold) and 33 canine patients (4 each of mixed breeds and Boxers; 2 each of German shepherds, Greyhounds, Miniature schnauzers, Yorkshire terriers, and Old English sheepdogs; 1 each of 15 various pure breeds) were imaged with a variety of US machines and probes and frequencies. Cases spanned February 2004 through March 2011. Age at time of US ranged from 3-156 months with a mean and median of 33 and 12 months, respectively. Time between US and surgery ranged from 0 days to 2 years with a mean of 65 days and a median of 0.5 days. Seven patients had prior surgical attempts at castration and 3 had unknown surgical histories. Testes were identified in the abdomen (30), ranging from just caudal to the kidney to lateral to the urinary bladder trigone; the inguinal region (12); and subcutaneously in the pre-pubic region (2). Most testes appeared normal with a hyperechoic linear mediastinum testis and adjacent epididymis; 4 appeared mass-like (histopathology revealed 2 Sertoli cell tumors, 1 seminoma, and 1 torsion). Surgical findings agreed with US findings in 27 of 36 patients (78%).

**Discussion/Conclusion:** US is useful in locating undescended testes in cats and dogs as well as determining whether the testes are normal or not. US identification of the mediastinum testis and/or epididymis helps ensure the structure is a normal testis. Scanning the patient from the level of each kidney, extending caudally to and including the scrotum, is recommended.

## CT AND MRI STUDY OF EQUINE EPIPHYSEAL DEVELOPMENT TOWARDS UNDERSTANDING OSTEOCHONDritis DISSECANS (OCD).

P. Fontaine<sup>†</sup>, L. Blond<sup>†</sup>, K Alexander<sup>†</sup>, E-N. Carmel<sup>†</sup> and S. Laverty<sup>†</sup>

<sup>†</sup> Département de sciences cliniques, Faculté de Médecine Vétérinaire, Université de Montréal, Québec.

**Introduction/Purpose:** Osteochondritis dissecans (OCD) arises from an abnormal endochondral ossification of the developing epiphysis leading to the development of cartilage flaps, joint surface irregularity and eventually secondary osteoarthritis. We postulate that greater relative thickness of the growth cartilage at OCD-susceptible sites is a factor in the pathogenesis of the disease process. Our goal was to study equine epiphyseal development to determine whether epiphyseal site maturation was a predisposing factor for OCD.

**Methods:** Equine foetuses (n =14) and full-term foals (n=4) were studied post-mortem. Specimens were allocated into 4 age groups; 4-5 months of gestation (MG), 6-7 MG, 8-9 MG and 10-11 MG including 3 first weeks post-partum. Both the stifle and tarsus were imaged with 1.5 T magnetic resonance imaging (MRI) using specific sequences to highlight cartilage structure. Joints were also scanned with computed tomography (CT) in order to determine the epiphyseal ossification pattern. Cartilage/bone percentages were compared between OCD-susceptible and control sites.

**Results:** At 8-9 MG the median cartilage/bone percentages were significantly higher at OCD-susceptible sites ( $p < 0.0001$ ). At 3 weeks post-partum the cartilage/bone percentage of the medial malleolus of the distal tibia (43%), the distal intermediate ridge of the tibia (27%), the lateral trochlear ridge of the distal femur (21%) and the lateral trochlear ridge of the talus (12%) remained high, indicating that these sites ossify later than those where OCD lesions do not occur, such as the medial trochlear ridge of the talus (8%). Epiphyses ossified progressively from 4 MG with the greatest progression occurring between 8-9 and 10-11 MG.

**Discussion/Conclusion:** Present findings corroborate recent literature of increased cartilage thickness at certain OCD-susceptible sites including the medial malleolus of the distal tibia and the lateral trochlear ridge of the talus and also provide new information concerning other sites known for frequent OCD occurrence such as the distal intermediate ridge of the tibia and the lateral trochlear ridge of the femur. Information about equine epiphyseal endochondral ossification provided by this study may also be used as a reference for future studies. In conclusion, MRI and CT scan are valuable imaging tools that allowed characterization of equine epiphyseal development and findings suggest that greater relative cartilage thickness at specific sites in the joint may predispose to OCD occurrence.

**MR CHARACTERIZATION OF VERTEBRAL ENDPLATE CHANGES IN THE DOG.**  
Karine Gendron<sup>1</sup>, Marcus Doherr<sup>1</sup>, Patrick Gavin<sup>2</sup>, Johann Lang<sup>1</sup>.<sup>1</sup> University of Bern, Switzerland, <sup>2</sup> MR Vets, Inc, Ponderay, ID 83852.

**Introduction/Purpose:** Although reactive endplate changes (Modic) are a common MR finding in people suffering from lower back and sciatic pain, descriptions of MR features of non-infectious and non-traumatic endplate changes are few in the veterinary literature. These changes distinguish themselves from other reported endplate pathologies, in that they are only visible on MR (Types 1 and 2), with MR characteristics sometimes overlapping those of other conditions. The purpose of this study was to describe and classify MR patterns of vertebral endplate changes in our canine patients as seen on low field MR, and to determine these changes' frequencies and associations.

**Methods:** Medical records of dogs with spinal MR performed at our institution between Jan 2003 and Feb 2010 were reviewed for mention of endplate or vertebral changes. All studies were performed with a 0.3T Hitachi Airis II system. MR criteria for the diagnosis of diskospondylitis were STIR-hyperintensity or contrast enhancement (CE) of the paravertebral soft tissues, T2w and STIR hyperintense as well as T1w hypointense signal at the endplates, endplate CE, CE of the intervertebral space, endplate erosion and collapse of the intervertebral space. Reactive endplate changes were defined by T2w and STIR hyperintensity and T1w hypointensity of the endplate, with or without endplate CE. Fatty infiltration of the endplates was defined as T1w and T2w hyperintensities that nulled in STIR. Osteochondrosis was diagnosed when a defect was observed on the dorsal edge of an endplate, with or without matching bone fragment. Focal, centrally located endplate defects, filled with disc-isointense material, were diagnosed as Schmorl's nodes.

**Results:** Of a total of 1348 spinal studies, seventy-six lesions were found in 75 dogs of 37 breeds. Presumptive diagnoses fell into 5 categories: diskospondylitis (29 dogs/38%), reactive endplate changes (10 dogs/13%), vertebral osteochondrosis (OC) (7 dogs, 9%), intravertebral disc herniation (Schmorl's nodes) (4 dogs/5%) and fatty infiltration (26 dogs/34%). The following criteria were not significantly different between diskospondylitis and other non-fatty endplate pathologies: irregular endplates, hyperintensity of the endplates in T2w or STIR, signal intensity of the endplates in T1w SE or T1w GRE, or contrast enhancement of the endplates. Fatty infiltrations occurred significantly more often in small breed dogs ( $P < 0.001$ ) and tended to be multifocal. Osteochondrosis was observed solely in the lumbosacral joint. Young male German Shepherds were overrepresented in this group.

**Discussion/Conclusion:** Similar to the human experience, reactive endplate changes in our population had a predilection for the lumbosacral joint (5/10: 50%), an association with degenerative disc changes (9/10: 90% with grade 4) and a tendency to affect older patients (6/10: 60% over 7 years of age). The occurrence of reactive endplate changes adjacent to a degenerate disc, the presence of mixed types, and the progression of Type 2 lesions in a subsequent MR study in one dog, suggests reactive endplate changes, may be as in people, dynamic changes. The apparent overlap between MR characteristics of non-fatty endplate changes should prompt cautious evaluation of adjacent structures.

## **RADIOGRAPHIC AND MAGNETIC RESONANCE IMAGING OF THE EQUINE FOOT: A FOCUS ON THE SOLE.**

I.N.M. Grundmann, W.T. Drost, L.J. Zekas, J.K. Belknap, R.B. Garabed, S.E. Weisbrode, M.V. Knopp, J. Maierl. The Ohio State University, OH 43210, Ludwig-Maximilians University, Munich 80539, Germany.

**Introduction/Purpose:** Equine laminitis may lead to rotation and/or sinking of the distal phalanx within the hoof capsule, causing damage and pain. Radiographs are used to diagnose severity and type of displacement to determine prognosis and guide treatment. Magnetic resonance imaging (MRI) has been used to evaluate soft tissue changes and help improve radiographic interpretation. Our study compares digital radiography (DR) and MRI for characterization of dorsal hoof wall structures and compares sole depth measurements.

**Methods:** 62 cadaver feet (31 left/right front feet) were radiographed before and after barium application to the surface of the sole. MRI was performed after application of lard to define hoof and sole surfaces. Image review and measurements were made by four reviewers (IG, LJZ, JKB, WTD), who were blinded to pre-mortem clinical status of the horse. Using DR the depth of the following areas were measured: sole, sole epidermal layer and sole dermal layer. Using MRI the depth of the following areas were measured: sole, sole epidermal layer, sole dermal layer, sole lamina and sole corium. Measurements were made from the tip of the distal phalanx to the sole margin and from the lateral and medial aspect of the distal phalanx to the sole margin. DR measurements were compared to MRI measurements. One reviewer (IG) measured these areas 3 times. Inter- and intra-observer variability was determined. For statistical analysis a mixed linear regression test was used.

**Results:** On DR images mean sole, dermis and epidermis depth was 12.8mm, 5.4mm and 8.0mm. Mean lateral sole, dermis and epidermis depth was 20.7mm, 7.4mm and 13.2mm. Mean medial sole, dermis and epidermis depth was 18.9mm, 7.2mm and 11.7mm. On MRI mean sole, dermis, epidermis, lamina and corium depth was 12.1mm, 4.5mm, 7.6mm, 1.4mm and 3.1mm. Mean lateral sole, dermis, epidermis, lamina and corium depth was 18.6mm, 5.8mm, 12.8mm, 1.6mm, and 4.1mm. Mean medial sole, dermis, epidermis, lamina and corium depth was 17.4mm, 5.7mm, 11.7mm, 1.6mm and 4.1mm. There was no statistical significant difference between DR and MR measurements. The intra- and inter-observer variability was better for MRI. Interobserver difference were 1mm for MRI and 0.5mm for DR measurements.

**Discussion/Conclusion:** There is good overall correlation of sole depth measurements between DR and MRI. Inter- and intra-observer variability was better for MRI. Ultimately, our data is used to determine what measurements will predict prognosis, guide therapy and help equine clinicians to better understand equine laminitis.

## **AGREEMENT BETWEEN T2 AND HASTE (HALF-FOURIER-ACQUISITION SINGLE-SHOT TURBO SPIN-ECHO) SEQUENCES IN THE EVALUATION OF INTERVERTEBRAL DISC DISEASE IN DOGS.**

J.M. Mankin, S. Hecht, W.B. Thomas. Department of Small Animal Clinical Sciences, University of Tennessee College of Veterinary Medicine, Knoxville, TN 37996-4544.

**Introduction/Purpose:** Magnetic resonance imaging (MRI) is commonly used when evaluating patients with intervertebral disc disease (IVDD). Heavily T2 weighted techniques such as HASTE (half-Fourier-acquisition single-shot turbo spin-echo) have proven useful by using the high signal obtained from cerebrospinal fluid. The purpose of this study was to compare T2-W and HASTE sequences in dogs with thoracolumbar IVDD.

**Methods:** MRI studies in 60 dogs (767 individual intervertebral disc spaces) were evaluated. Agreement between T2-W and HASTE sequences was assessed for presence of an extradural lesion, severity of compression, and treatment recommendation.

**Results:** There was moderate agreement between sequences as to presence of an extradural lesion ( $\kappa = 0.575$ ). HASTE was in agreement in 96.1% of the cases where no extradural lesion was identified on T2-W images, but only in 58.1% where lesions were identified. There was fair agreement between T2-W and HASTE sequence as to severity of compression ( $\kappa = 0.381$ ). There was moderate agreement between T2 -W and HASTE sequence as to treatment recommendations ( $\kappa = 0.476$ ). In 1.0% of cases considered not surgical and in 9.8% of cases considered equivocal based on T2 a surgical lesion was identified on HASTE.

**Discussion/Conclusion:** Acquisition of a HASTE sequence in addition to conventional sequences when evaluating the canine spine may be useful.

## **AIRSPACE DISEASE IN DOGS DETECTED DURING COMPUTED TOMOGRAPHY.**

N.Holmes<sup>1</sup>, P.Scrivani<sup>1</sup>, M.Thompson<sup>1</sup>, N.Dykes<sup>1</sup>, J.Gerdin<sup>2</sup>, T.Southard<sup>2</sup>.<sup>1</sup>Department of Clinical Sciences, <sup>2</sup>Department of Biomedical Sciences, Cornell University College of Veterinary Medicine, Ithaca, NY 14853.

***Introduction/Purpose:*** To investigate whether similar airspace opacity detected during thoracic CT in dogs with lung disease is associated with consistent and predictable microscopic lesions.

***Methods:*** The medical record was reviewed for dogs with lung disease evaluated by both thoracic CT and lung histology (surgical biopsy or necropsy). Inclusion criteria for CT scans included fully expanded lungs with increased opacity that partially or totally obscured the macroscopic pulmonary blood vessels and that was centered on the airspace but not the bronchovascular bundle.

***Results:*** CT findings in all 4 dogs included areas of similar airspace opacity. However, microscopic examination of lung tissue revealed a wide variety of histologic lesions, including filling of alveolar spaces with fluid or cells, capillary congestion and expansion of interstitial spaces.

***Discussion/Conclusion:*** Similar pulmonary changes on thoracic CT scans are associated with a wide spectrum of histopathologic lesions. Some of the terminology used in description of changes in human pulmonary CT images may be useful in dogs as these terms are descriptive of the imaging appearance, relate to the mechanism of image generation, and do not imply a specific histologic lesion that may be misleading and incorrect.

## **IMAGING FINDINGS IN DOGS WITH CAUDAL INTERVERTEBRAL DISC HERNIATION.**

C.M. Lawson, J.K. Reichle, T. McKlveen, M.O. Smith. Animal Surgical & Emergency Center, Los Angeles, California 90025.

**Introduction/Purpose:** Caudal intervertebral disc herniation is reported infrequently in dogs. S3-Cd1 and Cd1-Cd2 disc extrusion have been reported as isolated events in the miniature Dachshund.<sup>1-2</sup> The purpose of this study was to describe the radiographic and magnetic resonance imaging (MRI) abnormalities associated with Cd1-Cd2 disc disease in four dogs.

**Methods:** Dogs with caudal intervertebral disc herniation were identified by emailing American College of Veterinary Radiology (ACVR) members via the ACVR Forum and CT/MRI mailing lists in June 2010. Submitted material spanned January 1995-June 2010. Inclusion criteria were caudal intervertebral disc herniation identified using at least one form of imaging and availability of the medical records. Four dogs were identified with radiographic and/or MRI evidence of caudal intervertebral disc herniation. Review of radiographs and MRI was performed by a board-certified radiologist (J.R.) and a diagnostic imaging intern (C.L.). Disc herniation was classified as bulging, protrusion, or extrusion based on MRI.

**Results:** All four dogs had tail pain on manipulation. Two dogs demonstrated pain during defecation and two dogs maintained an abnormal tail position. In all dogs, pain was localized to the caudal lumbar, sacral, or caudal vertebral column. Radiographs of the lumbosacral and sacrocaudal vertebral column were performed on three dogs, demonstrating mineralized material in the disc space between the first and second caudal vertebrae. In two of the dogs, mineralized material was also identified within the vertebral canal at Cd1-Cd2. MRI of the lumbar and sacrocaudal vertebral column was performed on three dogs. All dogs undergoing MRI had evidence of intervertebral disc protrusion (1 dog) or extrusion (2 dogs) at Cd1-2.

**Discussion/Conclusion:** Caudal intervertebral disc herniation should be considered in dogs with caudal vertebral pain, pain with tail manipulation or during defecation, or abnormal tail carriage. Imaging the caudal vertebral column is important in dogs with clinical signs of tail pain to diagnose or rule out caudal intervertebral disc herniation.

1. Freeman P. Sacrococcygeal intervertebral disc extrusion in a dachshund. Vet Rec 2010;167:618-619.
2. Akin EY, Narak J, Simpson ST. What is your diagnosis? JAVMA 2011;238:153-154.

## **FEASIBILITY OF COMPUTED TOMOGRAPHY IN CONSCIOUS CANINE PATIENTS WITH PELVIC FRACTURE.**

Kichang Lee<sup>1</sup>, Jimo Chung<sup>1</sup>, Jinwon Kim<sup>1</sup>, Haebeom Lee<sup>1</sup>, Minsu Kim<sup>1</sup>, Namsoo Kim<sup>1</sup>, Hock Gan Heng<sup>2</sup>, Jacob J Rohleder<sup>2</sup>, James F Naughton<sup>2</sup>. <sup>1</sup> Chonbuk National University, Chonbuk Animal Medical Center, Jeonju, 561-756 Republic of Korea and <sup>2</sup>Purdue University, Department of Veterinary Clinical Sciences, West Lafayette, IN 47907.

**Introduction/Purpose:** In human medicine, radiography of traumatic pelvic fractures may not be adequate for complete evaluation, therefore computed tomography (CT) is performed for precise evaluation of the pelvis. In veterinary medicine, general anesthesia (GA) or sedation is generally required to immobilize animal patients during CT scanning. GA or sedation in traumatized patients is concerning due to various factors such as unstable patient condition, concerns of possible risks of anesthesia, and cost. This study was performed to evaluate the feasibility of pelvic CT examination in conscious traumatized animals.

**Methods:** CT scanning was performed in dogs with suspected pelvic fractures after vehicle accidents without GA or sedation (Purdue and Chonbuk University from Sep. 2010 to March 2010). All stable patients who were bright, alert, and responsive were included in the study. Under conscious conditions, physical restraint was performed by securing the body with medical tape and by sometimes wrapping the body in a towel. Scan position, cooperation on CT table, preparation time for CT scanning, scanning time, frequency of rescans, image quality, and complications related to physical restraint were evaluated.

**Results:** Out of seven canine patients, four patients were in lateral recumbency and three patients were in sternal recumbency. Most of them were cooperative with the exception of one that was slightly resisting to lay still on CT table. The physical restraint with tape or wrapping was enough for CT scanning. Preparation for CT scanning took less than five minutes and the scan time was typically 1 to 2 minutes with 3 mm slice thickness. No rescan was required in any cases. The axial CT image quality was good (5/7) and accepted (2/7) for interpretation. Three dimensional (3D) reconstructed volume rendered images were generally helpful (6/7) for better understanding of the pelvic fractures, especially sacral fractures which were not conspicuous on radiographs. No complications or additional injuries associated with physical restraint were noticed.

**Discussion/Conclusion:** Though a small number of canine patients were reviewed, non GA or non sedation CT scanning in dogs with pelvic fractures was performed easily without any complications. The good axial CT image quality, combined with three dimensional images, was helpful to evaluate pelvic fractures. This may be beneficial for surgical planning. This study indicates that pelvic CT scanning, without GA or sedation, is possible in veterinary medicine when GA or sedation is undesirable due to concerns about patient stability.

## **MAGNETIC RESONANCE IMAGING OF CANINE MAST CELL TUMORS.**

E. Pokorny, S. Hecht, P.A. Sura, A.K. LeBlanc, J. Phillips. Department of Small Animal Clinical Sciences, University of Tennessee College of Veterinary Medicine, Knoxville, TN 37996.

***Introduction/Purpose:*** Mast cell tumors (MCT) are the most common cutaneous tumors in dogs. The purpose of this study was to describe MR imaging characteristics of (sub)cutaneous MCT and associated lymph nodes.

***Methods:*** Eight dogs were included in the study. MR imaging was performed using a 1T magnet (MAGNETOM Harmony™, Siemens). Imaging characteristics of MCT and lymph nodes were described. Metastatic lymph nodes were compared to normal sentinel and contralateral lymph nodes. Lymph node pairs without biopsy of sentinel lymph nodes were excluded from evaluation.

***Results:*** 9 MCT were identified in 8 dogs. On T2-w sequences, 7/9 MCT were hyperintense and 2/9 were isointense to adjacent musculature. On T1-w sequences, 5/9 MCT were isointense and 4/9 were mildly hyperintense. 4/4 MCT were markedly hyperintense on STIR. All MCT were strongly contrast enhancing (5/9 homogeneous and 4/9 heterogeneous). 6 lymph node pairs were included in the evaluation. There were 5 sentinel lymph nodes with metastases and one without. All lymph nodes were T1 isointense. 5/5 metastatic and 1/7 normal lymph nodes were heterogeneously T2 hyperintense. Following contrast administration, all lymph nodes were contrast enhancing. 4/5 metastatic and 1/7 normal lymph nodes had heterogenous enhancement patterns.

***Discussion/Conclusion:*** Heterogeneous T2 hyperintensity and heterogenous contrast enhancement are more common in lymph nodes with metastatic MCT than in normal lymph nodes.

## **SONOGRAPHIC APPEARANCE AND AVERAGE SIZE OF THE NORMAL FELINE SPLEEN.**

<sup>1</sup>R.S. Sayre, <sup>2</sup>K.A. Spaulding. <sup>1</sup>Department of Small Animal Clinical Sciences, College of Veterinary Medicine, Texas A&M University, TX 77843. <sup>2</sup>Department of Large Animal Clinical Sciences, College of Veterinary Medicine, Texas A&M University, TX 77843.

**Introduction/ Purpose:** There are few reports in the literature on the sonographic appearance of the normal spleen in cats.<sup>1</sup> The overall shape of the spleen is not uniform but is fairly consistent among cats. Having a standard protocol including a reference range of the size of the spleen is needed. The purpose of this study was to describe the appearance and average size of the spleen in healthy cats and to develop a standard method of evaluation.

**Methods:** Data was obtained from 31 clinically healthy cats with no sonographic abnormalities. The sonographic appearance of the spleen's relative echogenicity compared to the central part of left renal cortex and the hepatic parenchyma was recorded. Spleen width was measured at 3 sites. Three measurements were determined at each site, and the mean value of these 3 measurements was determined and used for data analysis. A significance level of  $P < 0.05$  was used for analysis, which was performed using S-PLUS software (Version 8.1, TIBCO, Inc., Seattle, WA).

**Results:** The splenic parenchymal echogenicity was less than the left renal cortex echogenicity and greater than the liver in 17/31cats ( $S < K > L$ ); less than the left kidney cortex and equal to the liver in 5/31cats ( $S < K = L$ ); equal to the cortex of the left kidney and greater than the liver in 5/31 cats ( $S = K > L$ ); equal to the liver and renal cortex in 2/31cats ( $S = K = L$ ); and less than the liver and spleen with the renal cortex less than the liver in 2/31 cats ( $K < L > S$ ). The mean standard deviation (SD) of the proximal width of the spleen was 7.1 mm (1.19 mm); (range 5.1-to 9.1 mm). The mean (SD) of the sagittal width was 9.3 mm (1.51 mm); (range 6.0 - 12.8 mm). The mean (SD) of the width of the tail of the spleen was 8.7 mm (1.51 mm); (range 6.3 - 12.4 mm).

**Discussion/Conclusion:** The protocol recommended for consistent evaluation of the spleen in the cat should include measurements of the proximal extent of the spleen in a transverse plane when the splenic vein is apparent on the mesenteric surface. This provided the most consistent and least varied results {7.1 mm (1.19 mm); range 5.1- 9.1 mm}.

---

<sup>1</sup>McMahon Shona Louise. Effect of Sevoflurane Anesthesia and Blood Donation on the Sonographic Appearance of the Spleen and Hematology in healthy Cats. The Ohio State University 2010 Thesis.

## VISCERAL FAT MEASURED WITH CT CORRELATES WITH ADVERSE CARDIAC CHANGES IN OBESE DOGS.

T.I. Silver, J. Adolphe, L.P. Weber. WCVN, University of Saskatchewan, SK, S7N 5B4.

**Introduction/Purpose:** Obesity and cardiovascular disease are strongly linked in humans however this association is less clear in the dog. Elevations in heart rate and cardiac output have correlated with obesity in the dog, however specific heart function and structure changes have not been fully investigated. This study's objective was to evaluate the effects of obesity and fat distribution on cardiac function and structure.

**Methods:** Hemodynamic variables were measured before and after weight gain in nine neutered beagles. At baseline, dogs were fed a commercial dry diet in measured amounts to maintain a body condition score (BCS) of 3-5 on a 9-point scale. Subsequently, for 12 weeks the dogs were allowed free access to the diet with an additional 5% fat to encourage weight gain. Echocardiography was used to measure left ventricular volume, internal diameter, and free wall thickness in diastole and systole. Stroke volume, ejection fraction, cardiac output and fractional shortening were calculated. Blood pressure was measured by high definition oscillometry and total peripheral resistance was calculated. Hemodynamic parameters were compared using paired t-tests.

Abdominal computed tomography was used to quantify abdominal fat distribution in the dogs in the obese state. Regions of interest outlining the peritoneal space on a single slice image at the level of the third lumbar vertebra (L3) were used to quantify peritoneal fat area by counting the pixels within the fat attenuation range. Pearson correlations were performed between visceral fat and hemodynamic variables showing significance post weight gain.

**Results:** At baseline, mean body weight and BCS were  $9.8 \pm 0.6$  kg and  $3.9 \pm 0.1$ , respectively. After ad libitum feeding the higher fat diet, weight increased to  $12.1 \pm 0.7$  kg, BCS was  $6.4 \pm 0.2$ , and the percentage of ideal body weight was  $123 \pm 3\%$ . Hemodynamic variables were significantly increased after weight gain for cardiac output, heart rate and left ventricular systolic free wall thickness ( $p < 0.05$ ). Total peripheral resistance significantly decreased with obesity ( $p < 0.05$ ). A significant correlation between visceral fat and left ventricular systolic free wall thickness ( $r=0.7$ ;  $p=0.03$ ) was observed. No other significant correlations were noted.

**Discussion/Conclusion:** Increased systolic free wall thickness, coupled with elevated heart rate, in dogs likely reflects hyperdynamic cardiac function as opposed to a structural change in short term obesity. Visceral fat, measured by CT, correlates with detrimental effects in cardiac function in dogs that have been obese for only 12 weeks. From this observation, using CT scan to estimate visceral fat has the potential to be predictive for risk of cardiac disease in dogs. Moreover long term obesity may pose even greater cardiac risk.

## ESTIMATION OF FELINE RENAL VOLUME USING COMPUTED TOMOGRAPHY AND ULTRASOUND.

S.A. Logsdon, R. Tyson, G.B. Daniel, S.R. Werre. VA-MD Regional College of Veterinary Medicine, Blacksburg, VA 24061.

**Introduction/Purpose:** Renal volume estimation is becoming increasingly important with new techniques to determine renal function using dynamic computed tomography and magnetic resonance imaging. Renal volume has been shown to correlate well with the number of functional nephrons and the progression of chronic renal failure. The purpose of this study was to compare renal volume estimates using ultrasound and computed tomography with *ex vivo* volume measurements obtained using a “gold standard” modified Archimedes technique.

**Methods:** Ultrasound and computed tomography (16 detector, 1 mm collimation, 250 mAs, 120 kV, pitch 0.938, rotation time 0.5 sec) were performed on twelve cadaver cats, *in situ*. Ultrasound and computed tomography multi-planar volume reconstructions were used to obtain measurements for the prolate ellipsoid formula ( $\pi/6 L \times W \times T$ ) for volume estimation. In addition, computed tomography studies were reconstructed at 1-mm, 5-mm, and 1-cm, and transferred to a workstation where the renal volume was calculated using the voxel-count method (hand drawn regions of interest). The edge of the kidney image was manually traced halfway along the change in signal intensity between the kidney and any surrounding tissues. The kidneys were then removed from the cats and the renal vessels and ureters were ligated as close to the hilum and as much extra-renal tissue removed as possible. Maximum longitudinal length, from cranial to caudal pole, was measured with a Vernier caliper (accuracy 0.05 mm). A modified Archimedes principle, in which the weight difference (water displacement) of the kidney suspended in water on a balance, was utilized to determine renal volume.

**Results:** Renal volume was  $18.99 \pm 7.68 \text{ cm}^3$  (mean  $\pm$  SD) with a range from 7.40-29.83  $\text{cm}^3$ . A Bland-Altman plot was used to compare ellipsoid (\*) and voxel count (^) methods to the modified Archimedes “gold standard”. All data is expressed in  $\text{cm}^3$ .

	<u>US*</u>	<u>CT*</u>	<u>CT 1-mm^</u>	<u>CT 5-mm^</u>	<u>CT 1-cm^</u>
<b>Mean Difference</b>	-3.7701	-3.7907	0.0185	-0.6392	-1.9963
<b>Upper Bound</b>	0.0656	0.6877	3.261	0.7807	0.6784
<b>Lower Bound</b>	-11.4198	-11.2062	-2.756	-2.6586	-5.609

**Discussion/Conclusion:** The computed tomography voxel count method of 1-mm reconstructed images provided the best estimation of renal volume size, but is very time intensive. From the data obtained, inherent measurement error using any of the techniques should be considered when renal volume calculations need to be performed.

## **SPONTANEOUS ECHOCARDIOGRAPHIC CONTRAST IN HORSES: INCIDENCE AND SIGNIFICANCE.**

N. W. Rantanen. Fallbrook, CA 92088.

**Introduction/Purpose:** Spontaneous echocardiographic contrast (SEC) is defined as the presence of echogenic particulate matter seen on ultrasonographic studies of the circulating blood. This phenomenon is found in many disease conditions in man, especially atrial fibrillation, where its presence increases the risk of stroke. SEC is found in horses with atrial fibrillation as well as in other cardiac arrhythmias. It is prevalent in racehorses with history of exercise induced pulmonary hemorrhage (EIPH). Its sonographic appearance is indistinguishable from that in human studies. Endothelial damage and blood coagulation reactions accentuate platelet activation. SEC in horses could have multiple causes as it does in people. Low grade lung inflammation causes poor performance in racehorses and the high incidence of musculoskeletal injury in horses is a significant source of vascular compromise. The etiology of EIPH is still under scrutiny, however, there is general agreement that pulmonary hypertension during exercise is a significant part of the pathogenesis leading to pulmonary capillary rupture. In man, recurrent thromboembolic disease is one cause of pulmonary hypertension. Blood with aggregates transfused into lab animals causes alveolar hemorrhage. Interestingly, Intramedullary bone densities thought to be infarcts have been reported in horses.

**Methods:** Sonographic examination of horses was accomplished with a variety of different ultrasound machines using either rotating sector, convex or phased array transducers since 1984. All studies were stored on videotape and most recently on video clips. The initial studies were done with the same machine and blood analyses were performed primarily on Thoroughbreds (n=190). Since the initial study, a variety of other breeds using other machines have been added to the sonographic data. The original videos were analyzed using a computer based videodensitometric analysis. An 'aggregate' score was determined for all examinations that was the product of the 'number of particles counted x the mean brightness x the mean area'. Since that time, studies have been done and the amount of SEC was estimated without computer analysis.

**Results:** SEC is common in Thoroughbreds, but increased levels were found in racing Thoroughbreds that had EIPH (highest aggregate scores). The cell type responsible for the SEC hasn't been proven, but the leading candidate appears to be the platelet or platelet-neutrophil aggregates.

**Discussion/Conclusion:** The detection of increased SEC in horses with clinical findings of poor performance, cardiac disease, EIPH and presence of apparent medullary bone infarcts suggests aggregated blood components as a cause.

## **ELASTOGRAPHIC EVALUATION OF NORMAL TENDONS AND LIGAMENTS OF THE EQUINE DISTAL FORELIMB.**

G.S. Seiler, M. Lustgarten, W.R. Redding. North Carolina State University, NC 27607.

**Introduction/Purpose:** Elastography is an ultrasound technique that evaluates the stiffness of tissues by measuring the displacement of ultrasound echoes before and after compression. Elastography thereby provides information about the mechanical properties of tissues and is currently used in people to differentiate malignant from benign lesions in breast, prostate and thyroid tissue. Elastographic evaluation of musculoskeletal structures, particularly the human Achilles tendon, provides information enabling more accurate diagnosis of minor injuries and early tendinitis. The purpose of this study was to evaluate feasibility and repeatability of this method for imaging of the equine distal forelimb, as well as to establish the normal elastographic appearance of the equine digital flexor tendons and suspensory ligament branches.

**Methods:** Horses with no evidence of forelimb lameness at the trot, and with sonographically normal tendons and ligaments were included. Elastographic images of the superficial and deep digital flexor tendons, and the branches of the suspensory ligament were obtained in longitudinal and transverse planes. These measurements were also performed with the leg in a non-weight bearing (flexed) position. A second ultrasonographer then repeated the examination. Images were evaluated using qualitative and quantitative methods. A qualitative assessment of softness was scored as 1-4 (1=hard; 4=soft) on an image where tissue hardness is depicted by a color scale (blue=hard, red=soft). Where imaged at the same depth, a ratio of stiffness between the superficial and deep digital flexor tendons was calculated (MyLab 70, Biosound Esaote Inc. Indianapolis, IN). Weight bearing and non-weight bearing scores were compared using a paired Students t-test.

**Results:** Eleven forelimbs of 9 horses were included in the study. Normal weight-bearing tendons and ligaments were hard to intermediate in stiffness (1.26, SD 0.33), whereas non-weight bearing tendons and ligaments were significantly softer (1.72, SD 0.59) ( $P<0.001$ ). No significant differences were found between measurements obtained by the two observers ( $P=0.14$ ). The digital flexor tendons became progressively harder from proximal (1.80, SD 0.29) to distal (1.30, SD 0.41), the superficial aspects of the suspensory branches were softer (1.97, SD 0.81) than the deep aspects (1.58, SD 0.77). The peritendinous tissues were consistently soft. The average ratio of stiffness of the deep digital flexor tendon to the superficial digital flexor tendon was 0.978 (SD 0.166).

**Discussion/Conclusion:** We have found that elastography is a feasible, non invasive and repeatable method for evaluation of the equine superficial and deep digital flexor tendons, and the branches of the suspensory ligaments. The normal elastographic appearance of tendons and ligaments of the equine distal forelimb can be used as a baseline to investigate equine tendon and ligament injuries. Elastography complements conventional grayscale ultrasound by providing information about stiffness and therefore strength and integrity of the fiber structure.

## EFFECTS OF ALPHA-2 ADRENERGIC AGONIST SEDATION ON THE ULTRASONOGRAPHIC EVALUATION OF GASTROINTESTINAL MOTILITY IN THE ADULT HORSE.

D.A. Neelis, R.L. Tucker, J.S. Mattoon, G.D. Roberts. Washington State University, WA, 99163.

**Introduction/Purpose:** Colic, or abdominal pain, is a common equine condition that results from or causes an alteration in normal gastrointestinal motility. Many pharmacologic agents used in veterinary medicine, including alpha-2 agonist sedatives, have been shown to alter the motility of the equine gastrointestinal tract. Gastrointestinal motility has most commonly been studied using surgically implanted devices, auscultation, electrointestinalography, or markers of transit, however these methods are either invasive, subjective or not readily available. Ultrasound is noninvasive, available in many practices, and provides a real-time assessment of motility. The normal ultrasonographic parameters for evaluation of the equine abdomen have been reported, however few have looked at the ability of ultrasound to detect changes in motility following sedation. The aim of this study was to compare the effect of different alpha-2 agonist sedation protocols on the ultrasound evaluation of normal equine gastrointestinal motility.

**Methods:** Ultrasound examinations of the duodenum and cecum were performed in five teaching herd adult horses, before and after intravenous administration of four different sedation protocols and a saline control. The sedatives included detomidine, xylazine, xylazine combined with butorphanol, and romifidine. All horses received each sedative and the control once, with at least 1 week between treatments, using a randomized schedule. The ultrasonographer (D.N.) was blinded to the treatments administered. The number of contractions per minute were averaged over a three-minute time period at 10, 30, 60, 90, 120, 180 and 240 minutes after injection.

**Results:** All sedatives reduced motility to an average of 0 contractions/minute at 10-30 minutes in the duodenum (except xylazine in one horse) and 0 contractions/minute at 10 minutes in the cecum. Motility ranged from 0.3-4 contractions/min in the duodenum and 0.7-4.7 contractions/min in the cecum following the saline control, never reaching a value of 0 contractions/min. In most of the horses, after the decline in motility, an increase in the number of contractions was identified, approaching or often surpassing the initial baseline contraction frequency. Following this incline, the number of contractions typically decreased toward baseline, returning to normal by 4 hours after sedation.

**Discussion/Conclusion:** Ultrasound is a safe, effective way to evaluate gastrointestinal motility in the horse. The number of contractions visualized after sedation was decreased, as expected. The contraction frequency between horses and between sedatives was variable, however the frequency was never 0 contractions/minute in the saline control. The increase in motility following a period of amotility could be associated with a transient increase in intestinal intraluminal pressure or stimulation of presynaptic receptors in the central nervous system.

## **SIMULATED OCCUPATIONAL PERSONNEL SCATTER RADIATION EXPOSURE FOR RADIOGRAPHY OF THE EQUINE STIFLE.**

R. Tyson, D.C. Smiley, R.S. Pleasant, G.B. Daniel. Virginia-Maryland Regional College of Veterinary Medicine. Blacksburg, VA 24061.

**Introduction/Purpose:** Veterinary occupational personnel radiation exposure research is sparse. In a previous paper, we estimated tube leakage and scatter radiation exposure to occupational personnel holding a portable x-ray machine during simulated equine distal limb radiography. However, the expected greatest occupational exposure would be from holding the cassette, where individuals are in close approximation to the patient. For this project, we attempt to estimate scatter radiation exposure to occupational personnel holding the imaging receptor, or cassette, for simulated equine stifle radiography.

**Methods:** Each radiographic exposure was taken with a MinXray HF80 (MinXray, Inc., Northbrook, IL) at the following technique: 80 kVp; 15 mA; 0.5 msec; 24" FFD. A Model 1015C Radiation Monitor with a Model 10X5-180 Pancake Ion Chamber (Radcal Corporation, Monrovia, CA) was used to measure scatter radiation. The Radiation Monitor and Ionization Chamber were calibrated immediately before the study with an accuracy of  $\pm 4\%$ . The MinXray unit had been recently inspected and passed by a certified medical physicist. For each view, scatter radiation measurements were made of the following: at 2" from the radiographic image receptor, to simulate hand holding of the cassette, with a second measurement at the collar position; and at 12" from the image receptor, to simulate using an extended cassette holder, with a second measurement at the collar position. A person mimicking holding the cassette was used to determine the location of the hand and collar positions. Each measurement was repeated for ten exposures. The simulation was performed with an equine cadaver pelvic limb for lateral and caudo-cranial views of the stifle joint.

**Results:** All data expressed in mR (mean  $\pm$  SD) per exposure @ 80 kVp and 7.5 mAs.

	<u>Lateral Stifle</u>	<u>Cd-Cr Stifle</u>
<b>Hand Exposure (2" from receptor)</b>	5.700 $\pm$ 0.049	2.55 $\pm$ 0.040
Simulated Collar Position	0.369 $\pm$ 0.010	0.237 $\pm$ 0.004
<b>Hand Exposure (12" from receptor)</b>	1.560 $\pm$ 0.033	1.000 $\pm$ 0.010
Simulated Collar Position	0.271 $\pm$ 0.006	0.228 $\pm$ 0.003

**Discussion/Conclusion:** This data will allow an estimate of hand and body exposure associated with occupational personnel holding the radiographic imaging plate for a commonly performed equine radiographic procedure.

## MAGNETIC RESONANCE AND RADIOGRAPHIC DIAGNOSIS OF OSSEOUS RESORPTION AT THE ATTACHMENT OF THE DISTAL SESAMOIDEAN IMPAR LIGAMENT ON THE DISTAL PHALANX IN THE HORSE.

A.C. Young, A.N. Dimock, S.M. Puchalski, M. Spriet. University of California, Davis, CA 95616.

**Introduction/Purpose:** Distal sesamoidean ligament injury (DSIL) has been implicated as a causative factor in foot lameness. Osseous resorptive changes at the level of its insertion on the distal phalanx are occasionally identified with magnetic resonance (MR) imaging. These changes may also be visualized with routine radiography. The purpose of this study was to identify the prevalence of impar attachment resorption with MR imaging and evaluate the sensitivity and specificity of radiography for the detection of these changes.

**Methods:** Eighty-five distal extremities with MR and radiographic exams performed within 2 weeks of each other were included in the study. The contour of the distal phalanx at the site of DSIL attachment was assessed on MR images by consensus between two radiologists. The grading system used included: smooth osseous outline (grade 1), irregular osseous outline with defect(s) <2mm (grade 2) or osseous resorption with a defect(s) >2mm (grade 3). Two other radiologists, unaware of the MR findings, reviewed the dorso<sup>65</sup>proximal-palmarodistal oblique radiographs for changes at this same site using the following grading system: no evidence of lucency or small, round, well defined lucency <2mm (grade 1), heterogenous opacity or poorly defined lucencies <2mm (grade 2) or lucencies >2mm (grade 3). Inter-observer agreement for the radiographic grades was assessed using a Kappa-weighted test. A chi-square test was used to evaluate the association between the MR and radiographic grades. The sensitivity and specificity of radiography for identifying osseous resorption was calculated using the MR grade 3 as the gold standard.

**Results:** On MR imaging, 13% of the cases had distal phalanx resorption at the attachment of the DSIL (grade 3). Forty-five percent of the cases were grade 2 and 42% were grade 1. Inter-observer agreement for evaluation of the radiographs was fair (kappa weighted = 0.47). The chi-square test revealed an association between MR and radiographic grades ( $p < 0.001$ ). Both radiologists had a high specificity (0.96 and 0.96) but lower sensitivity (0.45 and 0.55) for identification of osseous resorption on radiographs.

**Discussion/Conclusion:** Distal phalangeal osseous resorption at the attachment of the DSIL was not an uncommon finding on MR images in our study population. Radiography was also useful for identifying some of these lesions with careful assessment of the dorso<sup>65</sup>proximal-palmarodistal oblique projection. The radiographic specificity was high, however, MR may still be warranted in many cases due to the lower sensitivity. The clinical significance of this lesion is yet unknown and requires further investigation. It is also unknown whether the irregular outline at the site of attachment of the DSIL in the absence of a larger defect (MR grade 2) represents an early stage of osseous resorption or a normal variant.

## CHARACTERIZATION OF THE PULMONARY SYSTEM IN ALPACAS WITHOUT THORACIC DISEASE USING COMPUTED TOMOGRAPHY.

SB Cooley, SM Stieger-Vanegas. Department of Clinical Sciences, College of Veterinary Medicine, Oregon State University, Oregon, 97333.

**Introduction/Purpose:** Camelids suffer from many of the same respiratory diseases as domestic livestock. However, identification of and differentiation between respiratory disease is difficult due to a variety of complicating factors including their limited display of clinical signs and restricted auscultation especially of the caudal lung fields. Thoracic radiographs are limited to lateral views and more invasive diagnostics are often avoided due to rapid decompensation in diseased animals. Computed tomography (CT), has proven to be a valuable technique for diagnosis and management of pulmonary disease in humans, especially when radiographs are normal. Only limited information regarding normal anatomy of the camelid respiratory system is available. The objective of this study was to characterize the normal pulmonary system and to identify anatomic landmarks to help evaluating thoracic CT studies in alpacas.

**Methods:** Ten female alpacas without evidence of thoracic disease ranging in age from 2-17 years were sedated and scanned in sternal recumbency before and after intravenous iodinated contrast administration. Volume data sets were acquired and reprocessed in axial, sagittal and dorsal planes with 3.0mm slice thickness. Measurements of trachea, bronchi, vertebrae and lungs were made using a bone window (WW/WL= 320/30 HU). All the bronchi were measured at their origin in axial images and the smallest diameter was recorded to eliminate the effect of obliquity.

**Results:** The normal branching pattern consisted of a left and right cranial bronchus and three ventral bronchi to both the left and right lungs, which supplied the caudoventral, mid-caudal and caudodorsal lung fields, respectively. The right lung dominated the cranial lung field and extended cranially as far as C7 and caudally as far as the caudal border of L2. The left lung extended as far cranially as the caudal aspect of C7 and as far caudally as L1. Caudal first generation bronchi diameters ranged in diameter from 3-8 mm with generally larger bronchi cranially. No significant difference between the diameter of the bronchi of the right and left lungs were observed. Individual lung lobes were not appreciated with the exception of the accessory lung lobe. The lung density was  $-866 \pm 50$  HU and no significant difference between the right and left lung was observed. In all animals, the caudal aspect of both lungs extended further axially than laterally.

**Discussion/Conclusion:** The bronchial tree was successfully measured and mapped to the level of the second-generation bronchi and a consistent branching pattern with minimal variation was identified. The difference between axial and lateral caudal extents of the left and right lungs demonstrated that a significant portion of the caudal lung field does not extend to the thoracic wall. CT is a valuable diagnostic tool evaluating the lungs and high quality images can rapidly be obtained using sedation.

## **COMPARISON OF MRI AND COMPUTED TOMOGRAPHY ARTHROGRAPHY FOR IDENTIFICATION OF PATHOLOGIC CHANGE IN THE EQUINE STIFLE.**

N.M. Werpy\*, C.P. Ho\*\*, C.E. Kawcak\*. \*Colorado State University, CO, 80523;

\*\*Steadman Philippon Research Institute, CO, 81658.

**Introduction/Purpose:** Magnetic Resonance Imaging (MRI) of the distal limbs is frequently performed to diagnosis lameness in horses. However, the equine stifle is difficult to image with MRI due to the size and configuration of the magnet bore in most available systems. One alternative that has shown promise and can accommodate a larger number of horses based on the gantry size is computed tomography arthrography (CTA). CTA will have limitations when compared to MRI for diagnosis of soft tissue injury and detection of osseous fluid. Having an understanding of the limitations is important when evaluating CTA studies of clinical patients.

**Methods:** Post mortem MRI and CTA studies were performed on 12 equine stifles. Pre- and post-contrast CT images were acquired. Iodinated contrast material (Optiray 300, 30 mg iodine/ml, 120 mls/joint compartment, 55 mls contrast agent/5 mls saline) was placed in the medial and lateral femorotibial joints as well as the femoropatellar joint. Sagittal, front and transverse images (3mm) were be obtained using proton density, proton density fat-saturated and T2-weighted images on a 1.5 GE Signal MR Imaging System. All osseous and soft tissue structures were evaluated for abnormalities. CTA studies were evaluated first, followed by the MR studies.

**Results:** Lesions that communicate with the joint were well demonstrated with CTA. Lesions that did not communicate with the joint, such as intrasubstance tears in the menisci or ligaments, were not detectable with CTA but could be identified MRI. Axial or femoral surface meniscal tears could be identified CTA. The complete margins of the cruciate ligaments could be identified for detection of enlargement, marked margin fraying and margin defects using CTA. Intrasubstance edema in the cruciate ligament was identified on MR image but not with CTA. Fluid in bone was not identified with CTA. However, CTA had superior bone detail. Stress fractures or other small osseous detects were more clearly evident on the CTA images.

**Discussion/Conclusion:** The study was used to demonstrate lesions which are detectable with computed tomography arthrography (CTA) as compared to MRI in order to enhance diagnostic capabilities when reading clinical case studies. Certain types of pathologic change in the equine stifle were detectable with MRI and not with CTA. However, CTA identified many lesions that may not be detected with other imaging modalities, such as ultrasound and radiographs. The use of CTA will improve the diagnosis of pathologic change in the equine stifle.

## EVALUATION OF AN FSE T2 WEIGHTED SEQUENCE WITH VARYING ECHO TIME TO REVERSE THE MAGIC ANGLE EFFECT IN THE COLLATERAL LIGAMENTS OF THE DISTAL INTERPHALANGEAL JOINT IN HORSES.

N.M. Werpy\*, C.P. Ho\*\*, E.B. Garcia\*\*\* C.E. Kawcak\*. \*Colorado State University, CO, 80523; \*\*Steadman Philippon Research Institute, CO, 81658; \*\*\*Louisiana State University, LA, 70803.

**Introduction/Purpose:** The magic angle effect has been described in horses in distal deep digital flexor tendons in high field systems and in collateral ligaments of the distal interphalangeal joints in both high and low field systems. The purpose of this study was to reverse the magic angle effect through manipulation of echo time (TE) using a T2-weighted FSE sequence.

**Methods:** Eight normal limbs from skeletally mature horses were imaged with the long axis of the limb parallel to the main magnetic field in a 1.0 Tesla system. Each limb was imaged with a TE of 80, 100, 120 and 140ms. The procedure was repeated with the limbs angled at 16° relative to the main magnetic field. Asymmetry between medial and lateral collateral ligaments was scored on all studies.

**Results:** Magic angle effect was found to decrease with increasing TE. A TE of 140ms was found to nearly eliminate the magic angle effect but resulted in a decrease in the overall signal intensity of the tissues as well as a decrease in the signal to noise ratio. A TE of 120ms was found to substantially reduce magic angle effect while preserving image quality. However, these images were heavily T2-weighted with dark connective tissue and trabecular bone. Using a TE of 100ms there was great variability in the asymmetry scores at 16 degrees relative to the main magnetic field. A TE of 80ms did not adequately reverse the magic angle effect. At TE of 80ms, 7 of the 8 limbs had moderate asymmetry when evaluating the collateral ligaments and one limb had mild asymmetry.

**Discussion/Conclusion:** Magic angle effect can be observed in sequences with short TE. Reversal of the magic angle effect can be achieved by using sequences with long TE. However, the long TE will affect the signal intensity of the images and the signal to noise ratio. The longest TE that does not significantly compromise image quality and still creates contrast between tissues is recommended. Magnetic resonance imaging of the equine distal limb should include sequences with both long and short TE to avoid confusing magic angle effect with pathologic change.

## **MAGNETIC RESONANCE IMAGING CHARACTERISTICS OF CONFIRMED NAVICULAR BURSA ADHESIONS AND RESPONSE TO TREATMENT.**

M.E. Holowinski, M. Solano, J. Garcia-Lopez, L. Maranda. Tufts Cummings School of Veterinary Medicine, MA, 01536.

**Introduction/Purpose:** Adhesions occur in the navicular bursa between the deep digital flexor tendon (DDFT) and multiple other structures. The appearance of navicular bursa adhesions on MR images has been described, but only a limited number of cases described in the literature were confirmed using a gold standard for diagnosis. The purpose of this study was to describe the appearance of navicular bursa adhesions on MR images using navicular bursoscopy as the gold standard for diagnosis, to determine the occurrence of other lesions of the podotrochlear apparatus in conjunction with navicular bursa adhesions, and to describe the response of horses with navicular bursa adhesions to debridement and administration of hyaluronic acid solution (HAS).

**Methods:** Sixteen limbs from 14 horses were included in the study. Horses that had undergone MR imaging of the foot and subsequent navicular bursoscopy within one week were eligible for inclusion. All horses had a lameness that was localized to the affected foot using diagnostic analgesia. Adhesions were assigned a grade 1 when they were characterized by a focal discontinuity in the navicular bursa fluid signal between two structures, a grade 2 when the navicular bursa fluid signal was disrupted and ill-defined extraneous tissue was present between the two structures, and a grade 3 when the fluid signal was disrupted and well-defined tissue was present between the two structures.

**Results:** Twenty-eight adhesions were suspected on MR images, twenty-one of which were confirmed at surgery. Adhesions were confirmed between the DDFT and the collateral sesamoidean ligaments (CSL) in 15 limbs, between the DDFT and the navicular bone in 4 limbs, and between the DDFT and the T ligament in 2 limbs. No adhesions were visualized at surgery that were not suspected on MR images. Adhesions were best visualized on transverse PD and STIR images. The positive predictive value was 43% for grade 1 adhesions, 57% for grade 2 adhesions, and 100% for grade 3 adhesions. Additional lesions were detected in the navicular bursa in 15 limbs, the DDFT in 13 limbs, the navicular bone in 15 limbs, the CSL in 9 limbs, and the distal sesamoidean impar ligament in 8 limbs. Ten out of 14 horses were sound after treatment.

**Discussion/Conclusion:** A focal discontinuity in the navicular bursa fluid signal between two structures with well-defined extraneous tissue between the structures is diagnostic for a navicular bursa adhesion. If well-defined tissue is not seen, the diagnosis of adhesion should be made with caution. DDFT, navicular bursa, and navicular bone lesions were common in the horses in this study. Horses with navicular bursa adhesions may respond favorably to surgical debridement and intra-bursal administration of HAS.

## CLINICAL SIGNIFICANCE AND PROGNOSIS OF DDFT LESIONS ASSESSED OVERTIME USING STANDING EQUINE MRI.

M.Vanel\*, J.Olive\*, S.Gold<sup>ϕ</sup>, †R.D.Mitchell, <sup>o</sup>L.Walker. \*University of Montreal, Saint-Hyacinthe, QC, Canada; <sup>ϕ</sup>B.W. Furlong and Associates, Oldwick, NJ; †Fairfield Equine Associates, Newtown, CT; <sup>o</sup>California Equine Orthopedics, San Marcos, CA.

**Introduction/ Purpose:** Deep digital flexor tendonopathy (DDFT) has been identified as one of the most frequent causes of foot lameness since the advent of magnetic resonance imaging. The prognosis is considered guarded. Some clinicians may perform recheck MR examinations to follow the healing process of a lesion, so as to adapt the rehabilitation program. The purpose of this retrospective study was to determine whether MR findings and their evolution would help the clinician to define the horse's prognosis.

**Methods:** Files from all horses that had undergone at least two low field standing MR examinations of the foot, in three US-based clinics (Furlong B.W. and Associates, Fairfield Equine Associates and California Equine Orthopedics), between 2007 and 2010, were reviewed. Based on first examination, 35 horses were diagnosed with a DDFT lesion, which was imaged  $2.5 \pm 1.27$  times.

Signalment, activity and level, onset, duration and grading overtime of lameness of all horses were recorded. Follow-up information was obtained by phone or email interviews with the owner, the trainer or the referring veterinarian. Two observers, unaware of clinical history, reviewed independently MR images and a consensus was reached for the final data. Lesion length, maximal percentage transverse area, semiquantitative signal intensity, location, and concomitant lesions (in the distal interphalangeal joint and collateral ligaments, navicular bone, navicular bursa, impar and sesamoidian collateral ligaments, and adhesions within the navicular bursa) were recorded for each MR examination, in all available sequences.

**Results:** No horse having a T1-GRE hyperintense lesion over 30mm in length or 15% in transverse area of a tendon lobe, on the first MR exam, returned to previous activity. Besides, no horse with a lameness grade higher than 1/5 at recheck examination, returned to its previous level, regardless of time between both exams. Horses with concomitant lesions (bone marrow lesion, bursitis, cyst-like lesion) had a statistically worse prognosis than horses with DDFT lesions only ( $p=0.005$ ). However, suspected adhesions within the navicular bursa were not statistically related to the prognosis ( $p=0.41$ ).

On all horses including those with an excellent outcome, the lesion persisted, even faintly, in T1-GRE and PD sequences. Horses whose DDFT lesion had resolved on STIR FSE images on recheck examination had a statistically better prognosis ( $p=0.0004$ ). All horses that returned to their previous level of performance had complete resolution of signal hyperintensity on STIR FSE sequence.

**Discussion/Conclusion:** Though rehabilitation remains multifactorial, characteristics of DDFT and concomitant lesions on first MR and recheck examinations can give clues to the clinician about the horse's prognosis.





## **American College of Veterinary Radiology**

### **ACVR 2011 Conference Special Activities**

**Wednesday, October 14, 2011**

The Sendero Ballroom  
Reception supported by  
Universal Medical Systems, Inc.  
6:30 – 7:30 p.m.

Special dedication to the memory of Dr. Myron “Mike” Bernstein

**Lunch Sponsor**  
Orthopedic Foundation for Animals

# IDENTIFICATION OF REGISTRANTS

*Blue name badges*

ACVR Diplomates

*Gray name badges*

ACVR Residents in Training

*Green name badges*

Post Trainees  
ACVR Society Members  
Veterinarians

*Yellow name badges*

Exhibitors/Sponsors